Das Glykoprotein M6a beeinflusst Endozytose und Rezyklisierung, sowie die Desensibilisierung des μ-Opioidrezeptors

Dissertation

zur Erlangung des akademischen Grades

doctor rerum naturalium
(Dr. rer. nat.)

genehmigt durch
die Fakultät für Naturwissenschaften
der Otto-von-Guericke-Universität Magdeburg

von	Magister Daifei Wu
geb. am	03. April 1969
in	Fujian, China

Gutachter:	Prof. Dr. Volker Höllt
	Prof. Dr. Eckart D. Gundelfinger
	Prof. Dr. Klaus-Armin Nave

Eingereicht am:	28. November 2005
Verteidigung am:	04. Juli 2006

1 Introduction

1.1 Opioid receptors

Opium has been known to relieve pain and alter mood since the advent of recorded history (Gourlay, 2005). To date, opiates such as morphine are still the best analgesic choice in the treatment of chronic and serious pain, such as cancer pain. However, their extensive and long-term use is limited due to the development of opiate tolerance and dependence. In addition, drug treatment can lead to drug abuse. Opiate drugs mediate their physiological effects by binding to opioid receptors, which are also activated by endogenously produced opioid neuropeptides (von Zastrow, 2004). Under the tremendous efforts of the past years, we now understand mechanisms of opioid receptor signal transmission in considerable detail. However, a definitive mechanism for opioid receptor regulation, especially in the complex physiological circumstance of intact nervous system, is still far from clear.

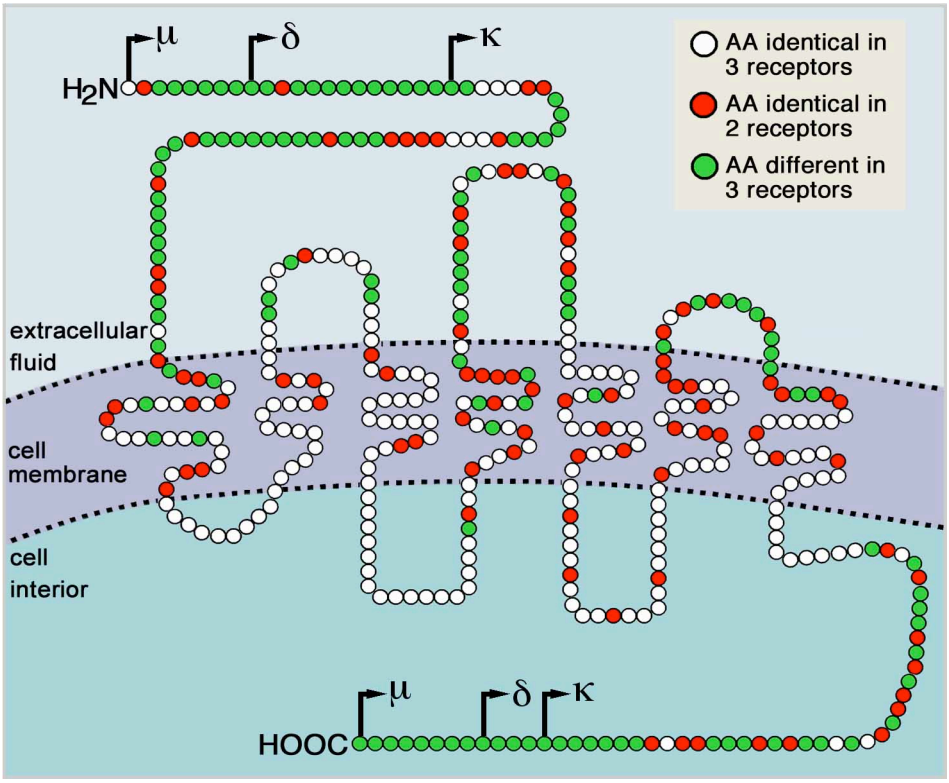

Figure 1.1. Structure of opioid receptors (modified from LaForge et al., 2000). Opioid receptor has a central common core made of seven transmembrane helices connected by three intracellular and three extracellular loops. The differences in N-terminal and C-terminal length for each receptor type are shown.

Three independent reports on the identification of opioid receptors in 1973 (Pert and Snyder, 1973; Simon et al., 1973; Terenius, 1973) marked the advent of a new era of the opioid research. 20 years later, genes encoding three well-defined or "classical" types of the opioid receptors, μ-, □- and □-opioid receptors, were cloned (Kieffer et al., 1992; Evans

et al., 1992; Chen et al., 1993a; Minami et al., 1993; Fukuda et al., 1993; Li et al., 1993; Meng et al., 1993; Yasuda et al., 1993; Wang et al., 1993).

Sequence analysis of these cloned opioid receptors revealed that they belong to the superfamily of G protein-coupled receptors (GPCRs) and the subfamily of rhodopsin receptors. As shown in Figure 1.1, the μ-, δ- and κ-opioid receptors have the putative seven domains of 20-25 hydrophobic residues that form α-helices and span the plasma membrane, an extracellular N-terminus, three extracellular loops, three intracellular loops and an intracellular C-terminal tail (Evans et al., 1992; Kieffer et al., 1992; Chen et al., 1993a; Fukuda et al., 1993; Li et al., 1993; Meng et al., 1993; Yasuda et al., 1993; Waldhoer et al., 2004). These receptors are about 60% identical to each other, with the greatest homology found in the transmembrane domains (73–76%) and intracellular loops (86–100%). The lowest homology in amino acid sequence is found in the N-terminus (9–10%), extracellular loops (14–72%), and the C-terminus (14–20%) (Chen et al., 1993b; Law et al., 2000b).

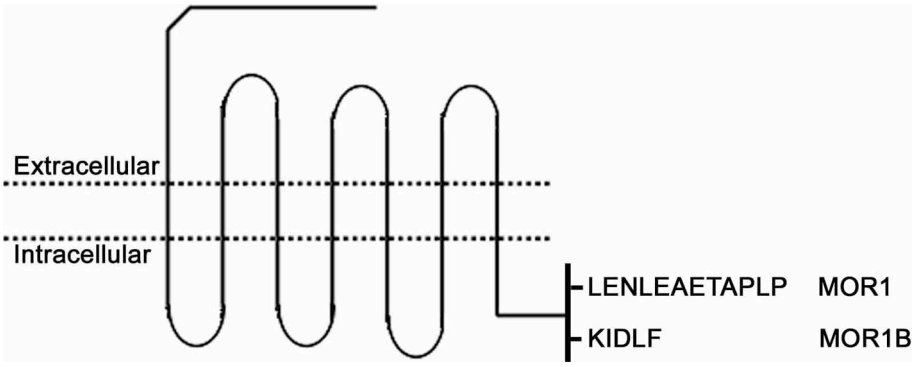

Figure 1.2. Different amino acid sequence between rat MOR1 and MOR1B.

Numerous pharmacological studies have suggested subtypes of the μ-opioid receptor (MOR1) and studies have raised the possibility that some of these may reflect splice variants of the MOR1 gene (Wolozin and Pasternak, 1981; Pasternak, 1993; Pasternak and Standifer, 1995). Two MOR1 variants, MOR1A and MOR1B, were identified shortly after the initial cloning of MOR1 (Bare et al., 1994; Zimprich et al., 1995). MOR1 and MOR1B differ at the C-terminus as shown in Figure 1.2. Thereafter, additional MOR1 splice variants such as MOR1C, D, E and F were identified (Pan et al., 1999, 2000). All these splice variants are identical in the first 386 amino acids. Though MOR1 and its splice variants are derived from the same gene, and exhibit similar binding properties, they differ in their functional properties and regional distributions (Schulz et al., 1998; Koch et al., 1998; Pan et al., 1999, 2000; Abbadie et al., 2000; Bolan et al., 2004). Recently, more carboxyl-terminal splice variants of the μ-opioid receptor were continually identified and characterized (Pasternak et al., 2004; Pan et al., 2005).

The μ-opioid receptor (MOR1) mediates the action of most clinically important opiate drugs, e.g. morphine, as well as drugs of abuse such as heroin (Matthes et al., 1996;

Kieffer, 1999; Kieffer and Gaveriaux-Ruff, 2002). MOR1 is thought to be responsible for opioid analgesic effects, and for unwanted effects, e.g. respiratory depression, euphoria, sedation, tolerance and dependence.

1.2 Functional activities of opioid receptors

Stimulation of opioid receptors by the binding of specific ligands activates $G_{i/o}$ proteins, as a result of which the G_{α} subunit exchanges its GDP for GTP. G protein thus dissociates from the receptor and both G_{α} and $G_{\beta\gamma}$ dimer carry the signal to their effectors, which may be enzymes and/or ion channels.

Generally, stimulation of opioid receptors inhibits adenylate cyclase (AC), activates inwardly rectifying potassium channels and inhibits voltage-sensitive calcium channels. All result in decreased neuronal excitability and inhibition of neurotransmission (see Law et al., 2000b and Williams et al., 2001 for reviews).

1.3 Intracellular trafficking of opioid receptors

Similar to other GPCRs, agonist binding to opioid receptors is followed by receptor phosphorylation, which is mediated by G protein-coupled receptor kinases (GRKs) (Kovoor et al., 1997; Pak et al., 1997; Wolf et al., 1999; Deng et al., 2000; Wang, 2000; Law et al., 2000b; Schulz et al., 2004) and second messenger-regulated protein kinases, such as Ca^{2+}/calmodulin-dependent kinase II (Mestek et al., 1995; Koch et al., 1997, 2000; Brüggemann et al., 2000) and mitogen activated protein (MAP) kinase (Polakiewicz et al., 1998; Schulz and Höllt., 1998; Schmidt et al., 2000). The binding of β-arrestins to phosphorylated receptors leads to receptor uncoupling from G-proteins, which in turn causes receptor desensitization. In addition, β-arrestins bind to both the clathrin heavy chain and the β2-adaptin subunit of heterotetromeric AP-2 adaptor complex, and target the receptors to clathrin-coated pits, thereby linking the receptors to endocytic membranes. The coordinated interaction of both clathrin and AP-2 with β-arrestins is necessary for heptahelical receptor internalization via clathrin-coated pits (Goodman et al., 1996, 1997; Gurevich and Benovic, 1997; Krupnick and Benovic, 1998; Laporte et al., 1999, 2000; Ferguson, 2001; Claing et al., 2002; Pierce et al., 2002). Once the plasma membrane is invaginated, GTPase dynamin wraps around and constricts the necks upon GTP hydrolysis, thus vesiculation occurs. These vesicles soon shed their clathrin coats and become early endosomes. The ligands and receptors are separated in an acidified perinuclear compartment. Dissociation of β-arrestins also occurs. Cytosolic phosphatases may dephosphorylate the receptors. The ligands are degraded while the receptors are either recycled to the plasma membrane for resensitization or degraded in the lysosomes for down-regulation (see Law and Loh, 1999; Ferguson, 2001; Williams et al., 2001; Claing et al., 2002; Pierce et al., 2002; von Zastrow, 2003; Mousavi et al., 2004 for reviews).

The processes of agonist-induced intracellular trafficking of opioid receptors are diagrammed in Figure 1.3.

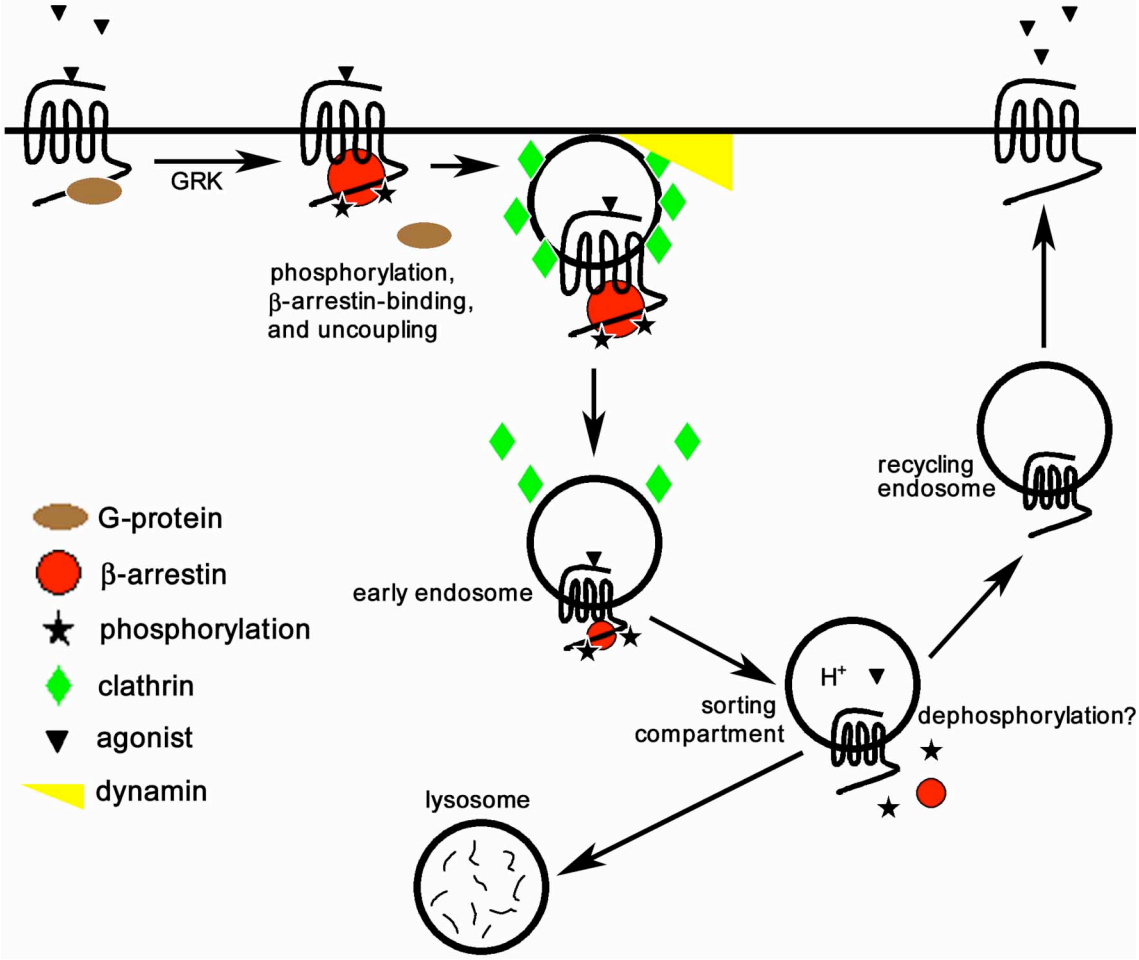

Figure 1.3. Typical pathways of opioid receptor trafficking.

1.3.1 Role of phosphorylation in the regulation of opioid receptor internalization

As shown above, one of the first events following receptor stimulation is the recruitment of G protein-coupled receptor kinases (GRKs) to the plasma membrane and receptor phosphorylation. GRK-mediated receptor phosphorylation enhances the interaction between receptors and β-arrestins.

MOR1 is phosphorylated at a low level in the absence of agonist, and receptor phosphorylation is significantly enhanced in the presence of etorphine or DAMGO (Arden et al., 1995; Whistler et al., 1999). Morphine was observed to promote phosphorylation of MOR1 to a lesser extent than opioid peptides and certain other alkaloid agonists (Arden et al., 1995; Yu et al., 1997; Zhang et al., 1998). Consistent with these findings, etorphine or DAMGO promotes rapid internalization of MOR1, whereas morphine fails to promote significant receptor internalization. However, over-expression of GRK2 enables morphine to promote rapid phosphorylation and internalization of MOR1 (Zhang et al., 1998). The absence of agonist-induced phosphorylation by the mutation of putative phosphorylation sites to alanine completely blocks or significantly attenuates the agonist-induced μ-opioid receptor internalization (El Kouhen et al., 2001; Schulz et al., 2004). The rapid

internalization of the □-opioid receptor (DOR1) is totally blocked in the presence of heparin, an inhibitor of GRKs (Hasbi et al., 2000).

1.3.2 Post-endocytic sorting of internalized receptors

Some internalized GPCRs are dephosphorylated in sorting endosomes and recycled rapidly to the cell surface, while others are sent to lysosomes for degradation. Trafficking of GPCRs to lysosomes requires specific sorting events involving ubiquitin-dependent or -independent interactions of receptors with cytoplasmic sorting proteins (Marchese and Benovic, 2001; Tanowitz and Von Zastrow, 2002; Whistler et al., 2002; Shih et al., 2002).

MOR1 and DOR1 differ significantly in their intracellular sorting. The internalized DOR1 is mainly targeted to lysosomes for degradation, whereas MOR1 and its spliced variants have distinct properties to recycle back to the cell surface upon agonist treatment (Koch et al., 1998, 2001; Wolf et al., 1999; Ko et al., 1999; Tsao and von Zastrow, 2000; Wang et al., 2003; Tanowitz and von Zastrow, 2003; Marie et al., 2003). The role of the carboxyl tail in directing opioid receptor trafficking has been established (Afify et al., 1998; Kouhen et al., 2000; Koch et al., 1998, 2001; El Kouhen et al., 2001; Wang et al., 2003). Recently, GASP (G protein-coupled receptor-associated sorting protein), was identified as a candidate of lysosomal sorting protein, which binds strongly to the DOR1 carboxyl tail, and plays a key role in modulating DOR1 endocytic sorting to lysosomes (Whistler et al., 2002).

Recycling of internalized opioid receptors to the plasma membrane is associated with dephosphorylation of receptors (Tsao and von Zastrow, 2001). The efficient recycling of opioid receptors requires a specific sequence that is conserved in the carboxyl tail of MOR1 but is absent in DOR1. The MOR-derived endocytic recycling sequence (MRS) distinguishes the endocytic trafficking of MOR1 from that of DOR1 (Tanowitz and von Zastrow, 2003). However, this finding cannot explain why MOR1B (a splice variant of MOR1) without this MRS shows faster recycling compared with MOR1 (Koch et al., 1998). Thus, additional domains of MOR1 might exist to control the regulation of μ-opioid receptor recycling.

The regulation by which opioid receptors are “sorted” between divergent recycling and degradative pathways after receptor internalization is of particular interest due to its importance on cell signaling and opiate responsiveness after long-term exposure to opiate drugs.

1.4 Down-regulation of opioid receptors

Down-regulation is characterized by a decrease in the total number of receptors in a cell, and is caused by long-term exposure to agonists for hours or days; recovery from down-regulation is slow. From a physiological viewpoint, it is probably rare that a cell is exposed continuously to opioids, since efficient mechanisms exist to remove them from the extracellular fluid. However, down-regulation may occur under pathological circumstances

and long-term administration of opiate drugs. Opioid receptor down-regulation may result from a proteolytic degradation of internalized receptors and/or a decrease of newly synthesized receptors.

Receptor internalization is considered as the first step in the down-regulation of opioid receptors after chronic exposure to agonists. Trafficking of internalized receptors to lysosomes promotes proteolytic degradation. In HEK293 cells, the rapid morphine-induced endocytosis of MOR1D and MOR1E permits receptor down-regulation. In contrast, the lack of morphine-induced internalization of MOR1 and MOR1C prevents receptor down-regulation (Koch et al., 2001).

The observed decrease in the mRNA level of the opioid receptors after chronic agonist treatment is suggested to be due to changes in the intracellular cAMP level (Kraus et al., 1995; Kim et al., 1995). The cAMP dependent PKA has been shown to phosphorylate CRE binding protein (CREB) and thereby to enhance receptor transcription. Promoter analysis of rat MOR1 revealed that an increase of intracellular cAMP level by forskolin enhances promoter activity in transfected SH SY5Y cells, whereas DAMGO by inhibiting cAMP formation decreases transcription driven by MOR1 promoter (Kraus et al., 1995).

In theory, down-regulation of opioid receptors would lead to tolerance by reducing the number of functional receptors. Previous studies showed that μ-opioid receptor downregulation contributes to opioid tolerance in vivo (Stafford et al., 2001). In fact, in vitro, opioid receptor downregulation has been reported following chronic agonist treatment (Law et al., 1983; Puttfarcken and Cox, 1989; Zadina et al., 1993, 1994; Yabaluri and Medzihradsky, 1997). However, opioid receptors in brain have been reported to decrease, increase or remain unchanged following chronic administration of agonists (for reviews, see Liu and Anand, 2001; Harrison et al., 1998). Furthermore, the time course of receptor down-regulation observed in cultured cells fails to match the time course of the development of tolerance in vivo. Thus, it appears unlikely that receptor down-regulation is solely responsible for the development of opioid tolerance.

1.5 Desensitization of opioid receptors

The early events of signaling by GPCRs are usually rapidly attenuated by receptor desensitization (Lohse, 1993; Freedman and Lefkowitz, 1996), which reduces the ability of receptors to modulate second messengers (Law et al., 1983; Nomura et al., 1994; Mestek et al., 1995). Desensitization is a complicated process in receptor regulation, which can be regulated as a consequence of multiple processes of receptor uncoupling, trafficking, down-regulation, and so on.

An important component of receptor desensitization, which occurs within seconds to minutes of receptor activation, is uncoupling of the activated receptor from its G-protein by receptor phosphorylation. The phosphorylation facilitates the subsequent binding of β-arrestin, which acts as a damper for further signaling by preventing further G-protein

coupling (Böhm et al., 1997; Yu et al., 1997; Bohn et al., 1999, 2004; Law et al., 2000b; Kohout et al., 2001; Ahn et al., 2003). In mice lacking β-arrestin 2, MOR1 remains coupled with G-protein, and its desensitization does not occur even after chronic morphine treatment (Bohn et al., 2000). The absence of agonist-induced phosphorylation by the mutation of putative phosphorylation sites to alanine completely blocks or significantly attenuates the agonist-induced receptor desensitization (Deng et al., 2000; Wang et al., 2002; Schulz et al., 2004). The enhanced phosphorylation of MOR1 has been correlated with the desensitization of MOR1 in thalamus of rats chronically treated with morphine (Deng et al., 2001). Over-expression of GRK2 increases agonist-induced receptor phosphorylation and promotes MOR1 desensitization (Zhang et al., 1998). However, phosphorylation and β-arrestins do not appear to be necessary in all cases for desensitization to occur in neurons and some test cell models (Kovoor et al., 1997; Capeyrou et al., 1997; Cheng et al., 1998; Law and Loh, 1999; Williams et al., 2001), implying that mechanisms other than receptor phosphorylation and the subsequent interaction with β-arrestin mediating receptor desensitization exist.

The ability of cells to respond to opioids requires the presence of opioid receptors at cell surface, where they can interact with agonists in the extracellular fluid. After receptor internalization, the dephosphorylation and subsequent recycling of receptors back to the plasma membrane therefore contribute to a reversal of the desensitized receptor state (resensitization), which partially counteracts the receptor desensitization (Böhm et al., 1997; Wolf et al., 1999; Hasbi et al., 2000). A MOR1 mutant, MOR363D, which does not recycle after internalization, was observed to desensitize faster than that of wild type MOR1 upon agonist activation (Qiu et al., 2003). The block of recycling pathway by monensin, which traps internalized receptors within endosomes, enhances receptor desensitization (Koch et al., 1998; 2004; Law et al., 2000a). Consistent with this, agonists that could promote rapid receptor internalization and recycling lead to less receptor desensitization (Koch et al., 2005).

1.6 Adenylate cyclase superactivation

Early studies revealed that opioids acutely inhibit AC activity in NG108-15 cells. Later it has been shown that in the continued presence of morphine, there is an upregulation of AC activity (Sharma et al., 1975). The phenomenon that chronic opiate treatment followed by opiate withdrawal leads to enhanced forskolin-stimulated AC activity and cAMP accumulation, has been termed AC superactivation. This has been considered as a cellular hallmark of opiate withdrawal (Bohn et al., 2000; Fin and Whistler, 2001). Mechanisms that are responsible for AC superactivation are still controversially discussed (for review, see Liu and Anand, 2001).

AC superactivation, originally observed in several cell lines and many types of neurons, has been suggested to represent a general means of cellular adaptation to the

activation of inhibitory receptors, and to play a role in the development of opiate tolerance and dependence (Childers, 1991; Self and Nestler, 1995; Avidor-Reiss et al., 1995, 1996; Nestler and Aghajanian, 1997; Williams et al., 2001; Liu and Anand, 2001; Fin and Whistler, 2001; Johnston and Watts, 2003).

1.7 Opiate tolerance and dependence

Morphine and other opioids are used and abused for their analgesic and rewarding properties. Tolerance to these effects, as well as physical and psychological dependence, develops over hours/days to weeks. Tolerance is a decrease in responsiveness manifested as a loss of response to a given dose of an agonist, or the requirement for an increased dose to achieve the original effect. Dependence is a different phenomenon, much more difficult to define and measure, which involves two separate components, namely physical and psychological dependence. Physical dependence is associated with a physiological withdrawal syndrome (or abstinence syndrome), manifesting as extreme restlessness and distress accompanied by a strong craving for drugs. Re-administration of morphine rapidly abolishes the abstinence syndrome. Drug users who are no longer physically dependent can still show psychological dependence and relapse.

It is increasingly evident that opiate-induced tolerance and dependence occur at multi-levels in the nervous system, beginning with regulation of opioid receptors themselves and extending to a complex network of direct and indirect modifications of "downstream" signaling machinery. Traditional mechanisms thought to underlie opiate tolerance and dependence include receptor phosphorylation, G-protein uncoupling, receptor down-regulation, desensitization, AC superactivation, the amount of effector proteins or the capacity of an effector to be regulated by opioid receptors (reviewed in Nestler and Aghajanian, 1997; Lefkowitz, 1998; Liu and Anand, 2001; Ferguson, 2001; Von Zastrow et al., 2003; Bailey and Connor, 2005). Despite the delineation of many of the physiological, biochemical, and molecular biological sequelae of persistent exposure to opioids, elucidation of the biochemical underpinnings of tolerance and dependence formation remains elusive.

1.8 Membrane glycoprotein M6 and its family

Using a monoclonal antibody, called M6 (Lagenaur et al., 1992), Yan and collaborators (1993) identified two distinct membrane glycoprotein M6 (designated M6a and M6b). M6a is one of the neuronal surface molecules in the central nervous system (CNS) (Lagenaur et al., 1992; Yan et al., 1993). As shown in Figure 1.4B, at the amino acid level, M6a is 54% identical with M6b, and shows greater homology to DM20 (42%) than to proteolipid protein (PLP) (Yan et al., 1993; Olinsky et al., 1996; Mukobata et al., 2002). DM20 differs from PLP by an internal deletion of 35-amino acid residues (116-150) from the major hydrophilic domain in the intracellular loop of PLP (Nave et al., 1987; Macklin et al., 1987; Simons et al., 1987).

A.

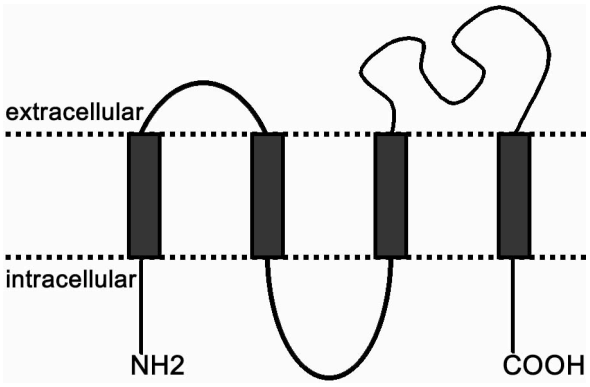

B.

```
M6b MKPAMETAAEENTEQSQERKGCFECCIKCLGGVPYASLVATILCFSGVALFCGCGHVALA 60
M6a -------MEENMEEGQTQKGCFECCIKCLGGIPYASLIATILLYAGVALFCGCGHEALS 52
DM20 ----------------MGLLECCARCLVGAPFASLVATGLCFFGVALFCGCGHEALT 41

M6b GTVAILEQHFSTN--TSDHALLSEVIQLMQYVIYGIASFFFLYGIILLAEGFYTTSAVKE 118
M6a GTVNILQTYFELARTAGDTLDVFTMIDIFKYVIYGIAAAFFVYGILLMVEGFFTTGAIKD 112
DM20 GTEKLIETYFSKN--YQDYEYLINVIHAFQCVIYGTASFFFLYGALLLAEGFYTTGAVRQ 99

M6b LHGEFKTTACGRCISGMFVFLTYVLGVAWLGVFGFSAVPVFMFYNIWSTCEVIKSPQSNG 178
M6a LYGDFKITTCGRCVSAWFIMLTYLFMLAWLGVTAFTSLPVYMYFNVWTICR--NTTLVEG 170
DM20 IFGDYKTTICGKGLSATFVGITYALTVVWLLVFACSAVPVYIYFNTWTTCQSIAFPSKTS 159

M6b TSGVEQICVDVRQYGIIPWNAFPGKICGS--ALENICNTNEFYMSYHLFIVACAGAGATV 236
M6a AN----LCLDLRQFGIVTIGEEK-KICTASENFLRMCESTELNMTFHLFIVALAGAGAAV 225
DM20 AS-IGSLCADARMYGVLPWNAFPGKVCGS--NLLSICKTAEFQMTFHLFIAAFVGAAATL 216

M6b IALIHFLMILSSNWAYLKDASKMQAYQDIKAKEEQELQDIQS-RSKEQLNSYT 288
M6a IAMVHYLMVLSANWAYVKDACRMQKYEDIKSKEEQELHDIHSTRSKERLNAYT 278
DM20 VSLLTFMIAATYN FAVLKLMGRGTKF---------------------- 242
```

Figure 1.4. A. Proposed structural model of PLP/DM20 family. Members of the PLP/DM20 family are tetraspan proteins, with four transmembrane domains, and with the NH2 and COOH termini both located on the cytoplasmic face of the membrane. **B. Alignment of mouse M6a, M6b and DM20 amino acid sequences.** Analyzed by the program of "Multiple Sequence Alignment" in http://workbench.sdsc.edu. Green amino acids (AA) represent identical sequence in these three molecules, and red AA represents identical sequence in at least two molecules. The AA residues were numbered on the right, respectively. Blue and gray regions represent transmembrane domains of M6a and DM20, respectively (Mukobata et al., 2002; Greer and Lees, 2002).

The identification of M6a and M6b indicated the formation of a new gene family, the PLP/DM20 family (Yan et al., 1993). Later, new members of this family, DM□, DM□, DM□ (Kitagawa et al. 1993) and Rhombex-29 (Shimokawa and Miura, 2000), were also identified. Members of PLP/DM20 family have four transmembrane domains with the N- and C-terminus localized intracellularly (Figure 1.4A). They show a very high degree of conservation within their hydrophobic domains, and less conservation in their hydrophilic regions. PLP is highly conserved through evolution. PLP from mouse, rat and human have identical amino acid sequence (Milner et al., 1985; Diehl et al., 1986). Similarly, M6a from mouse, rat and human share over 99% amino acid sequence (Mukobata et al., 2002).

PLP and its spliced isoform DM20 constitute about 50% of the protein in CNS myelin sheath (Readhead et al., 1994). It is generally believed that PLP/DM20 plays an

essential structural role in maintaining the multilamellar state required for normal myelin function by promoting adhesion of bilayers. However the idea that PLP/DM20 is more than a structural protein for myelination is gaining increasing support (Campagnoni, 1988; Campagnoni and Skoff, 2001; Greer and Lees, 2002). Although PLP appears to be expressed by mature oligodendrocytes only, DM20 has been found in oligodendrocytes well before myelination (Schindler et al., 1990). Moreover, a widespread distribution of DM20 in diverse non-nervous tissues further supported a PLP/DM20 function unrelated to myelination (Nadon et al., 1997). Consistent with this view, a role of PLP/DM20 family in ion transport was previously suggested (Lin and Lees, 1982; Helynck et al., 1983; Diaz et al., 1990; Inouye and Kirschner, 1991). Thus, a function of PLP/DM20 family other than its structural role in myelination is possible. It is tempting to speculate that M6a has a function similar to that of PLP/DM20 since they share a high sequence homology. Recently, Mukobata and coworkers (2002) reported that M6a functions as a nerve growth factor-gated Ca^{2+} channel and is involved in neuronal differentiation. This is in line with previous reports that M6a might be involved in vectorial transport and multi-ion transport (Diaz et al., 1990; Inouye and Kirschner, 1991; Lagenaur et al., 1992; Kitagawa et al., 1993). Furthermore, previous studies suggested a role for M6 protein (M6a and M6b) in some aspects of neurite growth. The M6 antigens located on neurites, especially in growth cones, and the M6 antibody inhibited neurite extension of cultured cerebellar neurons, presumably resulting from the interference of antibody with a surface antigen of the neurites by altering intracellular ion concentration (Lagenaur et al., 1992; Yan et al., 1993). However, according to the observation of M6a localization by immunoelectron microscopy, Roussel and colleagues (1998) excluded the possibility that the M6a antigen was responsible for the neuritic inhibition in response to M6 antibody because the M6a antigen localized at the cytoplasmic side of various membranes. Nevertheless, up to now, the definitive function of M6a is still unclear.

1.9 The present research project

The process by which extracellular signals are transferred from cell membrane to specific intracellular sites is an essential facet for cellular regulation. Various proteins within plasma membrane and/or by recruitment from cytoplasm greatly affect opioid receptor trafficking and signaling (Heydorn et al., 2004; Bockaert et al., 2004). Therefore, identification of opioid receptor-interacting proteins might provide new insights into the regulatory mechanisms of receptor trafficking and signaling.

Using a yeast two-hybrid system to screen a rat brain cDNA library for proteins that interact with the μ-opioid receptor, our group identified over fifty proteins interacting with MOR1 and/or MOR1B. We have employed co-immunoprecipitation to analyze these interacting proteins. Co-immunoprecipitation relies on in vitro assays that require solubilization with detergents, which could promote artificial aggregation of hydrophobic proteins such as transmembraneous proteins. In contrast, BRET (bioluminescence resonance energy transfer) technology is a living cell-based proximity assay, which overcomes the drawback of co-immunoprecipitation (Boute et al., 2002; Pfleger and Eidne, 2003; Wang et al., 2005). In BRET assay, the proteins are more likely to be in their native conformations, which may lead to increased sensitivity and accuracy of detection. Here, we employ BRET to confirm interactions of MOR1 with those proteins. Of all of those proteins, M6a shows the strongest interaction with MOR1.

In humans, a variety of mutations of the PLP gene are known to cause the dysmyelinating disorders Pelizaeus-Merzbacher disease (PMD) and spastic paraplegia (Hodes and Dlouhy, 1996; Garbern et al., 1999; Inoue, 2005). In mammalian cells, cholesterol is thought to form membrane microdomains termed lipid rafts that regulate protein trafficking (Lusa et al., 2001; Golub et al., 2004). PLP directly interacts with cholesterol in myelin lipid raft (Simons et al., 2000). In normal conditions, internalized cholesterol is distributed to early and recycling endosomes from where it can recycle back to the plasma membrane (Mukherjee et al., 1998; Gagescu et al., 2000; Kobayashi et al., 2001; Lusa et al., 2001). However, over-expression of PLP induces the abnormal accumulation of PLP and cholesterol in the late endosomal/lysosomal compartment (Simons et al., 2002). Thus, it is interesting to test whether the interaction between MOR1 and M6a changes the regulation of MOR1 trafficking.

In this thesis, we focus on demonstrating the MOR1-M6a interaction and characterizing the possible role of M6a in the intracellular trafficking and signal regulation of the μ-opioid receptor.

2 Materials

2.1 Instruments

Gene Pulser II and Pulse Controller Plus (Bio-Rad, USA) for Electroporation
dNA sequencer, model 4000 (Li-cor, Germany)
Leica TCS-NT laser-scanning confocal microscope (Leica Microsystems, Germany)
Fusion™ Universal Microplate Analyzer (BioSignal Packard BioScience)
PTC-0200 DNA Engine (MJ Research, Inc. USA) for PCR
TRI-CARB 1900 TR Liquid Scintillation Analyser (Packard, USA)
Expert Plus Microplate Reader (ASYS, Austria)
Electrophoresis power supply (Bio-Rad)
Gel electrophoresis system (Bio-Rad)
Semi-dry Transfer Cell (Bio-Rad) for electroblotting

2.2 Kits

PCR purification Kit, Gel extraction Kit, Plasmid Midi Kit (QIAGEN, Germany)
EndoFree Plasmid Maxi Kit (QIAGEN, Germany)
MinElute Reaction Cleanup Kit (QIAGEN, Germany)
RNeasy Tissue Kit (QIAGEN, Germany)
Cyclic AMP (^{3}H) assay system (Amersham Biosciences, Braunschweig, Germany)
Sequencing kit with 7-deaza-dGTP (Amersham Pharmacia Biotech)
Micro Bio-Spin columns P-30 (BIO-RAD)
Rat Neuron Nucleofector Kit (Amaxa Inc. USA)

2.3 Chemicals

DAMGO (Bachem, Heidelberg, Germany)
[^{3}H]DAMGO (NEN, Köln, Germany)
Morphine (Synopharm, Barsbüttel, Germany)
Etorphine (Gampian Pharamceutical Limited, Dundee Scotland, UK)
Naloxone (Tocris)
Monensin (Sigma)
DPDPE (Bachem, Heidelberg, Germany)
Forskolin (Biotrend, Köln, Germany)
Lipofectamine™ 2000 (Life technologies, Invitrogen)
Dithiobis-(succinimi-dylpropionate)(DSP) (Pierce)
Enhanced chemiluminescence detection system (Amersham Biosciences)
DPX mountant for histology (resinous mounting media) (Fluka, NeuUlm, Germany)
Deep Blue C (coelenterazine) (BioSignal Packard Biosciences)
Protein A-agarose beads (Amersham Biosciences, Sweden)
ABTS solution (Roche Molecular Biochemicals)
Triton-X100 (Merck, Darmstadt, Germany)

Ammonium persulfate (Sigma)
30% acrylamide mix (Carl Roth GmbH & Co)
HEPES, TEMED (Serva)

2.4 Bacterium and eukaryotic cell line

E. coli XL1 (Promega)
Human embryonic kidney HEK 293 cell (ATCC CRL 1573)

2.5 cDNAs and plasmids

pCMV-SPORT6-M6a (RZPD, Germany) (GI: 31981997)
pRc/CMV-MOR1 from Dr. Lei Yu (Indianapolis, IN) (GI: 6981309)
pcDNA3.1-MOR1B from Alexander Zimprich (Zimprich et al., 1995)
pCMV-M6b from Prof. Klaus-Armin Nave (Göttingen, Germany) (GI:9502118)
pCMV-DM20 from Prof. Klaus-Armin Nave (Göttingen, Germany) (GI: 200408)
pRK5-mGluR1a and 5a from Dr. Helmut Schröder (IPT,Magdeburg Univ., Germany)
pcDNA3.1-DOR1 from Dr. Manuela Pfeiffer (IPT, Magdeburg Univ., Germany)
pGFP-sst2A from Dr. Stefan Schulz (IPT, Magdeburg Univ., Germany)
pEAK10 expression vector (Edge Bio Systems, Gaithersburg, MD)
pRluc-N_3/C_1 and pGFP-N_3/C_3 vectors (BioSignal Packard BioScience)
pGEM-T easy vector (Promega, Madison, USA)
pCMV-HA, pCMV-Myc (Clontech)
pcDNA3.1 (Invitrogen)

2.6 Mediums

DMEM with 4.5g/L Glucose and L-Glutamine (Cambrex, Belgium)
OPTIMEM I (Modified Eagle's Minimum Essential Medium) (Invitrogen)
RPMI medium with Glutamine (Cambrex, Belgium)
Neurobasal medium (Gibco)
LB media and LB-Agar media (Gibco)
Fetal calf serum (FCS) (Bachem, Heidelberg, Germany)

2.7 Enzymes

All endonucleases from New England Biolab
Taq DNA polymerase, T4 ligase, M-MLV reverse transcriptase from Promega
SP6, T7 polymerase from Roche
RNase A from Sigma

2.8 Antibodies and antibiotics

Mouse anti-Myc monoclonal antibody (Clontech)
Fluorescent conjugated second antibodies (Jackson ImmunoResearch, PA)
Rat anti-mouse M6a antibody (Medical & biological laboratories CO., LTD.)
Peroxidase-conjugated anti-rabbit antibody (Amersham Biosciences)

HRP-conjugated second antibodies (Amersham Biosciences)
Hygromycin B (PAA Laboratories GmbH, Pasching, Germany)
Puromycin, Ampicillin, Penicillin and Streptomycin (Sigma)
Zeocin (Life technologies, Invitrogen)
G418 (Gibco)

2.9 Buffers and solvents

Zamboni's fixative:

4% paraformaldehyde and 0.2% picric acid in phosphate buffer, pH 6.9.

Immunoprecipitation buffer:

50 mM Tris-HCl, pH 7.4, 150 mM NaCl, 5 mM EDTA, 10 mM NaF, 10 mM disodium pyrophosphate, 1% Nonidet P-40, 0.5% sodium deoxycholate, 0.1% SDS, and the following proteinase inhibitors: 0.2 mM phenylmethyl-sulfonyl fluoride, 10 µg/ml leupeptin, 1 µg/ml pepstatin A, 1 µg/ml aprotinin, and 10 µg/ml bacitracin. (Proteinase inhibitors were added prior to use)

SDS-sample buffer:

62.5 mM Tris-HCl, pH 6.8, 2% SDS, 20% glycerol, 0.005% bromphenol blue, 100 mM DL-dithiotreitol. (Dithiotreitol was added prior to use)

1 x TPBS (Tris/phosphate-buffered saline):

10 mM Tris, 10 mM phosphate buffer, 137 mM NaCl and 0.05% thimerosal, pH 7.4.

In situ hybridization buffer:

600 mM NaCl, 10 mM TrisCl pH 7.5, 1 mM di-Na-EDTA, 0.05% (w/v) tRNA, 1 x Denhardt's solution, 50% dextransulfate, 100 µg/ml sonicated salmon sperm DNA, 50% formamide, 20 mM DTT.

Buffer 1:

100 mM maleic acid, 150 mM NaCl, pH 7.5

Buffer 2:

100 mM Tris, 100 mM NaCl, 50 mM $MgCl_2$, pH 9.4, 0.05% Triton-X100.

RNase-buffer:

10 mM TrisCl, pH 8.0, 0.5 M NaCl, 1 mM EDTA, 40 µg/ml RNase A, 1 unit/ml RNase T1.

SSC (sodium chloride/sodium citrate), 20x:

3.0 M NaCl, 0.3 M Na_3citrate.$2H_2O$, PH7.0

3 Methods

3.1 Gene subclone

In the following experiments, the related PCR, ligation, transformation by calcium chloride or electroporation, plasmid preparation, purification and identification were carried out using a standard molecular clone protocol or according to manufacturer's instruction.

3.2 Plasmid sequencing

To confirm the plasmid constructions, all subclones were sequenced using the Thermo Sequenase fluorescent labelled primer cycle sequencing kit according to the manufacturer's protocol.

3.3 Co-immunoprecipitation

The pCMV-Myc-M6a plasmid was constructed by the subcloning of M6a gene (pCMV-SPORT6-M6a) into pCMV-Myc expression vector by PCR. In 100-mm dish, HEK293 cells stably expressing HA-MOR1 (in method 3.7) were transiently transfected with pCMV-Myc-M6a plasmid using Lipofectamine 2000 according to the manufacturer's protocol. 48 h after transfection, cells were incubated in OPTIMEM I medium for at least 30 min before incubating with 6 ml cross-linking buffer (PBS containing 10 mM Hepes (pH 7.4) and 2 mM DSP) for 20-30 min at room temperature. Subsequently, cells were lysed in 1 ml of ice-cold immunoprecipitation buffer at 4°C for 45 min with gentle shaking. After centrifugation at 40,000 x g for 1 h, the supernatant was collected. The receptor proteins were then immunoprecipitated with 100 μl of protein A agarose beads preloaded with 10 μg anti-HA antibodies at 4^{o}C for over night. Beads were washed five times with the immunoprecipitation buffer, and immunoprecipitates were eluted from the beads with 100 μl of SDS-sample buffer at 60°C for 20 min. The receptor or M6a protein was separated with regular 8% or 12% SDS-polyacrylamide gel electrophoresis. After electrophoresis, proteins were transferred from the gel to nitrocellulose membrane by electroblotting. Then membranes were incubated with either mouse monoclonal anti-Myc or affinity-purified rabbit anti-HA antibody at a concentration of 1 μg/ml for over night at 4°C. Immunoreactive bands were visualized by detection using an enhanced chemiluminescence detection system.

3.4 BRET assay

3.4.1 Principle

Bioluminescence resonance energy transfer (BRET) technology is a proximity assay based on non-radiative transfer of energy between a bioluminescent donor (Renilla luciferase, Rluc) and a fluorescent acceptor (Green Fluorescent Protein, GFP) that allows real time monitoring of protein-protein interaction in living cells. In our experiments, an

advanced BRET (also termed BRET^2, BioSignal Packard BioScience) was used. For BRET principle, see Figure 3.1.

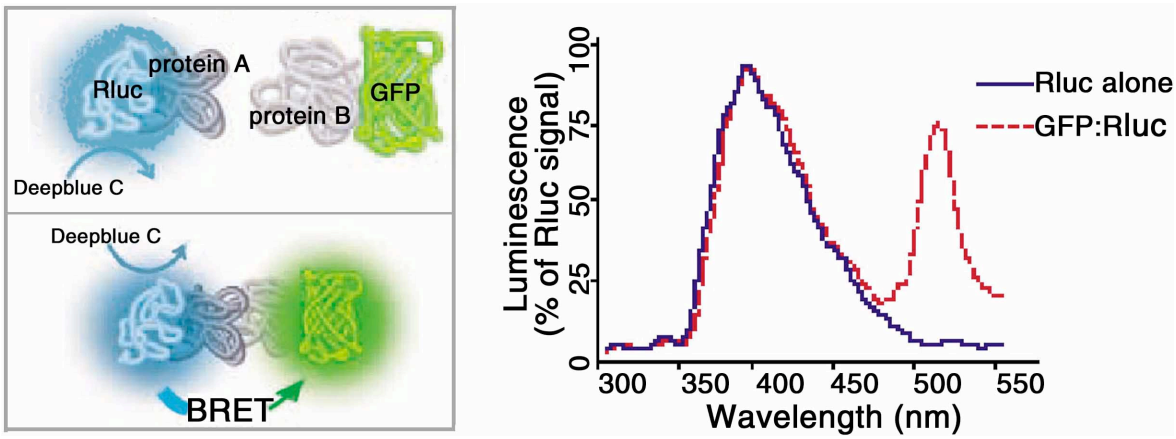

Figure 3.1. BRET principle. Resonance Energy Transfer occurs when part of the energy from DeepBlueC (DBC)-bound Rluc is transferred to GFP, which in turn, emits green light. If Rluc and GFP are not in close proximity (upper left panel), energy is not efficiently transferred and only the blue light emitted by the Rluc/DBC reaction is detected. When Rluc and GFP are brought into close proximity (lower left panel), by means of a specific biological interaction between protein A and protein B (fused to Rluc and GFP, respectively), energy is efficiently transferred from DBC-bound Rluc to GFP resulting in the production of green light. The BRET signal is determined by measuring the ratio of green light (515nm) over blue light (410nm) (right panel).

3.4.2 Donor and acceptor plasmid construction and co-transfection

The coding sequences without a stop codon of MOR1 and its truncations, or MOR1B, DOR1, sst2A, mGluR1a and mGluR5a were amplified by PCR, and then were ligated into humanized pRluc-N_3 expression vectors to produce BRET donors. The coding sequences of M6a and its truncation, or M6b and DM20 were amplified by PCR, and then were subcloned into humanized pGFP-C_3 expression vectors to produce BRET acceptors.

The day prior to transfection, HEK293 cells were seeded in a 24-well plate. Cells were 90-95% confluent before transfection. Cells were co-transfected with donor and acceptor plasmids using Lipofectamine 2000 according to the manufacturer's protocol.

3.4.3 BRET detection

45 h post-transfection, cells were detached with PBS/0.5mM EDTA and resuspended in PBS containing 0.1% glucose and 2µg/ml aprotinin. Cells were then transferred to 96-well microplates at a density of about 1 x 10^5 cells/well. Deep Blue C was added at a final concentration of 5 µM, and readings were collected immediately using the Fusion™ Universal Microplate Analyzer that allows the sequential integration of the signals detected in the 330-490 nm and 485-545 nm windows using filters with the appropriate band pass. The following settings were used: Mode: dual wavelength; Read length: 1 second per wavelength; PMT: 1100 volts; Gain: 100; Filter pair: 410/80 nm (Rluc emission) and 515/30 nm (GFP emission). The values were corrected by subtracting background signal

detected in untransfected cells. The BRET signal was determined by calculating the ratio of the light emitted by the GFP over the light emitted by the Rluc as shown in the following formula.

$$\text{BRET signal} = \frac{\text{(emission at 515 nm)-(background emission at 515 nm)}}{\text{(emission at 410 nm)-(background emission at 410 nm)}}$$

3.5 Immunocytochemistry

Cells were grown on poly-L-lysine-treated coverslips for overnight. After treatment as indicated in text or without treatment, cells were fixed with Zamboni's fixative for 40 min at RT. Then cells were washed several times with TPBS. Specimens were then incubated for 3 min in 50% and 100% methanol respectively to permeabilize membrane. Subsequently specimens were washed several times in TPBS and then preincubated with TPBS containing 3% normal goat serum for 2 h at room temperature. Then cells were incubated with mouse anti-Myc antibody and/or rabbit anti-HA antibody at a concentration of 0.5 □g/ml in TPBS containing 1% normal goat serum overnight. Bound primary antibodies were detected with relative cyanine 2.18 (Cy2)- and/or 3.18 (Cy3)-conjugated second antibodies (1:400 or 3.75 □g/ml). Cells were then permanently mounted in DPX. Specimens were examined using a Leica TCS-NT laser-scanning confocal microscope, equipped with a krypton/argon laser. Cyanine 2.18 was imaged with 488 nm excitation and 530 nm emission filters, and cyanine 3.18 was imaged with 568 nm excitation and 570-630 nm band pass emission filters.

To observe the trafficking of surface MOR1 and/or M6a, cells were firstly surface-labeled with rabbit anti-HA and/or rat anti-M6a antibody at a final concentration of 1.0 μg/ml at 4°C for 1.5 h. Cells were subsequently treated as shown in text, and then fixed normally. The bound primary antibodies were detected as described above.

3.6 In situ hybridization

3.6.1 Brain section preparation

Male Wistar rats aged 8 weeks (Dimed, Schonwalde, Germany) were housed under controlled laboratory conditions (12 h light/dark cycle, temperature 20 ± 2°C, humidity 50−60%). For all procedures, ethical approval was obtained according to the requirements of the German National Act on the Use of Experimental Animals.

Animals were killed by chloral hydrate (1 g/kg body weight, i.p.). The removed brains were frozen in isopentane at –30°C to –40°C and cut in a cryostat (15 μm). Sections were mounted on adhesive slides (Superfrost), and stored at –70°C. Before hybridization, frozen slides were air-dried, fixed in 4% paraformaldehyde dissolved in phosphate-buffered saline (PBS) at 4°C for 1 h. After washing in PBS, the slides were treated for 10 min with 0.4% Triton-X 100 in PBS. Next, slides were rinsed in distilled water, and then treated for 10 min with 1.5% tri-ethanolamine/PBS, containing 0.25% acetic anhydride

(Sigma). Finally, slides were washed in distilled water and dehydrated in 50% and 70% iso-propanol, air dried, and stored at -20°C.

3.6.2 Synthesis of RNA probes for in situ hybridization

The previously characterized probe of rat MOR1 (Stumm et al., 2004) was kindly provided by Dr. Ralf Stumm. To generate the probes of M6a, M6b and DM20, their coding sequences were amplified by PCR, and then subcloned into the pGEM-T easy vector. For in-vitro-transcription, the plasmids were linearized with restriction endonucleases and purified using the MinElute Reaction Cleanup Kit. Synthesis of [^{35}S]-labelled probes was done in the presence of 100-150 pmol [^{35}S]-labeled UTP in a total reaction volume of 10 µl. The reaction mix further contained 1 µg linearized plasmid-DNA, 10 mM dithiothreitol (DTT), 0.5 mM unlabeled nucleotides (without UTP). For digoxigenin-labeled probes, a 1 mM nucleotide mixture containing 0.35 mM digoxigenin-11-UTP (Roche, Mannheim) was used. The transcription was performed with SP6 or T7 polymerase. To improve permeability, the probes were subjected to partial alkaline hydrolysis, which produces short probes (final size: 200-300 nucleotides). The labeled probes were finally purified with Micro Bio-Spin columns P-30.

3.6.3 Hybridization and washing

Radioactive probes were diluted at 50,000 dpm/µl in in situ hybridization buffer. To each dried slide containing two sections, 45-µl hybridization mixture was added. Hybridization was performed overnight at 60°C in a humid chamber containing 50% formamide. Post-hybridization procedures consisted of a sequence of washes with decreasing salt concentration. Briefly, the slides were washed in 2 x SSC and 1 x SSC before a 30 min treatment in RNase-buffer at 37°C. Then the slides were extensively washed in 1 x and 0.2 x SSC at room temperature and subsequently in 0.2 x SSC for 60 min at 60°C. After washing in water, the tissue was dehydrated in 50% and 70% isopropanol.

3.6.4 Detection of signals

A sheet of x-ray film (β-max, Amersham) was laid over the sections and exposed for 1 to 3 days. For high-power bright- and dark-field microscopic analyses, autoradiographic detection of ^{35}S was performed by coating the slides with 50% NTB-2 nuclear emulsion (Eastman Kodak, Rochester, NY). Exposure time for autoradiography varied between 1 and 3 weeks. After emulsion coating, sections were stained with 0.5% cresyl violet (Fluka, NeuUlm) in 60 mM sodium acetate and 340 mM acetic acid. In each experiment, the comparison of slides hybridized with sense and antisense probes allowed to decide if a particular signal was due to specific hybridization or was background.

3.6.5 Double in situ hybridization histochemistry

The visualization of two different mRNA transcripts in the same tissue section was performed by combining radioactive and nonradioactive in situ hybridization as described

(Stumm et al., 2002). Digoxigenin-labeled riboprobes were diluted in radioactive hybridization solution to 1 µg/ml, hybridized, and washed as above. To detect nonradioactive hybrids, slides were equilibrated in buffer 1 containing 0.05% Triton-X100. After blocking for 1 h in blocking buffer (buffer 1 containing 2% blocking reagent (Roche) and 0.05% Triton-X100), alkaline phosphatase conjugated anti-DIG Fab fragments (Roche) were applied overnight at a concentration of 0.5 unit/ml blocking buffer. Next, slides were washed twice for 15 min in buffer 1 and equilibrated in buffer 2 prior to a chromogenic reaction using 0.2 mM 5-bromo-4-chloro-3-indolyl phosphate and 0.2 mM nitroblue tetrazolium salt (Roche). The reactions (5h for DM20, 22h for M6a and M6b) were stopped by washing the slides in distilled water. The slides were then dehydrated, and the ^{35}S-labeled probes were detected by 50% K5 photo-emulsion (Ilford).

3.7 Cell culture and generation of stable cell lines

HEK293 cells were maintained in DMEM supplemented with 10% FCS in a humidified incubator with an atmosphere containing 10% CO_2, at 37°C.

MOR1 and DOR1 were tagged at their NH2 terminus with HA epitope tag using PCR and then subcloned into pEAK10 expression vector. M6a was tagged at its NH2 terminus with Myc epitope tag using PCR and then subcloned into pcDAN3.1 expression vector. According to manufacturer's protocol, HEK293 cells were first transfected with pEAK10-HA-MOR1, pEAK10-HA-DOR1 or pcDAN3.1-Myc-M6a plasmid using the Lipofectamine 2000. Stable transfectants were selected in the presence of 1.25 µg/ml puromycin or 400 µg/ml hygromycin B. To generate the cell line co-expressing HA-MOR1 and Myc-M6a, cells stably expressing HA-MOR1 were subjected to a second round of transfection with pcDAN3.1-Myc-M6a plasmid as above, and stable transfectants were selected in the presence of 1.25 µg/ml puromycin and 400 µg/ml hygromycin B. Stably transfected multi-clones in similar receptor density identified by radioligand binding assay and ELISA quantitative assay were used for further studies. Receptor and/or M6a expression were monitored using radioligand binding assay, western blot analysis, and/or confocal microscopy.

3.8 Calcium-phosphate-mediated transfection of HEK293 cells

24 h before transfection, harvest exponentially growing cells by trypsinization and replate them at a density of about 2 x 10^5 cells per well in 12-well plates in 1ml complete growth medium (DMEM with 10% FCS). Incubate the cultures for 20-24 h at 37°C in a humidified incubator with an atmosphere containing of 10% CO_2. Change medium 1 h before transfection. For a transfection in one well of 12-well plate, prepare the calcium phosphate-DNA coprecipitate as follows: Combine suitable H_2O, 1.4 µg of plasmid DNA and 5 µl of 2.5 M $CaCl_2$ to a final volume of 50 µl. Mix 1 volume of this 2 x calcium-DNA solution with an equal volume of 2 x HEPES-buffered saline (280 mM NaCl, 50 mM HEPES, 1.5 mM Na_2HPO_4, pH 7.05). Quickly mix the ingredients and allow the solution to stand for 20 min at RT. Immediately transfer the calcium phosphate-DNA suspension

into the medium above the cell monolayer. Rock the plate gently to mix the medium, and incubate them for 16-18 h at 35°C in a humidified incubator with an atmosphere containing of 3% CO_2. Change the medium with complete growth medium and return the cells to the incubator (10% CO_2, 37°C) for 1-2 days.

3.9 Radioligand binding assay

The binding characteristics of the μ-opioid receptor were determined by saturation binding assays on membranes prepared from stably transfected HEK293 cells expressing HA-MOR1 with and without Myc-M6a. Dissociation constant (K_D) and number of [^{3}H]DAMGO binding sites (B_{max}) were calculated by Scatchard analysis using at least seven concentrations of radioligand in a range from 0.25 to 10 nM as previously described (Koch et al., 2003). Nonspecific binding was determined as radioactivity bound in the presence of 1 μM unlabeled DAMGO.

Radioligand binding assay is sensitive to calculate the receptor amount. The number of [^{3}H]DAMGO binding sites in membrane binding assay reflects the amount of total μ-opioid receptor, which can be used to evaluate the receptor down-regulation.

3.10 Quantitative analysis of receptor internalization and recycling by ELISA

To estimate receptor internalization, cells were seeded at a density of 5.0 x 10^4 per well and grown onto poly-L-lysine-treated 96-well plate overnight. Surface HA-MOR1 receptors were specifically labeled with anti-HA antibody (1 μg/ml) in OPTIMEM I at 4°C for 1.5 h. Cells were then incubated with or without 1 μM DAMGO at 37°C for 30 min. Subsequently, cells were fixed and incubated with peroxidase-conjugated anti rabbit antibody (1:1000) for 2 h at RT. Plates were developed with 50 μl ABTS solution per well. Colour reaction was analyzed at 405 nm using an Expert Plus Microplate Reader during 15-25 min in real time. Endocytosed receptors were evaluated as the loss of surface-labeled receptors. To measure receptor recycling, cells were first exposed to 10 μM etorphine for 2 h to drive agonist-induced receptor internalization to a steady-state level, then rinsed with OPTIMEM I, and subsequently incubated at 37°C for 30 and 60 min in the presence of 10 μM naloxone to block residual agonist-stimulated receptor internalization. Cells were then chilled with 4°C PBS to stop trafficking, and receptors were surface-labeled with anti HA antibody (1μg/ ml) at 4°C for 2h. Un-binding antibodies were washed out, cells were fixed and surface receptors were detected as described above. Recycling rate was estimated as a percent of recovered surface receptors to endocytosed receptors.

3.11 Cloning of M6a cDNA by RT-PCR

Total RNA of HEK293 cells was extracted according to manufacturer's instruction. Reverse transcription: Reverse transcription mix consisted of 1μg total RNA, 0.5μM oligo(dT)15, 0.5mM dNTPs, 100 units of reverse transcriptase and 2μl of 5x reaction buffer in a total 10 μl reaction volume. Simply, total RNA (1μg in 5μl) was firstly denatured at 65°C for 10 min, cooled on ice and then mixed with the other reaction

solution (5µl). The reaction mixture (10µl) was incubated at 42°C for 1 h, followed by 75°C for 15 min, and then frozen at -20°C. For contamination controls, water was used instead of total RNA. The total cDNA was used as template to amplify M6a coding sequence by standard PCR using the following primers. Forward primer 5′-GAA GAA GAA TTC CC ATG GAA GAG AAT ATG G-3′ introduced EcoR I restriction site, and reverse primer 5′-AGA GAA GGT ACC TTA TGT GTA CGC ATT GAG-3′ introduced Kpn I restriction site. PCR products were subsequently subcloned into humanized pGFP-C_3 vector for both sequencing and BRET assay.

3.12 Transferrin trafficking

A previously described "pulse-chase" assay (Tsao and von Zastrow, 2000; Tulipano et al., 2004) was used to estimate the degree to which a "pulse" of internalized opioid receptor and M6a was accessible to a subsequent "chase" of endocytosed transferrin. Stable HA-DOR1 cells transiently transfected with pCMV-Myc-M6a plasmid using calcium phosphate precipitation method, and cells stably co-expressing HA-MOR1 and Myc-M6a were used. Cells were grown on poly-L-lysine coated coverslip. Receptor and M6a were surface-labeled with rabbit anti-HA and rat anti-M6a antibody (1 µg/ml) at 4°C for 1.5 h. In the first set of experiments, cells were simultaneously incubated with 10 µM DAMGO (or DPDPE) and 5 µg/ml Alexa Fluor 488-conjugated transferrin (Molecular Probes) for 30 min at 37°C. In a second set of experiments, cells were first incubated with 10 µM DAMGO (or DPDPE) for 30 min at 37°C to drive the internalization of antibody-labeled receptor and M6a, then rinsed three times with calcium, magnesium-free PBS with 1.6% EDTA. Subsequently, cells were rewarmed at 37°C for 20 min in agonist-free media containing 5 µg/ml Alexa Fluor 488-conjugated transferrin, conditions which label both early and recycling endosomes (Dunn et al., 1989). Cells were then fixed, permeabilized. Subsequently, antibody-labeled receptor and M6a were detected using a mixture of cyanine 5.18-conjugated anti-rabbit and cyanine 3.18-conjugated anti-rat second antibodies. Alexa Fluor 488 was imaged with 488 nm excitation and 530 nm emission filters, cyanine 3.18 was imaged with 568 nm excitation and 570-630 nm bandpass emission filters, and cyanine 5.18 was imaged with 647 nm excitation and 665 nm long pass emission filters.

3.13 Primary neuronal cell culture, transfection and immunostaining

Neuronal cultures were prepared from rat cortex of embryonic day 17 embryos (E17). All animal procedures were approved by Otto-von-Guericke-University Magdeburg. Using 12-well plate with poly-D-lysine-coated coverslips, seed primary cortical cells at 4 x 10^5 cells/well in 1.5 ml Neurobasal medium supplemented with 2% B-27, 0.5 mM Glutamine, 100 units/ml penicillin and 100 µg/ml streptomycin. Cells were cultured at 37°C and 5% CO_2 in a humidified incubator. Remove 1/2 volume of the medium on day 3 after seeding and replace with fresh medium.

The cording region of MOR1 was amplified using PCR, and then subcloned into pCMV-HA expression vector, which generates amino-terminally HA-tagged MOR1. The

cording region of M6a was amplified using PCR, and then subcloned into pcDNA3.1 expression vector. These constructs and the construct of amino-terminally Myc-tagged M6a (pCMV-Myc-M6a) described in method 3.3 were used for transient transfection.

Primary neuronal cultures on day 4 were transfected with MOR1 and/or M6a plasmid using Lipofectamine 2000 following the manufacturer's instruction. 40 hours after transfection, cells were treated and subsequently fixed with Zamboni's fixative. To observe the trafficking of surface receptor and M6a, cells were surface-labeled by specific anti-HA antibody and/or anti-M6a antibody (2 μg/ml) at 4°C for 1 hour. Subsequently cells were treated or not treated as shown in text, and then fixed. Distribution of expressed interesting proteins was detected by immunocytochemistry as described above.

3.14 Determination of receptor desensitization

2.5 x 10^5 cells per well were seeded in poly-L-lysine-coated 24-well plate overnight. Cells were then exposed to agonist or agonist plus 50 μM monensin for different period. For the measurement of cAMP accumulation, cells were first washed one time with 0.5 ml serum-free RPMI medium. Immediately, medium was removed and replaced by 0.25 ml serum-free RPMI medium containing 25 μM forskolin with or without agonist. The cells were incubated at 37°C for 15 min. After one time wash with cold PBS, the intracellular cAMP was extracted immediately with 0.5 ml of cold HCl/ethanol (1 volume of 1 N HCl/100 volumes of ethanol, stored at -20°C). The supernatant was transferred into a 1.5 ml tube, and then evaporated by vacuum at 30°C. The residue of cAMP was frozen at -20°C or for further examination. The extracted cAMP content was determined using a commercially available cyclic AMP (^{3}H) assay system.

For the determination of receptor desensitization in primary neuronal cells, fresh prepared cortical cells (E17) were transfected with MOR1 and/or M6a plasmid using Rat Neuron Nucleofector Solution according to the manufacturer's protocol. After transfection, 6.0 x 10^5 cells per well were seeded into poly-D-lysine-coated 24-well plate, and grew in DMEM medium supplemented with 10% FCS, 100 U/ml penicillin and 100 μg/ml streptomycin. After overnight, carefully replace the medium with Neurobasal media supplemented with 2% B-27, 0.5 mM Glutamine, 100 U/ml penicillin, 100 μg/ml streptomycin. 4-5 days after transfection, cells were then exposed to 10 μM DAMGO for 0, 1 and 4 h. Cells were then washed one time with 0.5 ml serum-free DMEM medium. Subsequently, medium was removed and replaced by 0.25 ml serum-free DMEM medium containing 5 μM forskolin in the presence or absence of 10 μM DAMGO. The cells were incubated at 37°C for 10 min. The cAMP accumulation was determined as described above.

3.15 Data analysis

Statistic significant difference was analyzed by one-way ANOVA followed by bonferroni test using GraphPad Prism 4.0 software. All graphs in the following were drawed by the same software.

4 Results

4.1 Co-immunoprecipitation of MOR1 and M6a

To confirm whether the strong interaction of MOR1 with M6a in yeast also occurs in mammalian cells, we carried out co-immunoprecipitation experiments in HEK293 cell co-transfected with epitope tagged MOR1 and M6a. MOR1 was labeled with the HA epitope (HA-MOR1), and M6a with the Myc epitope (Myc-M6a) both at the amino terminus.

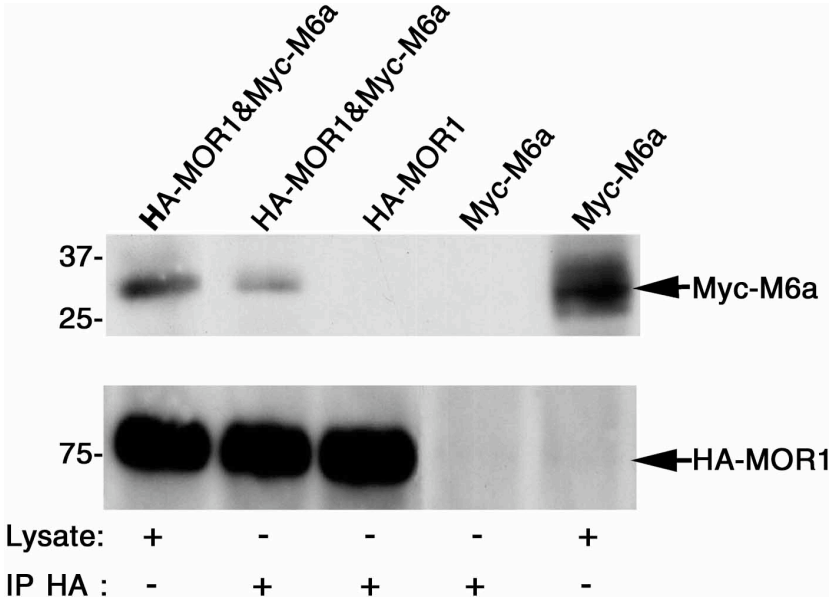

Figure 4.1. Co-immunoprecipitation of HA-MOR1 with Myc-M6a. Cell lysate proteins from cells co-expressing HA-MOR1 and Myc-M6a were extracted and either immunoblotted directly (lane 1, lysate) or immunoprecipitated using anti-HA antibodies (lane 2, IP HA). Cell lysate proteins from cells expressing HA-MOR1 alone were extracted and immunoprecipitated using anti-HA antibodies (lane 3, IP HA). Lysate proteins from cells transiently over-expressing Myc-M6a alone were extracted and either immunoblotted directly (lane 5, lysate) or immunoprecipitated using anti-HA antibodies (lane 4, IP HA). The resulting immunoprecipitates were electrophoretically separated, transferred to nitrocellulose membrane and detected with anti-Myc or anti-HA antibodies. The mobility of molecular mass standards (in kDa) is indicated to the left. Arrows point to M6a or MOR1. Two additional experiments gave similar results.

As shown in Figure 4.1, expression of HA-MOR1 and Myc-M6a was examined by directly immunoblotting lysates from these cells with specific antibodies against HA and Myc tag, respectively (lane 1 and 5, lysate). For co-immunoprecipitation, receptors were precipitated from the lysates of cells expressing HA-MOR1 with and without Myc-M6a using anti-HA antibodies. The resulting precipitates were immunoblotted with antibodies directed against Myc epitope tag. As shown in Figure 4.1 (lane 2, IP HA), Myc-M6a migrating at about 30 kDa was detected in immunoprecipitates from cells co-expressing HA-MOR1 and Myc-M6a, suggesting that MOR1 is physically associated with M6a in

vivo. In immunoprecipitates from HA-MOR1 or Myc-M6a expressing control cells, no Myc-M6a was detected (Figure 4.1, lane 3 and 4, IP HA, respectively), indicating the specific interaction between MOR1 and M6a.

4.2 Analysis of protein-protein interaction by BRET

Detergent solubilization of cells during co-immunoprecipitation studies could promote artificial aggregation of hydrophobic proteins such as transmembraneous proteins. We therefore analyzed protein-protein interaction in living HEK293 cells using a biophysical method, BRET. This technique is a proximity assay based on non-radiative transfer of energy between a bioluminescent donor (Rluc) and a fluorescent acceptor (GFP) that allows real time monitoring of protein-protein interaction in living cells. M6a is a member of the proteolipid protein (PLP)/DM20 family, and shows high homology with M6b and DM20 (Yan et al., 1993). We therefore investigate whether MOR1 also interacts with M6b and DM20.

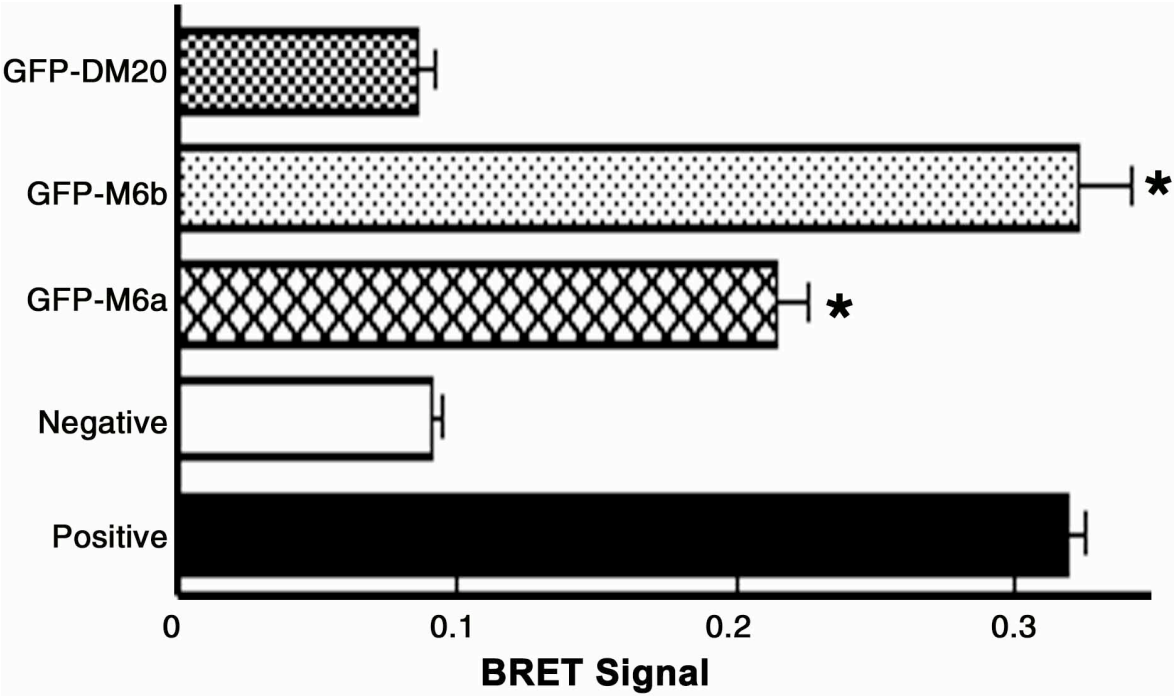

Figure 4.2. The interaction of MOR1 with members of PLP/DM20 family. HEK293 cells were transiently cotransfected with MOR1-Rluc in the combination with GFP (negative control), GFP-M6a, GFP-M6b or GFP-DM20. A treatment of GFP-Rluc fusion protein was used as positive control. Cells were harvested 45 h post-transfection, and were incubated in the BRET buffer for 30 min. The energy transfer was initiated by addition of 5 μM Deep Blue C, and BRET signal was assessed in a Fusion™ Universal Microplate Analyzer as described under "Methods". The results represent mean ± SEM of 3-5 independent experiments performed in duplicate. Asterisk indicates an extremely significant difference ($P<0.001$, compared with negative control) analyzed by one-way ANOVA followed by Bonferroni test.

In the BRET assay, the fusion construct linking Rluc to the MOR1 carboxyl terminus was co-transfected in combination with the fusion construct linking GFP to the amino

terminus of M6a, M6b or DM20 in HEK293 cells. 45 hours after transient co-transfection, the transfer of energy between the two partners was assessed following the addition of Deep Blue C. In the presence of oxygen, Rluc catalyzes the transformation of Deep Blue C into coelenteramide with concomitant light emission peaking at 395 nm (blue light) that can excite GFP, which in turn, re-emits fluorescence with a peak at 510 nm but only when the two partners are within the BRET-permissive distance (<10nm). The BRET signal is determined by calculating the ratio of the light emitted by the GFP fusion protein over the light emitted by the Rluc fusion protein.

As shown in Figure 4.2, a high BRET signal was obtained with the GFP-Rluc fusion protein in positive control (Positive), whereas a very low BRET signal was obtained when MOR1-Rluc was co-expressed with GFP in negative control (Negative). A significantly high BRET signal was obtained in cells co-expressing MOR1-Rluc with GFP-M6a or GFP-M6b, but not with GFP-DM20. This finding indicated that a specific constitutive interaction of MOR1 with M6a or M6b occurs in living cells.

4.3 Agonist-mediated subcellular distribution of MOR1-M6a/M6b

In baby-hamster kidney-cell line (BHK cells), cultured oligodendrocytes and transgenic mice, previous research showed that over-expression of the proteolipid protein (PLP) induces the abnormal accumulation of PLP, cholesterol, and other lipid raft components in the late endosomal/lysosomal compartment (Simons et al., 2002). Since M6a and M6b show high homology with PLP (Yan et al., 1993), it is interesting to analyze whether over-expression of M6a or M6b influences agonist-mediated subcellular distribution of the μ-opioid receptor (MOR1).

In HEK293 cells stably co-expressing HA-MOR1 and Myc-M6a, M6a was localized both at the plasma membrane and in the cytoplasm. MOR1 was predominantly distributed at the plasma membrane, and was shown to co-localize with M6a both at the plasma membrane and in the cytoplasm (Figure 4.3A, control). In MOR1-M6b co-expressing cells, M6b was mainly localized at the plasma membrane, and was shown to co-localize with MOR1 (Figure 4.3B, control).

After treatment of MOR1 with agonist together with the recycling blocker monensin, MOR1 and M6a were detected mainly in cytoplasm and showed strict co-localization (Figure 4.3A, lower panel). In remarkable contrast, there was no distinct change in M6b subcellular distribution and no major co-localization between MOR1 and M6b after MOR1 internalization (Figure 4.3B, lower panel) though the interaction between MOR1 and M6b was stronger than that of MOR1 and M6a (Figure 4.2).

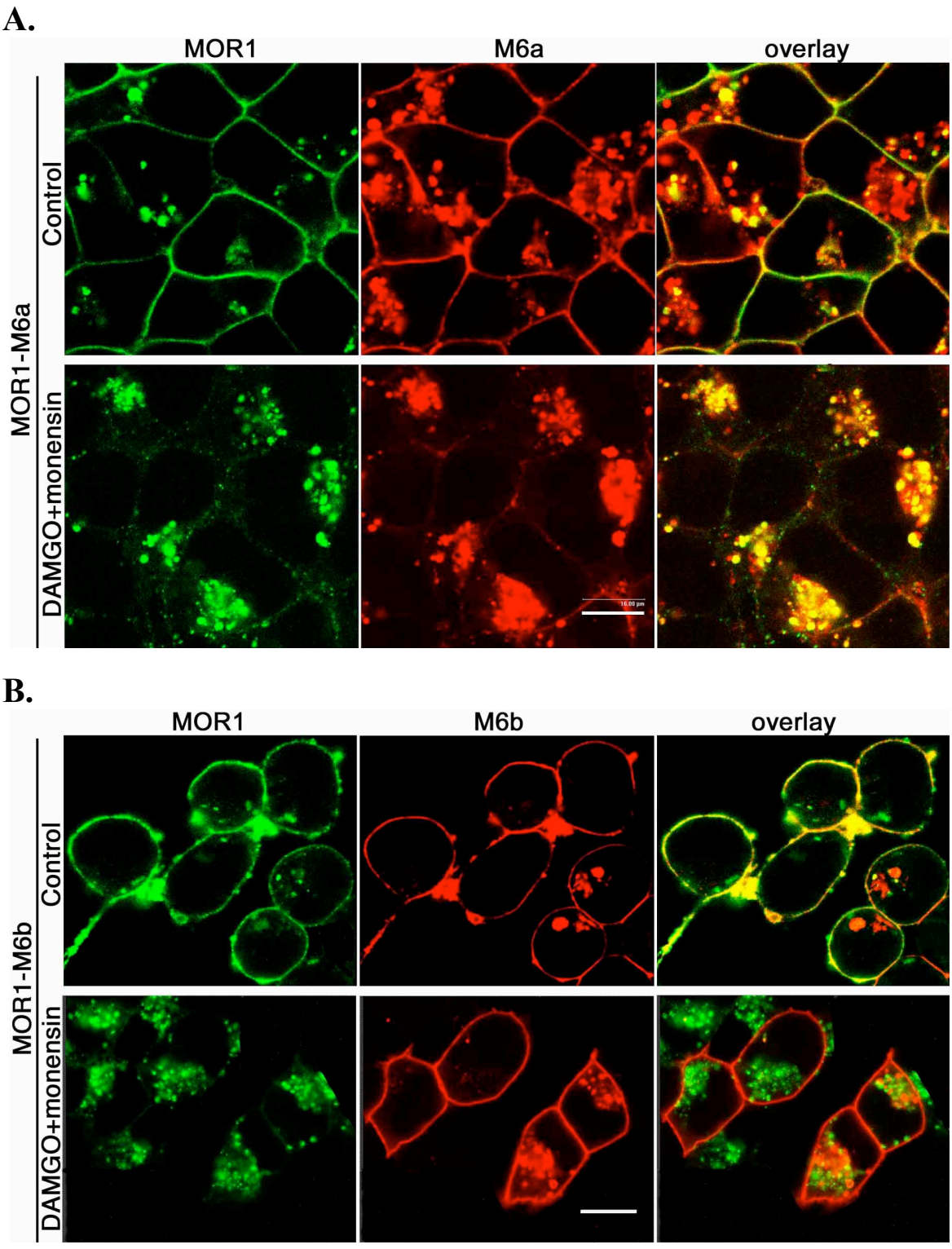

Figure 4.3. Agonist-mediated subcellular distribution of HA-MOR1 with Myc-M6a/M6b. HEK293 cells stably expressing HA-MOR1 were transiently transfected with Myc-M6b plasmid. Three days after transfection, cells were exposed to 1 μM DAMGO and 50 μM monensin for 2 hours at 37°C. Simultaneously, cells stably co-expressing HA-MOR1 and Myc-M6a were treated in the same way. Cells were subsequently fixed, and the receptor and M6a/M6b were visualized by confocal microscopy as described under "Methods". Representative images from two independent experiments are shown. Scale bar, 16 μm.

This finding that MOR1 and M6a co-localized and co-internalized in the presence of μ-opioid receptor agonist suggested that M6a might function as a scaffold, anchoring or adaptor protein in receptor trafficking. The absence of co-internalization of MOR1 and M6b implied that M6b might be involved in other steps of MOR1 regulation. Since our interest is the intracellular trafficking of the μ-opioid receptor, we first focus on the analysis of the possible role of M6a in MOR1 regulation.

4.4 Analysis of MOR1-M6a interacting domains by BRET

To estimate the binding domains of MOR1 and M6a, a series of truncation mutants of MOR1 and M6a were generated by PCR mutagenesis. The interactions between these truncations and full length of MOR1 or M6a were analyzed by BRET assay.

As depicted in Figure 4.4B, the carboxyl terminal tails (340-398aa) of MOR1 failed to interact with the full length of M6a, whereas the MOR1 truncation (1-339aa), like full length MOR1 (1-398aa), interacted strongly with the full length of M6a. This demonstrated that MOR1 carboxyl terminal tail, which plays a key role in the regulation of MOR1 signaling, is not the direct interacting domain for MOR1-M6a interaction. For the interaction between MOR1 truncations (1-124aa, 105-258aa or 258-339aa) and the full length of M6a, there was no significant BRET signal. Furthermore, we found that the truncation (186-303aa) of MOR1 plays an important role in MOR1-M6a interaction because only this short truncation can interact with the full length of M6a.

As shown in Figure 4.4C, according to BRET signals, the M6a truncation (108-278aa) interacted strongly with the full length of MOR1. When the M6a mutant (108-278aa) was truncated into two parts (108-163aa and 164-278aa), both fragments failed to interact with the full length of MOR1, suggesting that the second extracellular large loop of M6a plays a major role in MOR1-M6a interaction. However, the 2nd extracellular loop (152-225aa) itself showed no interaction with the full length of MOR1 (Figure 4.4C), indicating that the 3rd and 4th transmembrane domains together with the 2nd extracellular loop, are necessary to form a MOR1 binding domain. This is in agreement with the finding that there is an interaction between the M6a truncation (129-255aa, the 3rd and 4th transmembrane domains plus the 2nd extracellular loop) and the full length of MOR1. In addition, there was also an interaction between the amino terminal truncation (1-108aa) of M6a and the full length of MOR1. This finding suggested that M6a has two binding domains, and the region of 129-255aa is the predominant binding sequence. Taken together, the transmembrane domains of MOR1 and M6a are important for their interaction.

A.

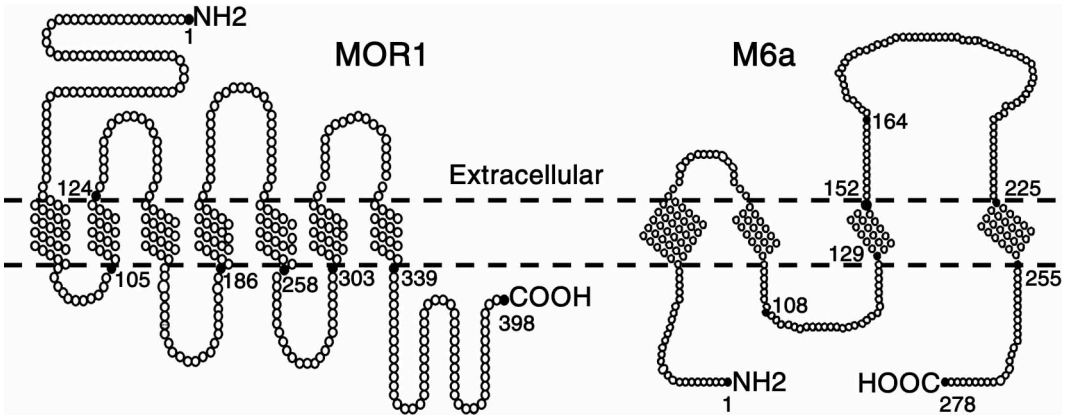
NH2
1
MOR1
M6a
Extracellular
124
105
186
258
303
339
COOH
398
164
152
225
129
255
108
NH2
1
HOOC
278

B. MOR1

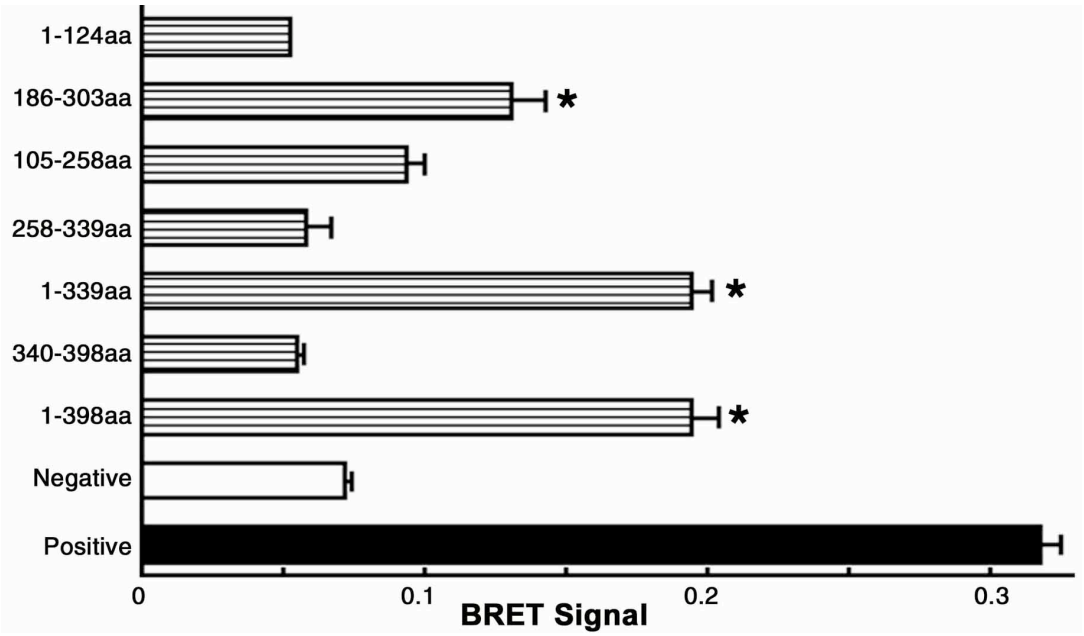
1-124aa
186-303aa
105-258aa
258-339aa
1-339aa
340-398aa
1-398aa
Negative
Positive
0
0.1
0.2
0.3
BRET Signal

C. M6a

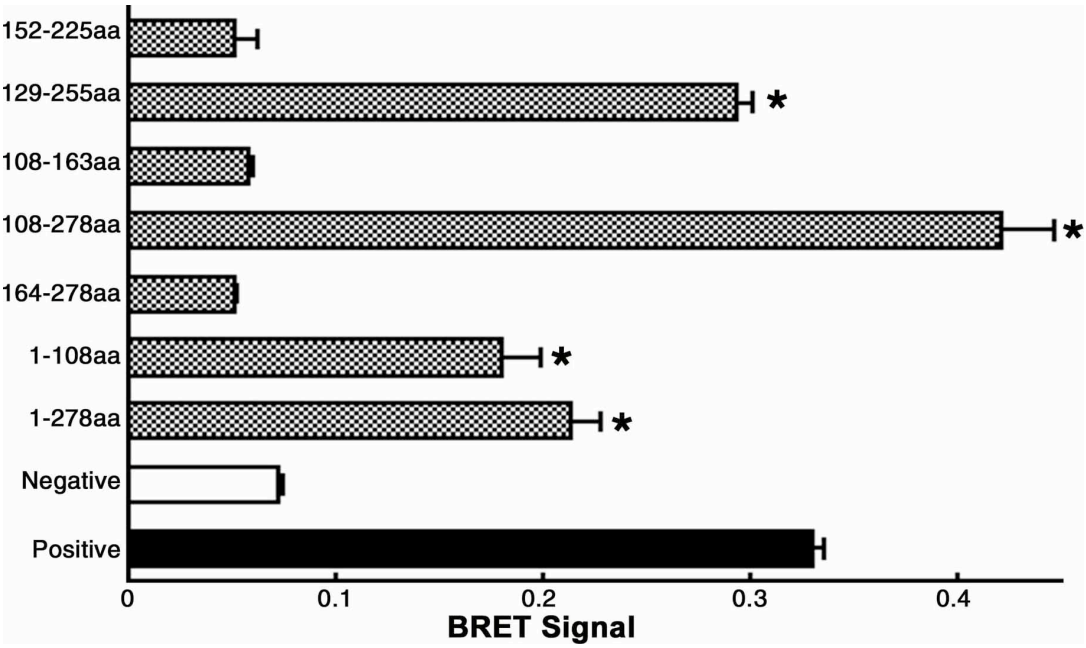
152-225aa
129-255aa
108-163aa
108-278aa
164-278aa
1-108aa
1-278aa
Negative
Positive
0
0.1
0.2
0.3
0.4
BRET Signal

Figure 4.4. Analysis of specific binding domains between MOR1 and M6a. A. Schematic structure of MOR1 and M6a, the number in the structure pattern represents the position of relative amino acid (black dot). **B.** Full length M6a interacted with different truncation mutants of MOR1. Cells were transiently cotransfected with GFP-M6a in combination with Rluc-tagged full length MOR1 (1-398aa) or its truncation mutants. MOR1-Rluc in combination with GFP was set as the negative control. Cells were harvested 45 h post-transfection. The energy transfer was detected as described under "Methods". **C.** The full length of MOR1 interacted with different truncation mutants of M6a. Cells were transiently cotransfected with MOR1-Rluc in combination with GFP (negative control), GFP-tagged full length of M6a (1-278aa) or its truncation mutants. The protein-protein interaction was detected as described above. The results represent mean ± SEM of 3-5 independent experiments performed in duplicate. Asterisk indicates an extremely significant difference ($P<0.001$, compared with negative control) analyzed by one-way ANOVA followed by Bonferroni test.

4.5 BRET-analysis of M6a interaction with various GPCRs

Next we asked, is it possible that M6a interacts with other GPCRs because of their high homology at transmembrane domains?

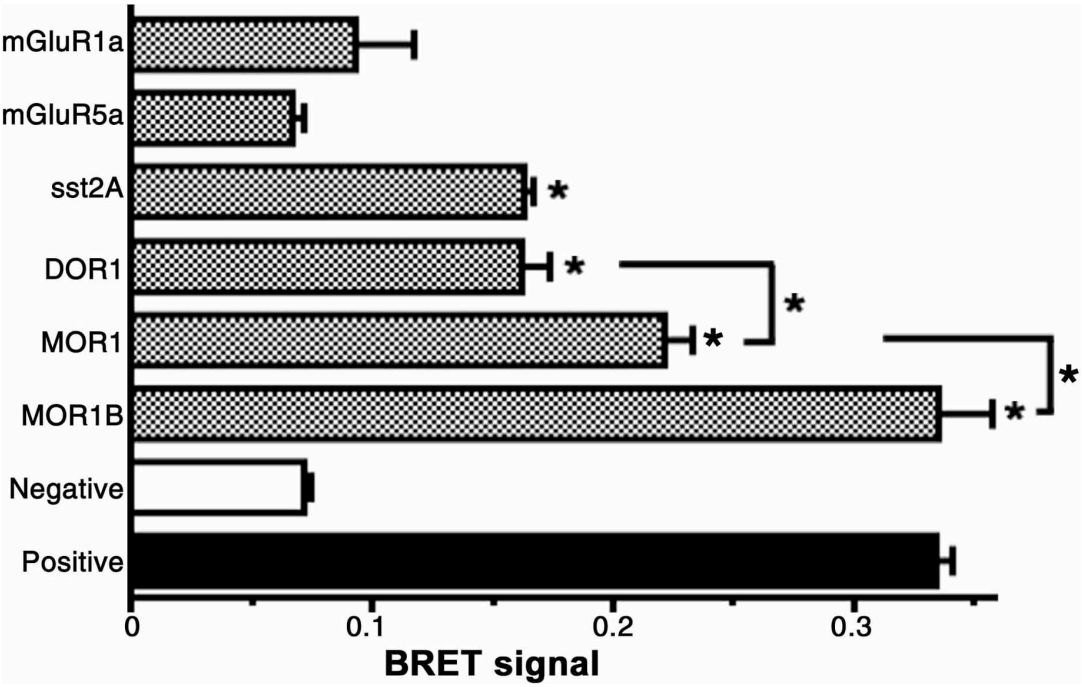

Figure 4.5. Analysis of M6a interaction with GPCRs. Cells were transiently cotransfected with GFP-M6a in combination with Rluc tagged GPCRs. MOR1-Rluc in combination with GFP was set as the negative control. Cells were harvested 45 h post-transfection. The energy transfer was detected as described under "Methods". Note that M6a interacts with μ- and δ-opioid receptors, the somatostatin receptor 2A (sst2A), but not with the metabotropic glutamate receptors (mGluR1a, 5a). Negative controls in the combination of different Rluc tagged receptors with GFP were used, and there was no significant difference between these negative controls. The results represent mean ± SEM of 3-5 independent experiments performed in duplicate. Asterisk indicates an extremely significant difference ($P<0.001$) analyzed by one-way ANOVA followed by Bonferroni test.

As shown in Figure 4.5, M6a interacted strongly with both μ-opioid receptor isoforms MOR1 and MOR1B. The stronger interaction of M6a with MOR1B as compared to MOR1, indicated that the carboxyl tail might influence the interaction though the carboxyl tail of MOR1 was not the direct interacting domain (Figure 4.4B). M6a interacted also with the δ-opioid receptor (DOR1)(Figure 4.5). In addition, M6a also interacted with the somatostatin receptor 2A (sst2A), suggesting that M6a interacts not only with opioid receptors, but also with other GPCRs. However, this does not mean that M6a is an associated protein for all GPCRs. For instance, we have not detected an interaction between M6a and metabotropic glutamate receptors (mGluR1a and 5a). This finding suggested that M6a might play a role in the regulation of certain GPCRs.

4.6 Formation of a dimer (oligomer) of MOR1 or M6a

Receptor dimerization/oligomerization is a potential mechanism for the modulation of receptor function, and involved in cell surface targeting, internalization and signaling of receptors (Salahpour et al., 2000). Dimerization/oligomerization of opioid receptors has been suggested to play a role in receptor activation and internalization (Cvejic and Devi, 1997; Jordan and Devi, 1999; George et al., 2002; He et al., 2002; Gomes et al., 2004; Waldhoer et al., 2005). The μ-opioid receptor has been shown to form the homo- and hetero-dimers in different transfected cell lines using biochemical assays (Koch et al., 2001; Gomes et al., 2000). In the present study, we investigated whether the formation of dimers (oligomers) of MOR1 can also be detected by BRET, a biophysical method. As shown in Figure 4.6A, the formation of a dimer (oligomer) of MOR1 was detected by BRET. Interestingly, the significant BRET signal of MOR1 dimerization occurred only in the combination of carboxyl-terminally Rluc- and GFP- tagged MOR1. This finding indicated that the formation of dimers occurs by the binding of MOR1carboxyl-parts.

A previous study has demonstrated that PLP and DM20 form stable dimers, which are involved in the transportation of PLP to the plasma membrane in HeLa cells (Sinoway et al., 1994). We therefore examined whether M6a also forms homo- and/or hetero-dimers (oligomers) in HEK293 cells. As shown in Figure 4.6B, M6a formed homo-dimers (or oligomers) with itself, and hetero-dimers (or oligomers) with M6b, but not with DM20. The formation of homo-dimers of M6a was further confirmed biochemically in Western blot experiment as shown in Figure 4.6C. These results indicated that M6a selectively dimerizes with M6a and M6b, but not with DM20.

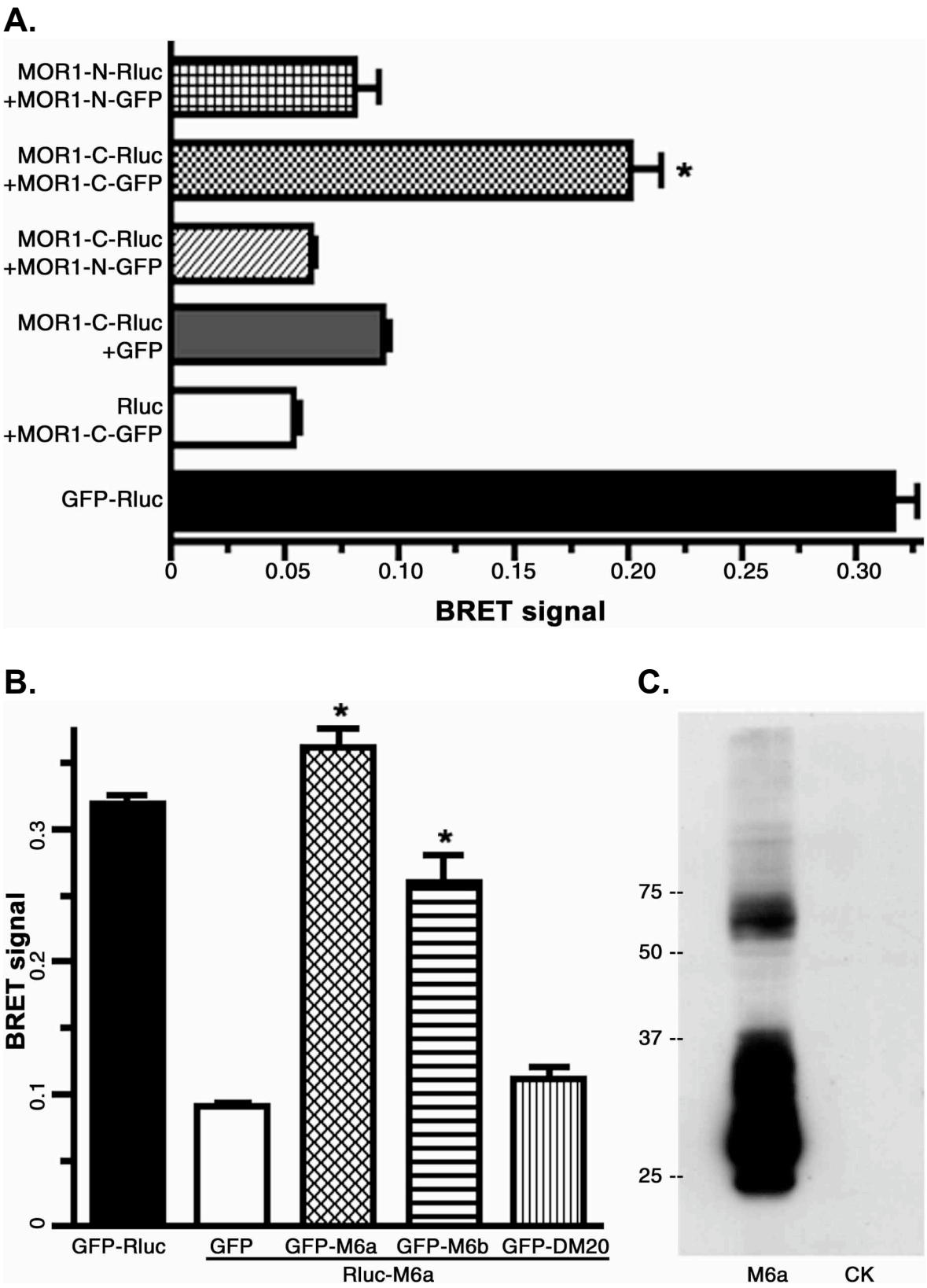

Figure 4.6. Formation of dimers of MOR1 or M6a. A. Cells were transiently cotransfected in different combinations with GFP or Rluc (negative control), Rluc- or GFP-tagged MOR1 as shown in the graph. GFP-Rluc was used as positive control. **B.** Cells were transiently cotransfected with amino-terminally Rluc-tagged M6a in combination with GFP (negative control), amino-terminally GFP-tagged

M6a, M6b or DM20. Cells were harvested 45 h post-transfection. The energy transfer was measured as described under "Methods". The results in A and B represent mean ± SEM of 3-5 independent experiments performed in duplicate. Asterisk indicates an extremely significant difference ($P<0.001$, compared with negative control) analyzed by one-way ANOVA followed by Bonferroni test. **C.** Cell lysate protein from HEK293 cells with expression of Myc-M6a (M6a), or without expression of Myc-M6a (CK), were extracted, and were electrophoretically separated, transferred to nitrocellulose membrane and detected with monoclonal anti-Myc antibody. The mobility of molecular mass standards (in kDa) is indicated to the left. Two additional experiments gave similar results.

4.7 Co-expression of MOR1 and M6a in rat brain

Co-localization is a prerequisite of protein-protein interaction under physiological conditions. Since an anti-M6a antibody for immunohistochemical studies is currently unavailable, we firstly evaluated the co-expression of MOR1 and M6a mRNAs using in situ hybridization techniques. In situ hybridization technique can be used to visualize cells that synthesize the respective proteins. Previous researchers reported that there is a good correlation between the distribution of mRNA and protein of MOR1 in the central nervous system (Delfs et al., 1994; Mansour et al., 1994, 1995a, 1995b; Stumm et al., 2004). In addition, the distribution of the M6a antigen has been demonstrated to fit well with the pattern of M6a mRNA expression (Yan et al., 1993, 1996; Roussel et al., 1998).

As depicted in Figure 4.7A, MOR1 mRNA was detected in many areas of rat brain. High expression of MOR1 mRNA was detected in the medial habenular nuclei and thalamic nuclei (Figure 4.7, A1-A2), including the mediodorsal thalamic nucleus, the central medial thalamic nucleus and intermediodorsal thalamic nucleus. MOR1 mRNA was also found in numerous scattered cells of the cerebral cortex (Cx), hippocampal formation (Hi), caudate putamen (CPu) and globus pallidus (GP). This expression pattern of MOR1 mRNA was in line with previous reports showing that MOR1 was expressed in neurons (Delfs et al., 1994; Arvidsson et al., 1995; Mansour et al., 1994, 1995a). High expression of M6a mRNA was detected in many regions (Figure 4.7B), including cerebral cortex, hippocampus, thalamus and striatum. The expression of M6b mRNA was detected in almost all regions (Figure 4.7C), including both white and gray matters in rat brain. The expression of PLP/DM20 mRNA was much higher when compared with that of M6a and M6b. PLP/DM20 mRNA was distributed in typical areas of oligodendrocyte, including the corpus callosum and fimbria/fornix (Figure 4.7D). This observation was in agreement with previous reports showing that M6a was expressed in neurons, and PLP/DM20 was limited to oligodendrocytes whereas M6b was expressed in both of neurons and oligodendrocytes in central nervous system (Yan et al., 1993, 1996). It is therefore plausible to predict a co-expression between MOR1 and M6a, but not between MOR1 and PLP/DM20 in rat brain.

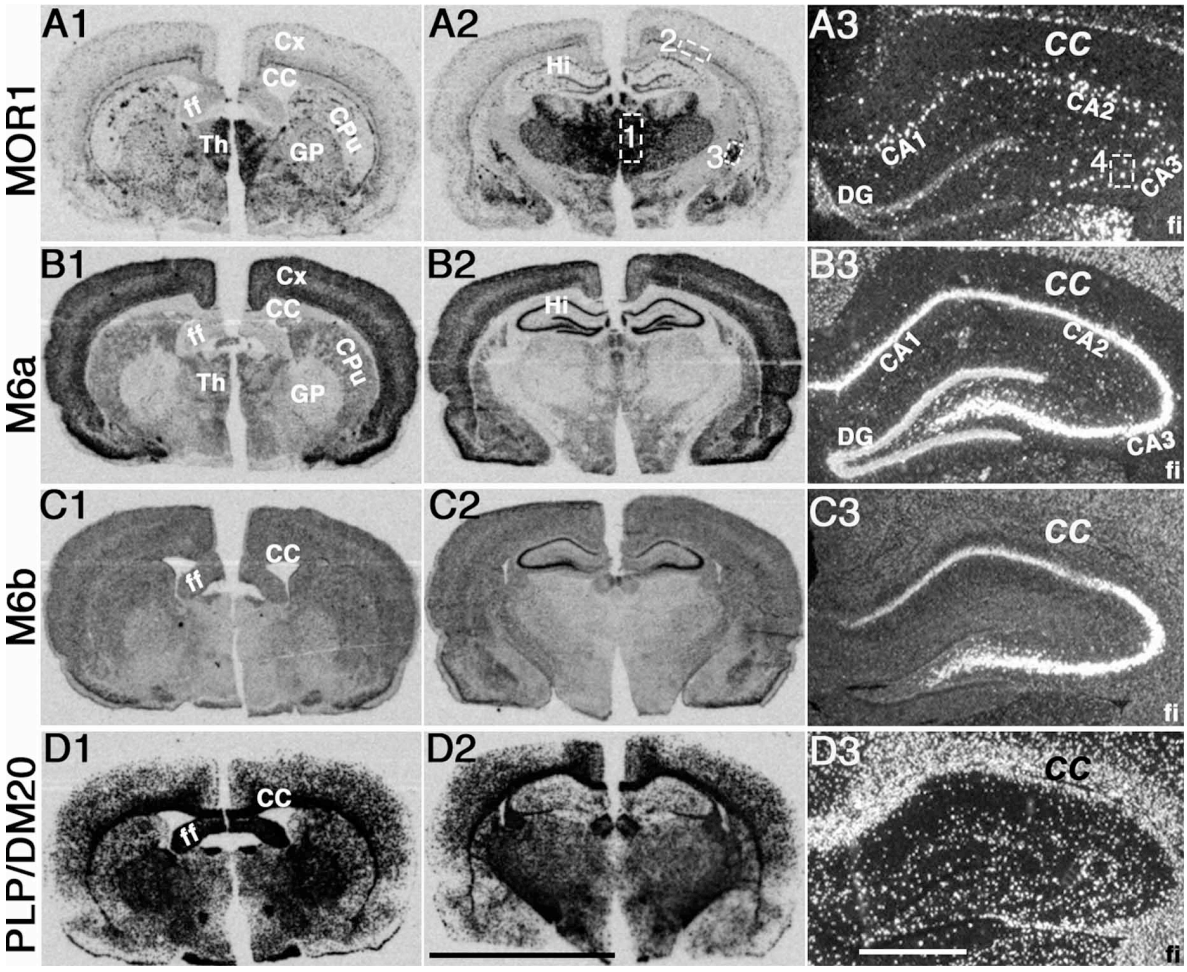

Figure 4.7. Expression patterns of MOR1, M6a, M6b and PLP/DM20 mRNAs. Rat brain sections were hybridized with [^{35}S]-labeled antisense probes. Low-power X-ray film autoradiographs through the forebrain at the level of bregma –1 mm (A1-D1, left panel) and –3 mm (A2-D2, middle panel) after in situ hybridization were shown for MOR1 (A), M6a (B), M6b (C) and PLP/DM20 (D) mRNAs. Darkfield micrographs of the hippocampal formation in a higher magnification were shown in A3-D3. **A1-A3:** MOR1 mRNA was expressed by numerous scattered neurons in many areas, including cerebral cortex, all layers of the hippocampal formation and striatum. Highly expressed MOR1 was detected in thalamic nuclei. **B1-B3:** M6a mRNA was most prominent in cerebral cortex and hippocampus. In addition, numerous cells expressing M6a mRNA were detected in striatum and thalamus. **C1-C3:** Moderate expression of M6b mRNA was seen in many regions of gray and white matters. **D1-D3.** PLP/DM20 mRNA was strongly expressed in typical regions of oligodendrocytes. Note: 1) CA1 (CA2, CA3): CA1 (CA2, CA3) field of the hippocampus; cc: corpus callosum; CPu: caudate putamen; Cx: cerebral cortex; DG: dentate gyrus; ff: fimbria/fornix; fi: fimbria hippocampus; GP: globus pallidus; Hi: hippocampus formation; Th: thalamus. 2) The white dashed rectangles with number shown in A2 and A3 were the similar regions for the representative observation in double in situ hybridization later (Figure 4.8). 3) Calibration bar in X-ray film autoradiographs (A1-D1, A2-D2): 8 mm; in darkfield micrographs (A3-D3): 1 mm.

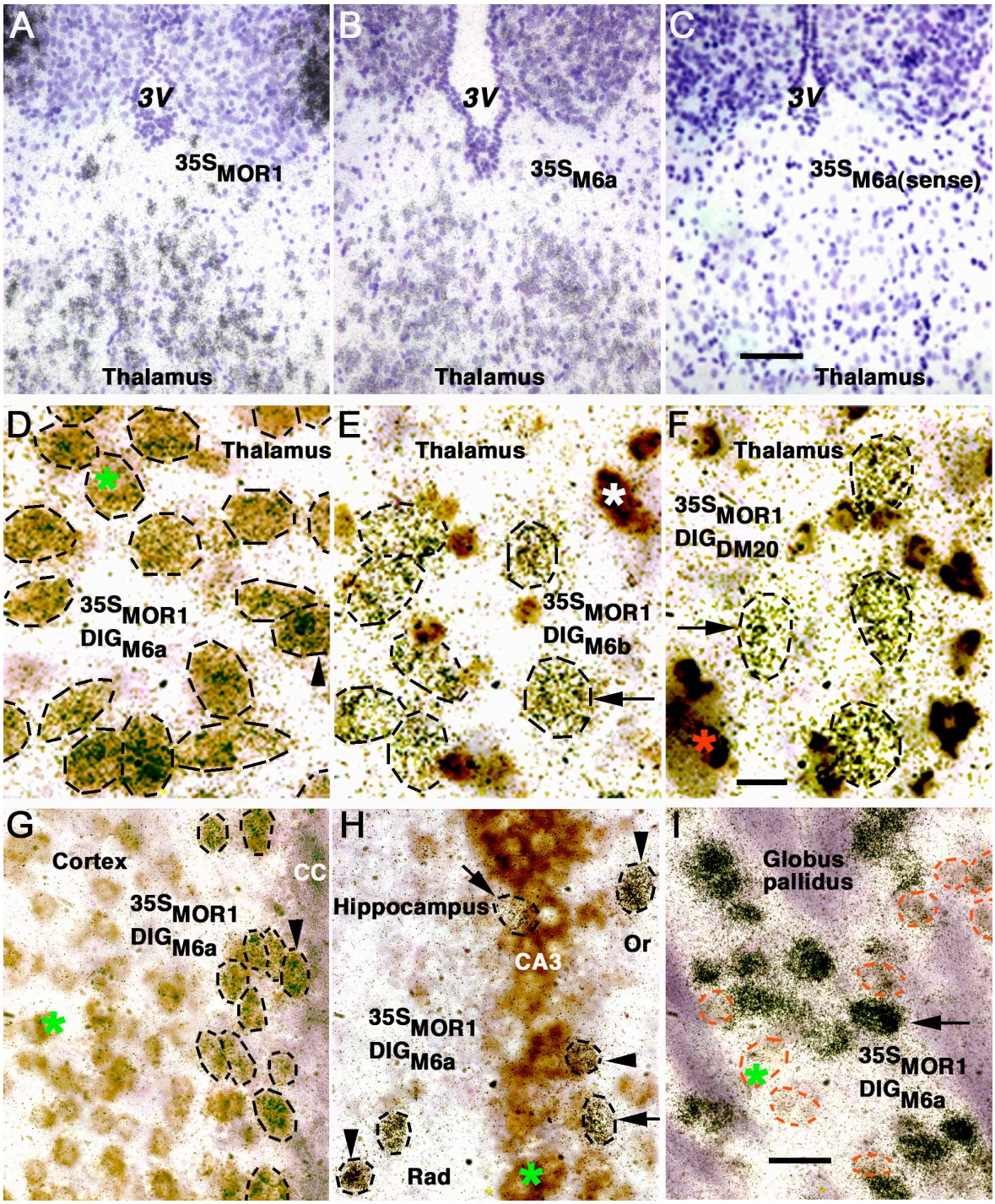

Figure 4.8. Co-expression pattern of MOR1 with M6a, M6b or PLP/DM20 in rat brain. A-B: In thalamus, wide expression of MOR1 and M6a mRNAs were detected, respectively. **C:** As a representative example, no in situ signal was detected using a [^{35}S]-labeled sense probe of M6a. **D:** In thalamus, most cells co-expressed both of MOR1 and M6a mRNAs. **E-F:** In thalamus, all MOR1 positive cells were M6b or PLP/DM20 negative, respectively. **G:** In cortex, all MOR1 positive cells were M6a positive whereas most M6a positive cells were MOR1 negative. **H:** In pyramidal cell layer, it appeared that few MOR1 positive cells were M6a positive. In the stratum radiatum (Rad) and oriens layer (Or), co-expression of MOR1 and M6a was often. **I:** In globus pallidus, co-expression of MOR1 and M6a was undetectable. Note that: 1) [^{35}S]-labelled mRNAs were shown as dark emulsion grains,

and DIG-labelled mRNAs were detected as chromogenic reaction products. 2) The investigated regions of D-F, G, I and H were from region 1, 2, 3 and 4, respectively in Figure 4.7A. 3) Cellular nuclei in A-C were stained with cresyl violet. 4) As an example, MOR1-M6a co-expressive cells (arrowhead), MOR1-positive cells (arrow) were shown in the images. The representative expressions of M6a, M6b and PLP/DM20 were shown as green, white and red asterisk, respectively. Dark or red dashed circles showed cell size. cc, corpus callosum. 3V, 3rd ventricle. Calibration bar: A-C, 100 μm; D-F, 20 μm; G-I, 40 μm.

The effect of opiate drugs depends on the presence of opioid receptors in specific brain regions. Both thalamus and cortex are significantly involved in analgesia and processing of pain information (Davis et al., 1998; Peyron et al., 2000; Sim-Selley et al., 2000; Zubieta et al., 2001; Maher et al., 2005). In particular, the thalamus is a main neural substrate in nociceptive pathways (Craig et al., 1994; Rausell et al., 1998; Ko et al., 2003). Both MOR1 and M6a mRNAs were expressed in large proportions of thalamic cells (Figure 4.8, A-B), suggesting the co-expression of the μ-opioid receptor and M6a in the same cell. As predicted, virtually all MOR1-positive cells expressed M6a mRNA, and most M6a-expressing cells were MOR1-positive in many thalamic nuclei (Figure 4.8D). In cerebral cortex, expression of M6a mRNA was more abundant than that of MOR1 mRNA. Cell counting of double- and single-labelled cells revealed that almost all of MOR1-positive cells expressed M6a mRNA whereas only a subpopulation of M6a-positive cells were MOR1-positive (Figure 4.8G).

We also investigated the co-expression pattern of MOR1 with M6a in other brain regions. Only very few of cells co-expressed MOR1 and M6a mRNAs in granule cells of dentate gyrus and the pyramidal cell layer of hippocampus (Figure 4.8, H). In the other layers of hippocampal formation, including the stratum radiatum and oriens layer, co-expression of MOR1 and M6a mRNAs was frequent (Figure 4.8, H). In globus pallidus, all cells expressing MOR1 mRNA were M6a negative (Figure 4.8, I).

In marked contrast to the frequent co-expression between MOR1 and M6a mRNAs, co-expression of MOR1 mRNA with M6b or PLP/DM20 mRNA was undetectable in thalamus (Figure 4.8, C and E). In fact, co-expression of MOR1 mRNA with M6b or PLP/DM20 mRNA was not found in any region tested (data not shown).

Based on the strong interaction of MOR1 with M6a and their co-expression in rat brain, we next investigated the potential role of M6a in MOR1 regulation.

4.8 M6a does not influence binding and inhibition of AC by MOR1 agonist

The endogenous M6a protein in HEK293 cells was undetectable using presently available antibodies (data not shown). To elucidate the effect of MOR1-M6a interaction on binding and signal transduction, we stably co-expressed HA-tagged MOR1 and Myc-tagged M6a in HEK293 cells. Co-expression of HA-MOR1 and Myc-M6a was monitored by radioligand binding assay, Western blot, and/or immunocytochemical analyses. As shown in table 4.1, saturation binding experiments revealed no substantial differences between MOR1 and MOR1-M6a expressing cells with respect to their affinities (K_D) to

[^{3}H]DAMGO and their numbers of maximal binding sites (B_{max}). For the functional properties to inhibit adenylate cyclase (AC), there was no significant difference on their maximal inhibition of 25μM forskolin-induced cAMP accumulation by 5 μM DAMGO. These results indicated that M6a has no substantial effect on MOR1 in HEK293 cells, both in agonist binding and maximum inhibition of adenylate cyclase.

Stable cell lines	K_D (nM)	B_{max} (pmol/mg)	Maximal inhibition of cAMP accumulation
HA-MOR1	2.25 ± 0.10	2.68 ± 0.26	98.8 ± 0.8 %
HA-MOR1&Myc-M6a	2.17 ± 0.22	2.10 ± 0.15	96.1 ± 1.3 %

Table 4.1 Functional properties of HA-MOR1 and HA-MOR1&Myc-M6a. The K_D and B_{max} for the binding of [^{3}H]DAMGO to MOR1 in stable cell line expressing amino-terminally HA-tagged MOR1 with or without co-expression of amino-terminally Myc-tagged M6a in HEK293 cells were determined by Scatchard analyses. The effect of 5 □M DAMGO on forskolin-stimulated cAMP accumulation was determined as described under "Methods." Values shown are the mean ± SEM of 4-5 independent experiments.

4.9 M6a augments *μ*-opioid receptor trafficking

Firstly, we investigated the subcellular distribution of M6a. As depicted in Figure 4.9, M6a was localized both at plasma membrane and in cytosolic vesicles of stably transfected HEK293 cells expressing amino-terminally Myc-tagged M6a. Interestingly, after exposure to monensin, an inhibitor of vesicle recycling, M6a accumulated in cytosolic vesicle-like compartments. Moreover, hypertonic sucrose (a blocker of protein internalization via clathrin-coated pits) significantly fixed M6a at the plasma membrane. These observations implied that M6a does internalize and recycle constitutively.

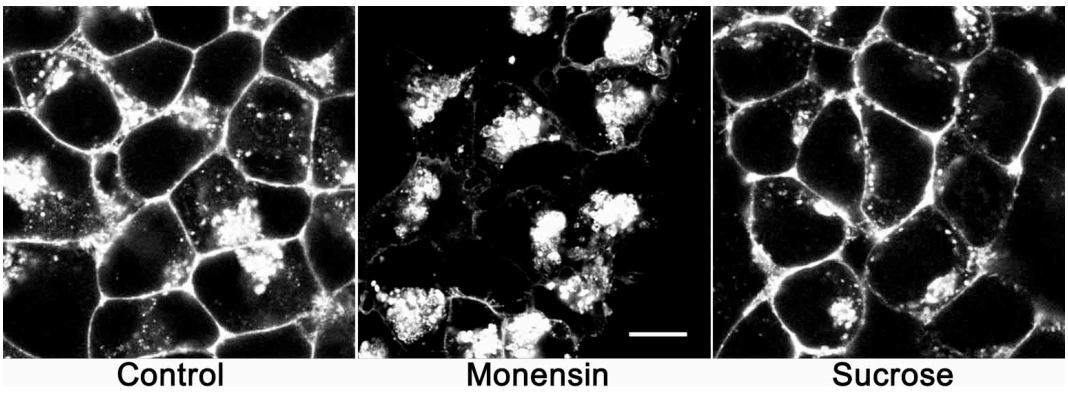

Figure 4.9. Intracellular trafficking of the membrane glycoprotein M6a. HEK293 cells stably expressing Myc-M6a were either not exposed (control) or exposed to 50 *μ*M monensin or 400 mM sucrose for 3 hours at 37°C. Cells were subsequently fixed, and the distribution of M6a were examined by confocal microscopy as described under "Methods". Representative images from two independent experiments are shown. Scale bar, 16 *μ*m.

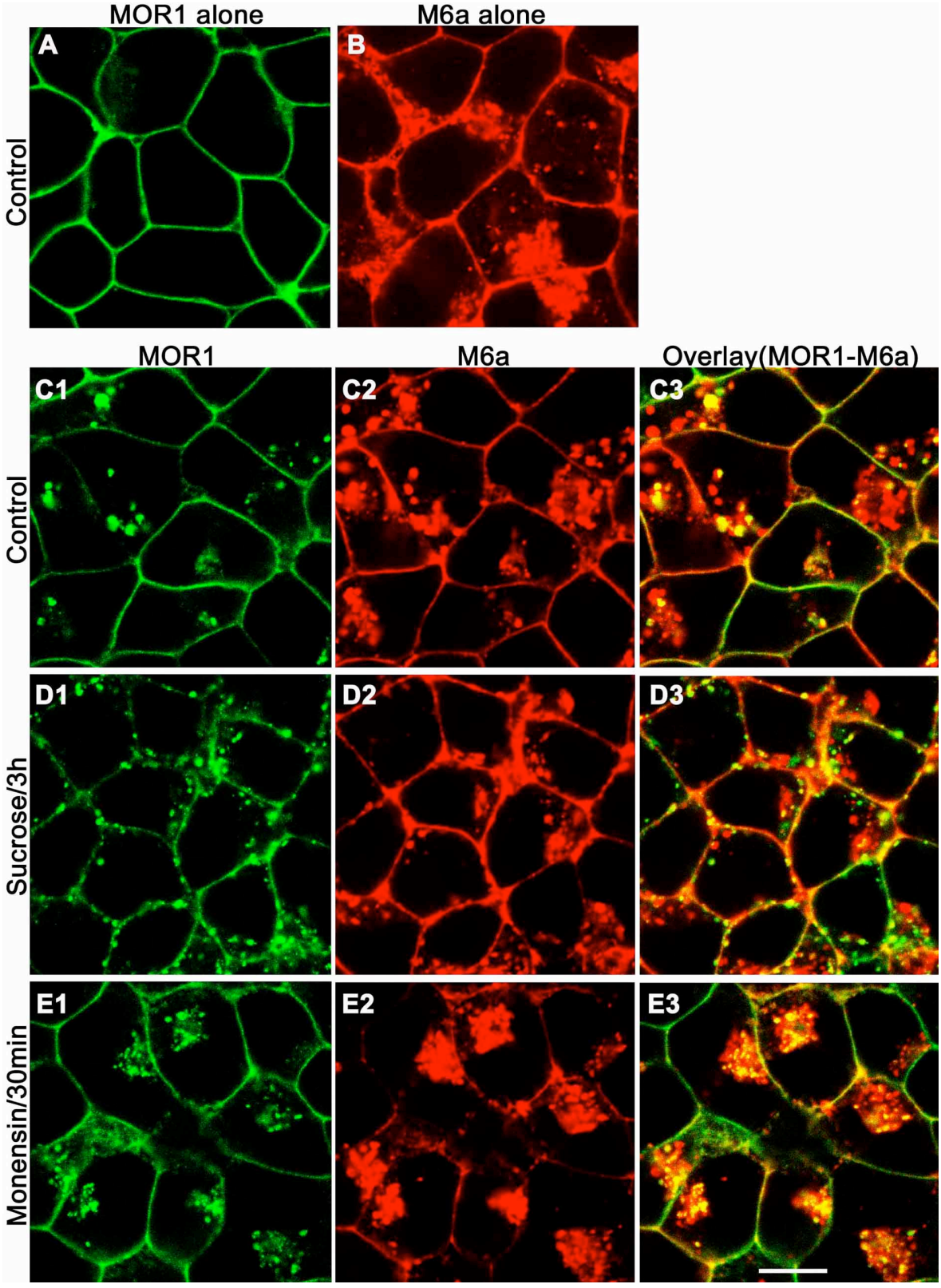

Figure 4.10. Subcellular distribution of HA-MOR1 and/or Myc-M6a. HEK293 cells stably expressing HA-MOR1 and/or Myc-M6a were either not exposed (A-C, control) or exposed to 400 mM sucrose for 3 hours (D) or 50 μM monensin for 30 minutes (E) at 37°C. Cells were subsequently fixed, and the receptor and M6a were examined by confocal microscopy as described under "Methods". Note that: 1) In untreated cells expressing MOR1 or M6a alone, MOR1 (A) was almost exclusively confined

to the plasma membrane whereas M6a (B) was distributed not only at plasma membrane, but also in cytoplasm. 2) In untreated cells co-expressing MOR1 and M6a, MOR1 (C1) was distributed not only at plasma membrane, but also in cytoplasm. 3) MOR1 showed strict co-localization with M6a (C3 and E3). 4) Sucrose decreased the accumulation of MOR1 and M6a in cytoplasm (D3), whereas monensin enhanced this accumulation (E3). 4) The punctual staining of MOR1 receptors (D) was partly due to high hypertonicity of sucrose. Representative images from two independent experiments are shown. Scale bar, 16 μm.

Next, we investigated whether the constitutive internalization and recycling of M6a (Figure 4.9) influences the intracellular trafficking of MOR1. In HEK293 cells stably expressing Myc-tagged M6a alone (Figure 4.10, B), M6a was localized both at the plasma membrane and in endosome like structures of the cytoplasm. In stably transfected HEK293 cells expressing amino-terminally HA-tagged MOR1 alone (Figure 4.10, A), almost all of receptors were localized at the plasma membrane with some occasional immunofluorescence within the intracellular compartments of the cells. However, in cells co-expressing HA-MOR1 and Myc-M6a, a significant immunoreactivity of receptors was found in endosome like structures in cytoplasm in addition to the distribution at the plasma membrane (Figure 4.10, C1), and showed a strict co-localization with Myc-M6a (Figure 4.10, C2-C3). M6a shows high homology with the proteolipid protein (PLP) (Yan et al., 1993). Over-expression of PLP has been shown to induce an abnormal accumulation of PLP and cholesterol in the late endosomal/lysosomal compartments (Simons et al., 2002). Analogously, it should be possible that over-expression of M6a induced an abnormal accumulation of receptors in cytoplasm. After exposed of MOR1 and M6a co-expressing cells to sucrose, both MOR1 and M6a were mainly localized at the plasma membrane (Figure 4.10, D). The treatment of monensin markedly enhanced the accumulation and co-localization of both MOR1 and M6a in cytoplasm (Figure 4.10, E as compared to C). These findings indicate that the M6a-mediated accumulation of MOR1 in cytoplasm is the result of an enhanced constitutive internalization and recycling of MOR1.

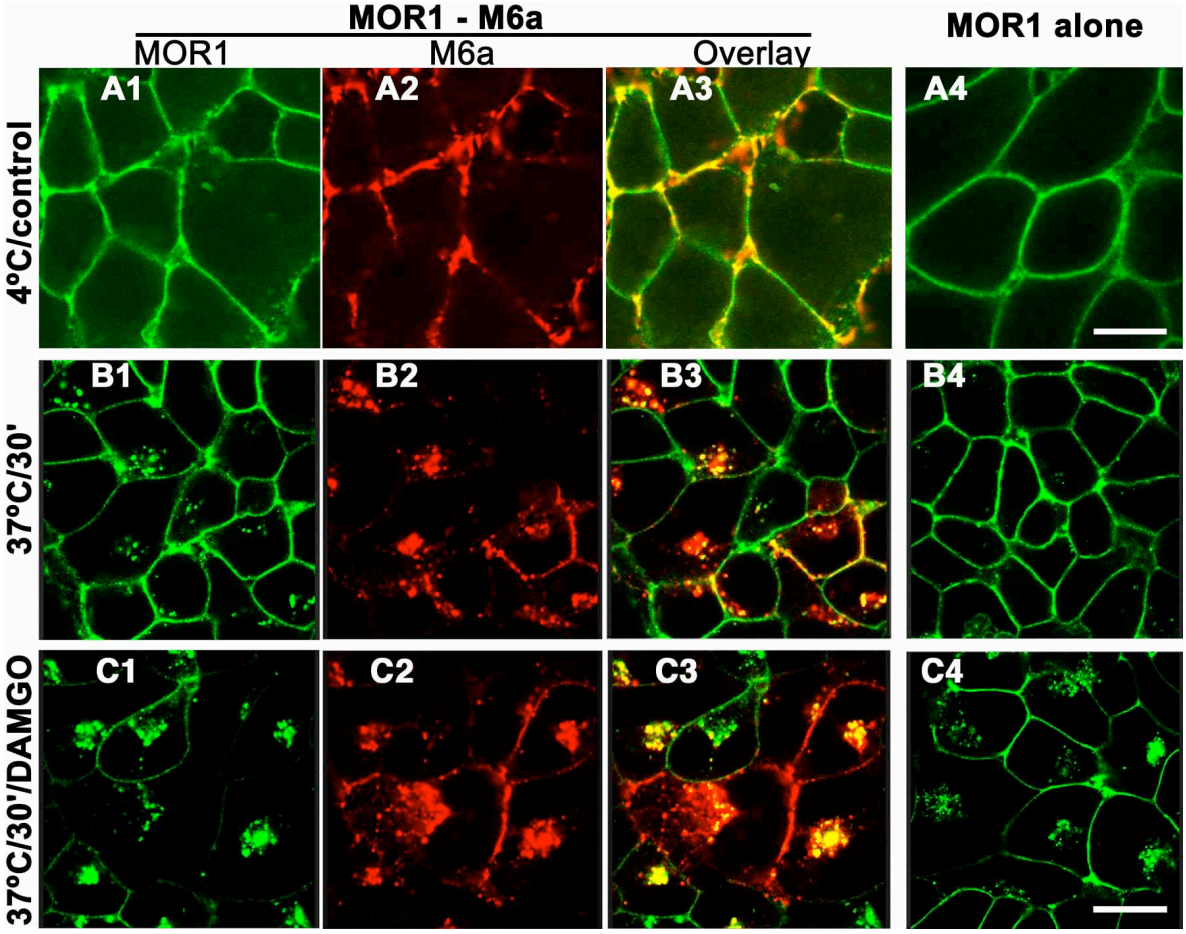

Figure 4.11. Co-internalization and co-localization of HA-MOR1 and Myc-M6a. Cells expressing HA-MOR1 and/or Myc-M6a were grown on poly-L-lysine coated glass coverslips. Receptor and/or M6a were surface-labeled at 4 °C with anti-HA and/or anti M6a antibodies. Subsequently, cells were either not exposed or exposed to 10 μM DAMGO at 37°C for 30 min. After fixation, MOR1 and M6a were detected by confocal microscopy as described under "Methods". Note that: 1) M6a augmented the MOR1 constitutive internalization (B1 as compared to B4). 2) Either in untreated cells or agonist-treated cells, MOR1 showed co-internalization and co-localization strictly with M6a (B3 and C3). 3) M6a enhanced agonist-induced internalization of MOR1 (C1 versus C4). Shown are representative results from one of three independent experiments. Scale bar, 16 □m in A, and 20 □m in B and C.

The anti-HA antibody recognizes the HA-epitope tag located in the extracellular N-terminal tail of HA-MOR1, and the anti-M6a monoclonal antibody recognizes the extracellular loop of the M6a antigen. These properties of the antibodies make it possible to specifically label MOR1 and/or M6a at the surface of living cells. Without membrane permeabilization, MOR1 and/or M6a at the cell surface can be specifically labeled using anti-HA and/or anti-M6a antibodies at 4 °C. As shown in Figure 4.11A, receptor and/or M6a were exclusively confined to the plasma membrane at low temperature (4 °C), which prevents the endocytosis of MOR1 and M6a. Incubation of the HEK293 cells expressing HA-MOR1 alone at 37 °C for 30 min did not induce substantial receptor internalization (Figure 4.11, B4). In remarkable contrast, in cells co-expressing M6a, the anti-HA and anti-M6a immunofluorescences were detected in cytoplasm (Figure 4.11, B1), confirming

that M6a-mediated intracellular accumulation of MOR1 (Figure 4.10C) was due to M6a-augmented receptor internalization. M6a showed co-internalization and co-localization during the constitutive internalization of MOR1 (Figure 4.11, B2-B3). Furthermore, after 30 min of 10 μM DAMGO treatment, cells co-expressing MOR1 and M6a exhibited an enhanced internalization (Figure 4.11, C1) as compared with cells expressing the receptor alone (Figure 4.11, C4). The agonist-induced co-internalization of M6a and MOR1 was evident by its strict co-localization within the intracellular compartments (Figure 4.11, C3). This indicated that M6a enhances the internalization of MOR1. In addition, like opioid pepide DAMGO, similar observations were also found when cells were treated with alkaloid agonist etorphine (data not shown).

4.10 Quantitative analysis of *μ*-opioid receptor trafficking

Analysis using confocal microscope indicated that M6a enhances both constitutive and agonist-stimulated internalization of MOR1. In addition, we quantified the rate of MOR1 trafficking by ELISA. As expected, there was an enhanced constitutive internalization of MOR1 in cells co-expressing M6a (9.4 ± 0.5 % versus 26.3 ± 1.4 % for MOR1 and MOR1-M6a, respectively, Figure 4.12, left panel). In the presence of 1μM DAMGO for 30 min, an augmented rate of agonist-mediated receptor internalization by M6a was also detected (32.4 ± 2.7 % versus 47.8 ± 1.0% for MOR1 and MOR1-M6a, respectively, Figure 4.12, left panel). In addition, in the presence of etorphine, M6a-augmented MOR1 internalization was also observed (data not shown).

The recycling rate of internalized receptors was examined using a modified form of ELISA previously described for estimating receptor internalization (Koch et al., 2003). The incubation of cells in the presence of 10 μM etorphine for 2 h led to an agonist-induced internalization to a steady-state level in cells both with and without co-expression of M6a. After receptor internalization, the agonists were washed out and then cells were incubated in agonist free medium for receptor recycling. In this experiment, the antagonist naloxone was added into incubation medium to block further endocytosis. As shown in Figure 4.12 (right panel), the recycling rate was estimated as a percent of the recycled receptors to endocytosed receptors. In cells co-expressing M6a, about 32% of endocytosed receptors was recycled after 30 min of agonist withdrawal. By contrast, in cells expressing receptor alone, only about 9% of internalized receptors was recycled. After 60 min of agonist withdrawal, over 30% of internalized receptors was recycled in both cell lines.

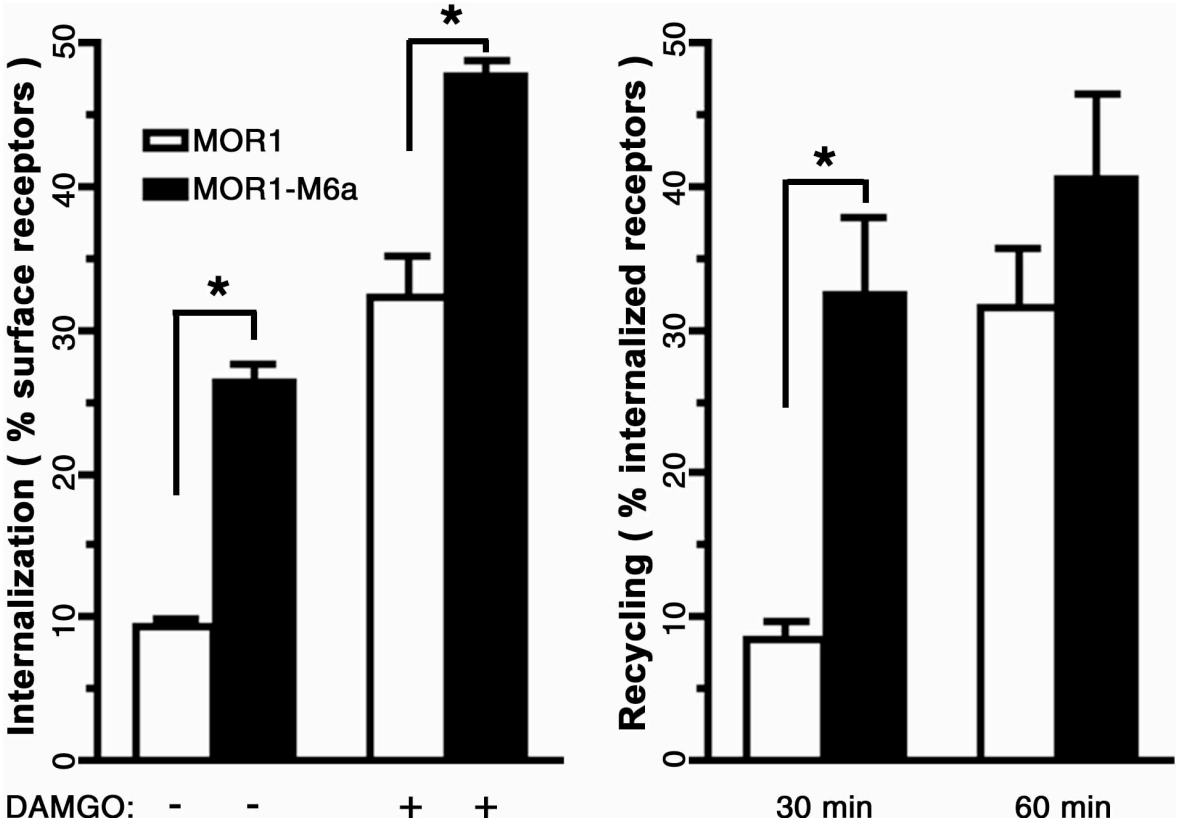

Figure 4.12. Quantitative analysis of MOR1 trafficking. Left panel. For the analysis of receptor internalization, cells expressing HA-MOR1 alone or co-expressing with Myc-M6a were surface-labeled with anti-HA antibody at 4°C for 1.5 h. Subsequently, cells were either not treated or treated with 1 μM DAMGO for 30 min, and then fixed. Receptor internalization, quantified as the percent loss of cell surface receptors, was measured by ELISA as described under "Methods". **Right panel**. For the analysis of receptor recycling, cells were first exposed to 10 μM etorphine for 2 h to drive receptor internalization to a steady-state level. After agonist washout, cells were exposed to 10 μM naloxone for 30 and 60 min. Afterwards, cells were chilled with 4°C PBS to stop receptor trafficking. Receptors were surface-labeled with anti HA antibody at 4°C for 2 h. Un-bound antibodies were washed out, cells were then fixed and the surface receptors were quantified as described above. The recycling rate was estimated as a percent of recovered surface receptors to internalized receptors. Data are presented as means ± SEM of 3-5 independent experiments performed in triplicate. Asterisk indicates an extremely significant difference ($p<0.001$) between MOR1 and MOR1-M6a expressing cells (One-way ANOVA followed by Bonferroni test).

These results are in excellent agreement with the observations by confocal microscopy, and provide convincing evidence that M6a enhances both internalization and recycling of the μ-opioid receptor in HEK293 cells.

4.11 Expression of M6a mRNA in HEK293 cell

In earlier reports, M6a antigen was detected at the apical surfaces of epithelial cells in mouse kidney (Lagenaur et al., 1992). In the human kidney cell line (HEK293 cells), we were unable to detect the endogenous M6a using presently available anti-mouse M6a antibodies (data not shown). This could be due to the low expression of M6a and/or the

low avidity of the available antibodies. Using RT-PCR, a high sensitive method, we were able to amplify and sequence the transcript of M6a in HEK293 cells.

```
1 ATGGAAGAGAATATGGAAGAGGGACAGACACAAAAAGGGTGTTTTGAATGCTGTATCAAA
  M  E  E  N  M  E  E  G  Q  T  Q  K  G  C  F  E  C  C  I  K  20

61 TGCCTGGGGGGCATT CCC TATGCCTCT CTG ATTGCC ACCATCCTGCTCTATGCGGGTGTT
  C  L  G  G  I  P  Y  A  S  L  I  A  T  I  L  L  Y  A  G  V  40

121 GCCCTGTTCTGT GGCTGC GGTCATGAAGCG CTTTCT GGAACTGTCAACATTCTGCAAACC
  A  L  F  C  G  C  G  H  E  A  L  S  G  T  V  N  I  L  Q  T  60

181 TACTTTGAGATGGCAAGAACTGCT GGAGACACACTG GATGTCTTTACC ATGATTGACATC
  Y  F  E  M  A  R  T  A  G  D  T  L  D  V  F  T  M  I  D  I  80

241 TTTAAGTATGTGGTCTAC GGCATCGCAGCTGCG TTC TTT GTGTATGGC ATTTTGCTGATG
  F  K  Y  V  V  Y  G  I  A  A  A  F  F  V  Y  G  I  L  L  M  100

301 GTGGAAGGTTTCTTCACAACTGGGGCCATCAAA GATCTC TATGGGGATTTCAAAATCACC
  V  E  G  F  F  T  T  G  A  I  K  D  L  Y  G  D  F  K  I  T  120

361 ACTCGTGGCAGATGTGTGAGCGCTTGGTTC ATT ATGCTG ACATATCTTTTC ATGTTG GCC
  T  R  G  R  C  V  S  A  W  F  I  M  L  T  Y  L  F  M  L  A  140

421 TGGCTGGGAGTCACGGCTTTCACCTCACTG CCA GTTTAC ATGTACTTCAATCTGTGGACC
  W  L  G  V  T  A  F  T  S  L  P  V  Y  M  Y  F  N  L  W  T  160

481 ATCTGCCGGAACACCACATTAGTGGAGGGAGCA AATCTCTGCTTGGACCTTCGTCAG TTT
  I  C  R  N  T  T  L  V  E  G  A  N  L  C  L  D  L  R  Q  F  180

541 GGAATTGTGACAATTGGAGAGGAAAAGAAAATTTGTACTGTCTCT GAGAATTTCTTGAGG
  G  I  V  T  I  G  E  E  K  K  I  C  T  V  S  E  N  F  L  R  200

601 ATGTGCGAATCTACTGAGCTGAACATG ACCTTCCAC TTGTTTATT GTGGCACTTGCTGGA
  M  C  E  S  T  E  L  N  M  T  F  H  L  F  I  V  A  L  A  G  220

661 GCTGGGGCAGCAGTCATTGCTATGGTTCACTACCTT ATGGTTCTG TCTGCCAACTGGGCC
  A  G  A  A  V  I  A  M  V  H  Y  L  M  V  L  S  A  N  W  A  240

721 TATGTGAAAGACGCCTGCCGGATGCAGAAGTATGAAGACATCAAGTCGAAGGAAGAGCAA
  Y  V  K  D  A  C  R  M  Q  K  Y  E  D  I  K  S  K  E  E  Q  260

781 GAGCTTCATGACATCCACTCTACT CGCTCCAAAGAGCGGCTCAAT GCGTACACATAA
  E  L  H  D  I  H  S  T  R  S  K  E  R  L  N  A  Y  T  *  278
```

Figure 4.13. Neucleotide sequence and deduced amino acid sequence of M6a cDNA from HEK293 cells. The nucleotide sequence and corresponding translated amino acid sequence of the M6a cDNA from HEK293 cells are shown. The nucleotide and amino acid residues were numbered on the left and right, respectively. In comparison to the human M6a cDNA (Olinsky et al., 1996), the difference in nucleotides and deduced amino acids were shown in bold, italic and underlined. Note that it is impossible that this cDNA derives from the genomic DNA because there is no intron inside.

Analysis of cDNA sequence of HEK293 M6a (Figure 4.13) revealed a 99%, 93%, 91% homology to the reported M6a nucleotide sequence of human (Olinsky et al., 1996; GI:21314625), mouse (Yan et al., 1993; GI:31981997) and rat (Mukobata et al., 2002; GI:57527945), respectively. In comparison with the reported human M6a protein sequence, there are only two amino acids different (Figure 4.13). This difference might be due to gene polymorphisms, although sequencing errors can not be completely excluded. The existence of M6a in HEK293 cells suggests that endogenous M6a can play a role in the intracellular trafficking of MOR1 in these cells.

4.12 The effect of M6a dominant negative mutants on MOR1 internalization

As shown above (Figure 4.4C), both the amino terminal truncation mutant (amino acids 1-108) and the truncation mutant (amino acids 129-255) of M6a interact with the full length of MOR1 (Figure 4.4C). This finding led us to test whether these truncations act as dominant negative mutants of MOR1 internalization in HEK293 cells with endogenously expressed M6a.

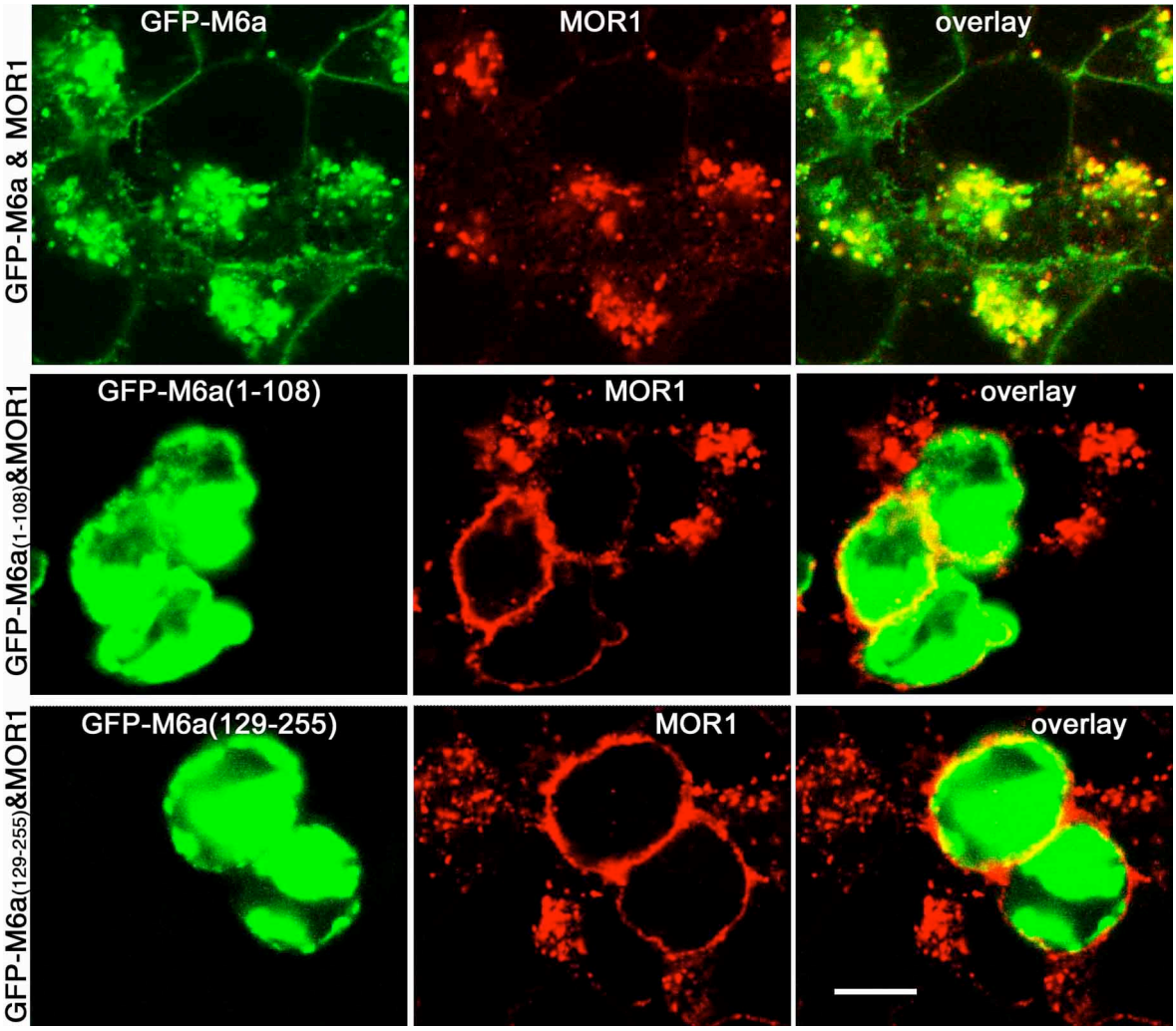

Figure 4.14. Effect of M6a dominant negative mutants on MOR1 internalization. HEK293 cells stably expressing HA-MOR1 were transiently transfected with plasmids encoding GFP-M6a, GFP-M6a(amino acids 1-108) or GFP-M6a(amino acids 129-255) as described under "Methods". About 60 h after transfection, cells were pretreated using 50 μM monensin for 30 min and then were exposed to 10 μM DAMGO in the presence of 50 μM monensin for another 30 min at 37°C. Cells were subsequently fixed, and the receptor was immunostained using rabbit anti-HA antibody and Cy3 conjugated anti-rabbit antibody. The GFP signal (green) and Cy3 signal (red) were taken by confocal microscopy. Representative images from two independent experiments are shown. Scale bar, 8 μm.

In cells co-expressing GFP-tagged M6a, a marked DAMGO-induced internalization of MOR1 was seen (Figure 4.14, upper panel). This was also confirmed by quantitative ELISA (data not shown). However, after over-expression of GFP-tagged truncation mutants (amino acids 1-108 and 129-255) of M6a, DAMGO-induced MOR1-internalization was almost blocked completely whereas receptors in adjacent cells that did not express these mutants internalized in response to agonist (Figure 4.14, middle and lower panel). It is likely that these mutants can function as dominant negative mutants to compete for binding of endogenous M6a to MOR1, and thus impairs receptor internalization. This finding further supports a physiological role of M6a in MOR1 internalization.

4.13 M6a increases accumulation of MOR1 and DOR1 in recycling endosomes

Next, we examined whether M6a modulates the trafficking pathway and post-endocytic sorting of opioid receptors. We carried out immunocytochemistry to estimate whether co-internalized receptor and M6a would be associated with the endocytic vesicles that can be identified by Alexa Fluor 488-labeled transferrin, a well-established marker of early and recycling endosomes (Hopkins and Trowbridge, 1983; Dunn et al., 1989; Tsao and von Zastrow, 2000).

Surface opioid receptors (MOR1, DOR1) and M6a were labeled by exposing intact cells to appropriate specific antibodies. When these cells were simultaneously incubated with selective agonists and Alexa Fluor 488-conjugated transferrin for 30 min, a high degree of co-localization among opioid receptor, M6a and endocytic transferrin was detected (Figure 4.15A), indicating that the opioid receptors and M6a co-internalize into early endosome via the same trafficking pathway as the transferrin receptor. Moreover, when cells were first incubated with 10 μM DAMGO to initiate a 30-min pulse of receptor internalization, and then chased for an additional 20 min in the presence of labeled transferrin in agonist-free medium, a high degree of co-localization among the pulse of internalized MOR1, M6a and the recycling endosome marker transferrin was still observed (Figure 4.15B, upper panel). Unexpectedly, in cells co-expressing M6a, co-internalized DOR1 still co-localized with transferrin whereas internalized DOR1 was mainly sorted into the other compartments in adjacent cells without co-expression of M6a (Figure 4.15B, lower panel). This demonstrated that over-expression of M6a did not change MOR1 trafficking pathway but enhanced post-endocytic sorting of receptors for the recycling pathway. Consistent with this, after agonist-induced endocytosis, MOR1 is sorted into recycling endosome for recycling whereas DOR1 is mainly targeted to lysosomes for degradation (Tanowitz and von Zastrow, 2003; Wang et al., 2003). This suggested that M6a directs internalized opioid receptors into recycling endosomes during receptor post-endocytic sorting.

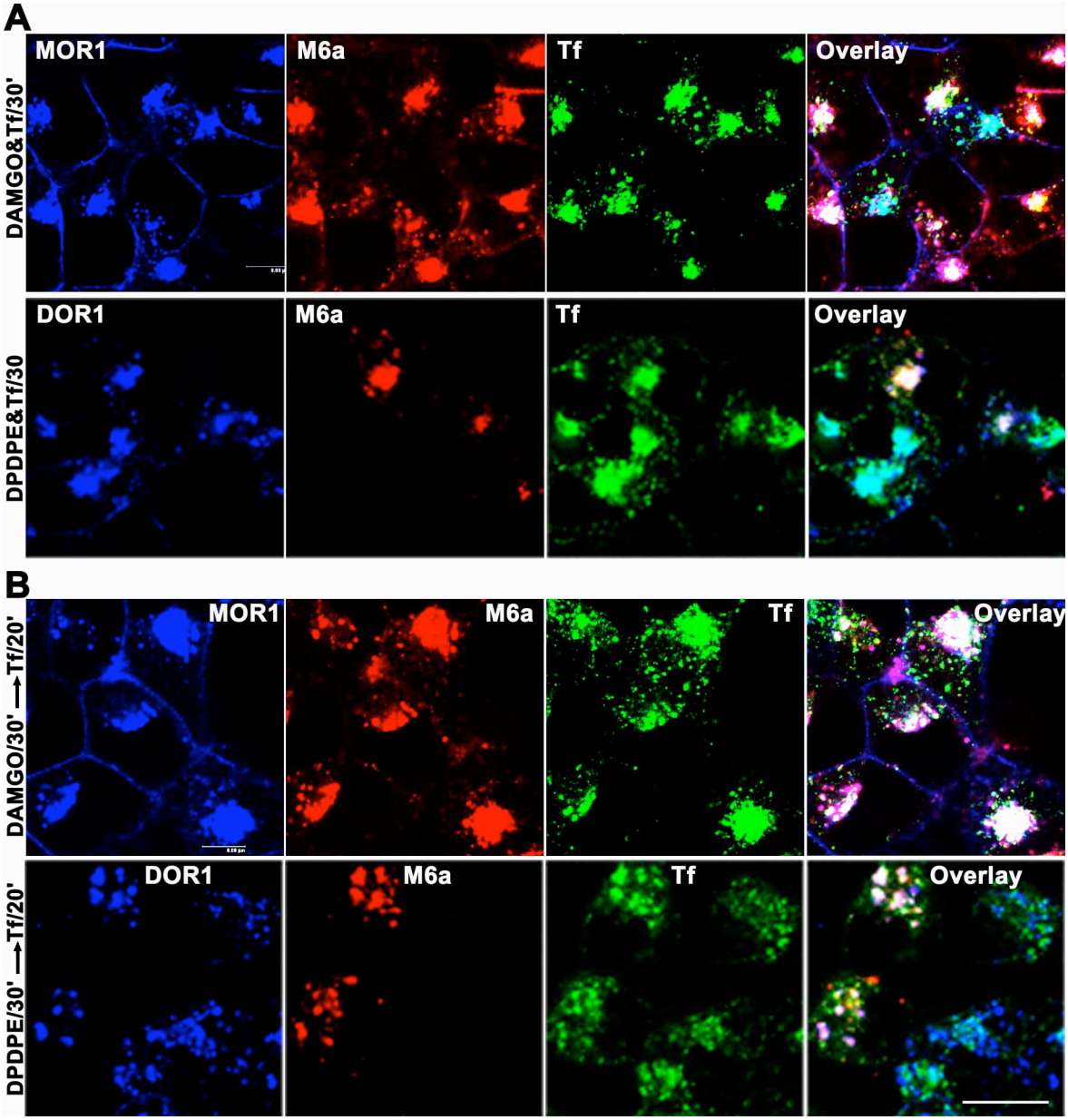

Figure 4.15. Trafficking pathway of MOR1, DOR1 and M6a. Stable HA-DOR1 cells transiently transfected with pCMV-Myc-M6a plasmid, and cells stably co-expressing HA-MOR1 and Myc-M6a were used. **A.** Co-internalization of MOR1/DOR1, M6a and transferrin. Cells were surface-labeled and exposed to 10 μM DAMGO (or DPDPE) and 5 μg/ml Alexa Fluor 488-conjugated transferrin for 30 min. Confocal microscopy was used to examine the internalization of antibody-labeled receptors, M6a and Alexa Fluor 488-conjugated transferrin, as described under "Methods". **B.** Post-endocytic sorting of internalized opioid receptors and M6a. Confocal microscopy of triple labeled cells was used to examine the co-localization of a 30-min agonist pulse of antibody-labeled receptors and M6a followed by a 20-min chase with transferrin in the absence of agonist, as described under "Methods". Note that: Overlap of MOR1 (blue), M6a (red) and transferrin (green) was denoted by the white vesicular structures visualized in merged image. Overlap of receptor with M6a generated magenta; Overlap of receptor with transferrin generated cyan; and Overlap of M6a with transferrin generated yellow. Representative images from one of three independent experiments are shown. Scale bar, 16 μm.

4.14 M6a attenuates down-regulation of the μ-opioid receptor

Down-regulation of opioid receptors in response to chronic opioid treatment is a long-term adaptive process, which results from the proteolytic degradation of internalized receptors. The present studies provided evidences that over-expression of M6a augments the recycling of μ-opioid receptors (Figure 4.12). The M6a-enhanced receptor recycling might decrease receptor endosomal sorting to lysosomes for degradation, and thus decrease receptor down-regulation.

As expected, and consistent with the observation that M6a augmented receptor recycling (Figure 4.12), agonist-induced down-regulation of MOR1 was significantly reduced in cells with co-expression of M6a. After an extended exposure (16 hours) to DAMGO, we observed that only 25% of MOR1 were downregulated in cells co-expressing MOR1 and M6a in contrast to the 42% down-regulation in cells expressing MOR1 alone (Figure 4.16). This is in agreement with the hypothesis that M6a-augmented receptor recycling decreases receptor degradation in lysosomes, and thus reduces receptor down-regulation.

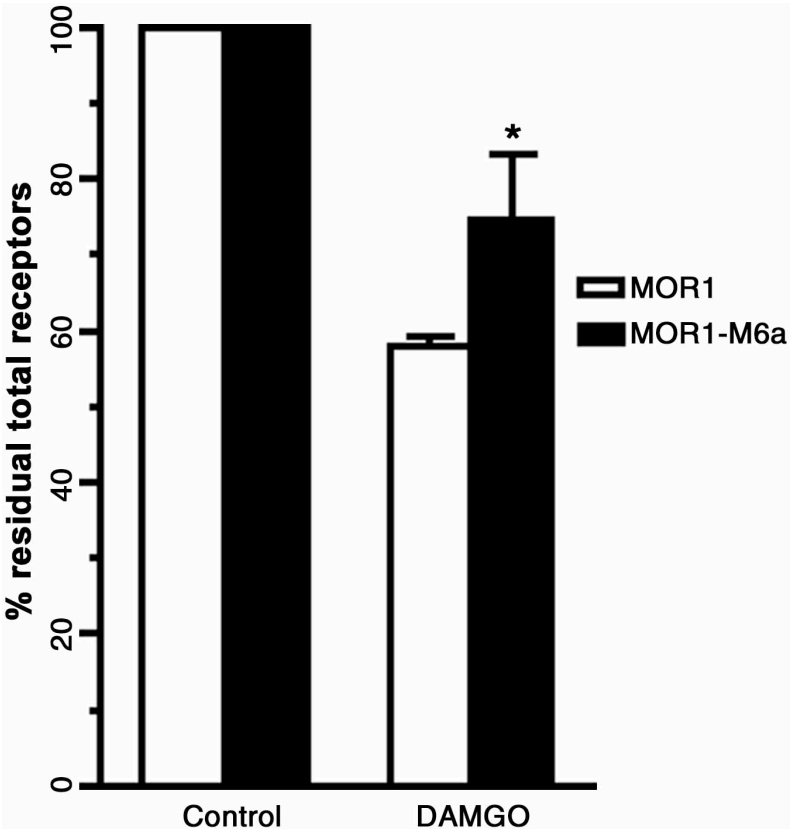

Figure 4.16. Effect of M6a on MOR1 down-regulation by DAMGO. Cells stably expressing HA-MOR1 with and without Myc-M6a were incubated at 37°C for 16 hours in the presence or absence of 5 μM DAMGO. The amount of total MOR1 was examined by membrane binding assay as described under "Methods". The total receptor without DAMGO treatment was set as 100% (Control). Values represent mean ± SEM of 3-5 independent measurements performed in triplicate. Asterisk indicates a significant difference ($p<0.05$) between MOR1 and MOR1-M6a expressing cells (One-way ANOVA followed by Bonferroni test).

4.15 M6a decreases agonist-induced desensitization of the μ-opioid receptor

Since receptor trafficking affects agonist-induced desensitization of the μ-opioid receptor, we investigated whether the observed effects of M6a on μ-opioid receptor trafficking influences agonist-induced MOR1 desensitization.

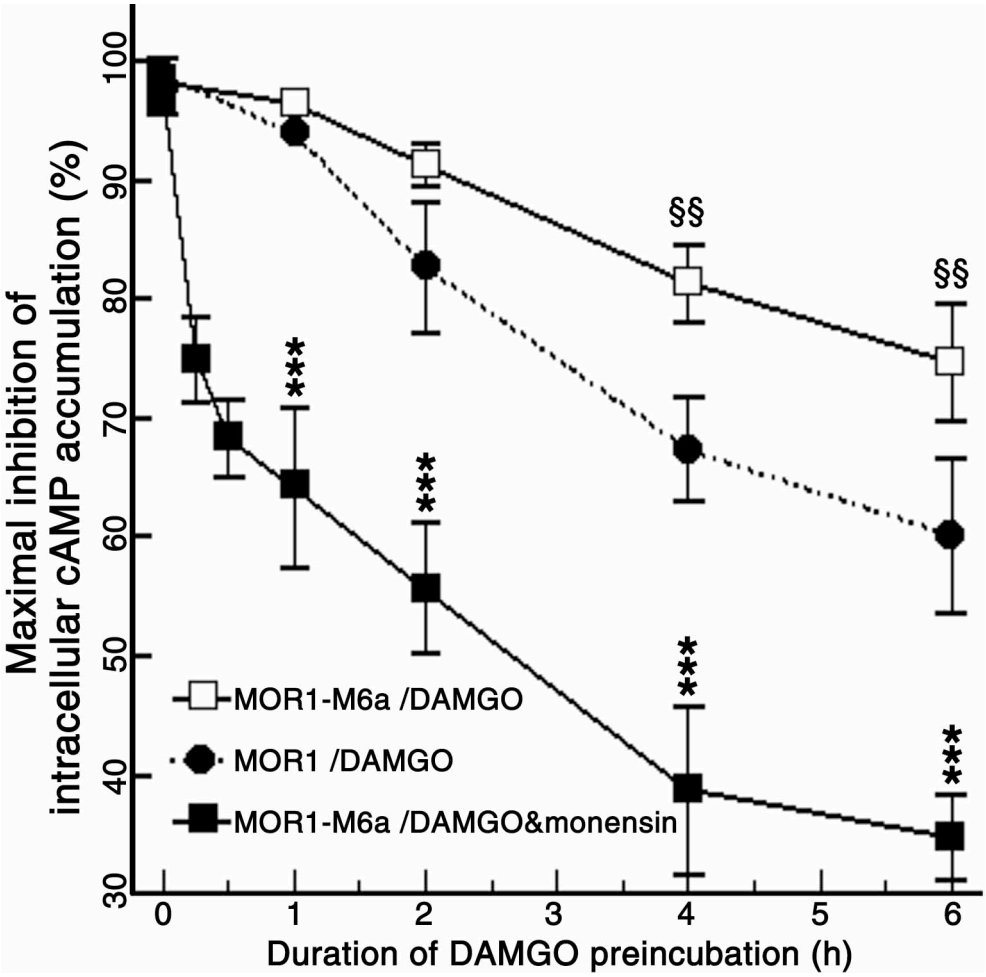

Figure 4.17. The effect of M6a on DAMGO-induced μ-opioid receptor desensitization. Cells stably expressing HA-MOR1 with and without Myc-M6a were exposed to 5 μM DAMGO in the presence or absence of 50 μM monensin for the indicated time periods. After removal of the preincubation medium, the cells were treated with forskolin (25 μM) or forskolin (25 μM) plus DAMGO (5 μM) for 15 min, and cAMP levels were determined as described under "Methods". Values represent mean ± SEM of 3-6 independent measurements performed in duplicate. Double paragraph indicate a very significant difference ($p<0.01$) in the absence of monensin between MOR1 and MOR1-M6a expressing cells, and triple asterisks indicate an extremely significant difference ($P<0.001$) in MOR1-M6a co-expressing cells compared with the absence of monensin (One-way ANOVA followed by Bonferroni test).

Cells expressing HA-MOR1 with and without Myc-M6a were pre-incubated with 5 μM DAMGO for various time periods followed by the measurement of agonist-induced inhibition of forskolin-stimulated cAMP accumulation. Receptor desensitization was monitored by the decreased ability of the MOR1 agonist to inhibit forskolin-stimulated adenylate cyclase activity, which represents loss of signaling caused by both receptor

uncoupling and internalization. As shown in Figure 4.17, prolonged exposure to the μ-opioid receptor selective agonist DAMGO led to a time-dependent decrease in the inhibition of cAMP accumulation. During the first hour of agonist treatment, there was no significant difference in MOR1 desensitization with and without co-expression of M6a. However, after the prolonged agonist treatment, cells co-expressing MOR1 and M6a exhibited a slower desensitization rate as compared to cells expressing MOR1 alone. After 6 hours of agonist exposure, about 40% loss of DAMGO activity was observed in cells expressing MOR1 alone, whereas in cells co-expressing M6a only about 25% loss in DAMGO activity was observed. In general, receptor internalization is expected to contribute to receptor desensitization. However, in case of MOR1, receptors are recycled back to the plasma membrane after internalization; the reactivated receptors, in turn, contribute to receptor resensitization, which partially reverses ongoing receptor desensitization (Koch et al., 1998, 2001, 2004, 2005; Law et al., 2000a; Qiu et al., 2003; Beyer et al., 2004). According this hypothesis, the lower receptor desensitization in M6a-expressing cells is most likely explained by the M6a-augmented receptor recycling.

To prove this hypothesis, we tested the effect of monensin, a blocker of receptor recycling, on receptor desensitization. In fact, as depicted in Figure 4.17, application of monensin in cells co-expressing MOR1 and M6a markedly enhanced DAMGO-induced desensitization of MOR1 in these cells. This is in clear agreement with the notion that the enhanced MOR1 recycling caused by M6a is responsible for the decreased MOR1 desensitization, since it can be reversed by the recycling blocker monensin.

Peptide agonists, such as DAMGO, induce a pronounced endocytosis of the μ-opioid receptor, whereas many clinical alkaloid drugs (e.g. morphine) are very weak in their ability to promote receptor internalization (Koch et al., 2005). We analyzed whether agonist-induced receptor desensitization would be a result of agonist-mediated receptor internalization by comparing DAMGO and morphine-induced receptor desensitization.

As depicted in Figure 4.18, a small but clear receptor desensitization was detected after pretreatment with morphine for 1 hour. At that time, the degree of desensitization after morphine was higher than that after the receptor internalizing opioid DAMGO (Figure 4.18). The recycling blocker monensin which caused a marked increase in the desensitization of the receptor-internalizing agonist DAMGO did not significantly change the desensitization of the non-internalizing agonist morphine (Figure 4.18). After a longer time period (4h), morphine induced a greater receptor desensitization than DAMGO (42.4 ± 3.3% versus 18.6 ± 3.0% for morphine and DAMGO, respectively) (Figure 4.18). Again, in contrast to the desensitization after DAMGO, monensin did not significantly affect the extent of receptor desensitization after morphine at this time-point. These findings show that the morphine-induced MOR1 desensitization does not require internalization and reflects most likely uncoupling of the receptors from the G-proteins. Internalization is, therefore, not a prerequisite for agonist-induced desensitization of MOR1.

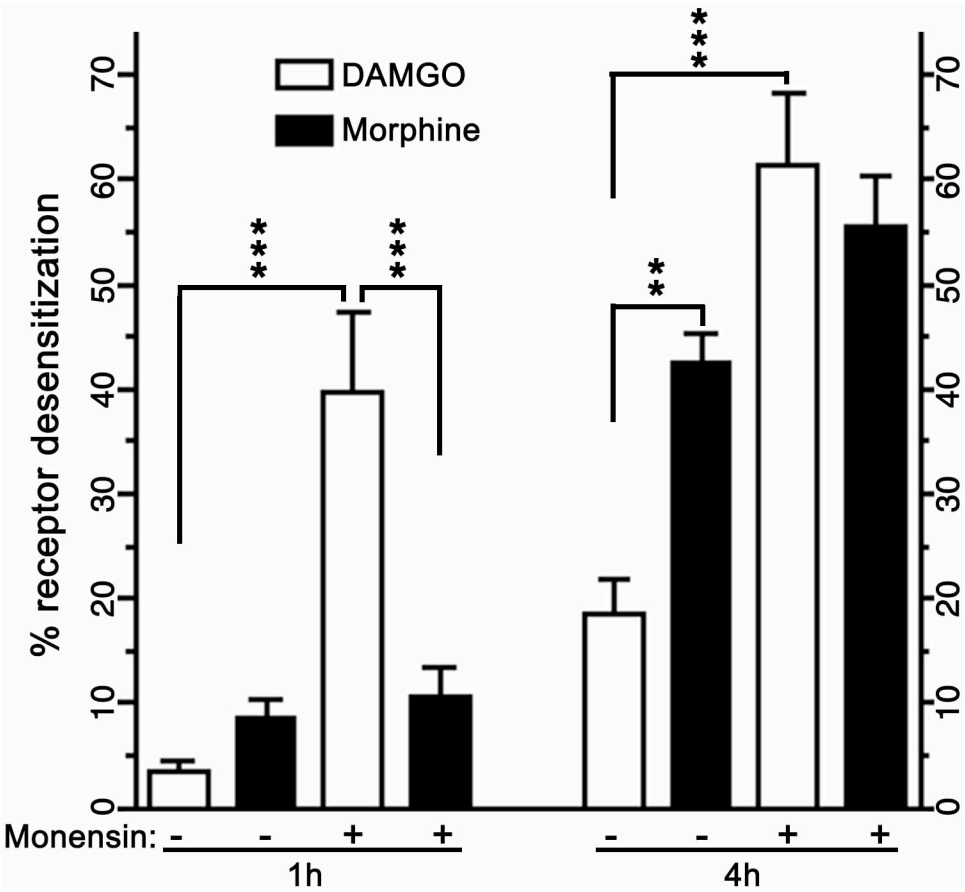

Figure 4.18. Comparison of DAMGO- and morphine-induced MOR1 desensitization. Cells stably co-expressing HA-MOR1 and Myc-M6a were treated with 5 μM DAMGO or morphine in the presence or absence of 50 μM monensin for 1 and 4h. The cAMP levels were determined as described under "Methods". Maximum agonist-induced inhibition of cAMP accumulation without agonist preincubation was defined as 100%. Values represent mean ± SEM of at least 3 independent measurements performed in duplicate. Double asterisks indicate a very significant difference ($p<0.01$), and triple asterisks indicate an extremely significant difference ($P<0.001$) as compared in this graph (One-way ANOVA followed by Bonferroni test).

4.16 Role of M6a in MOR1 internalization in primary cultured neurons

We have demonstrated the effect of M6a on MOR1 internalization and desensitization in HEK293 cells. MOR1 and M6a proteins are mainly expressed in neurons (Mansour et al., 1995b; Roussel et al., 1996; Drake and Milner, 1999; Kaplan et al., 2004). Non-neuronal cell models might not be appropriate for studying opioid receptor regulation owing to their potential lack of crucial components of regulatory pathway that exist in native neurons. Therefore, we investigated whether the observed co-localization and co-internalization of MOR1 and M6a in HEK293 cells also occur in primary cultured neurons.

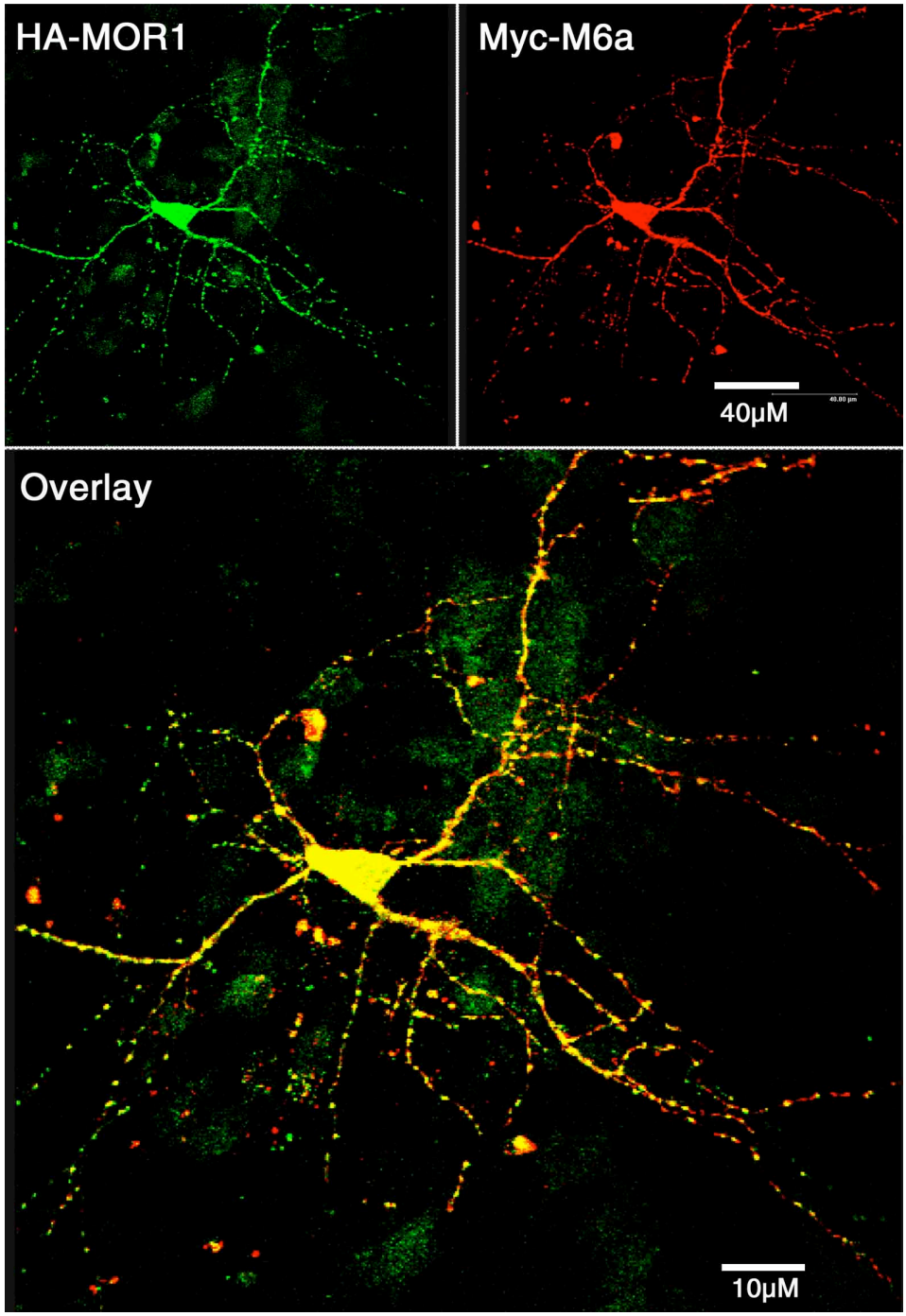

Figure 4.19. Subcellular distribution of HA-MOR1 and Myc-M6a in co-transfected primary cultured neurons. Newly prepared cortical cells (E17) were grown on poly-D-lysine-coated glass coverslips for about 100 hours, and then subjected to the co-transfection with pCMV-HA-MOR1 and pCMV-Myc-M6a plasmids. 40 hours after transfection, cells were fixed. HA-MOR1 and Myc-M6a were detected using anti-HA and anti-Myc antibodies as described under "Methods". The overlay image was shown in a higher magnification image (4 folds in comparison with single image). The green fluorescence (Cy2) represents the distribution of HA-MOR1, and the red fluorescence (Cy3) for Myc-M6a, the yellow for overlay. Shown is a representative result from one of three independent experiments.

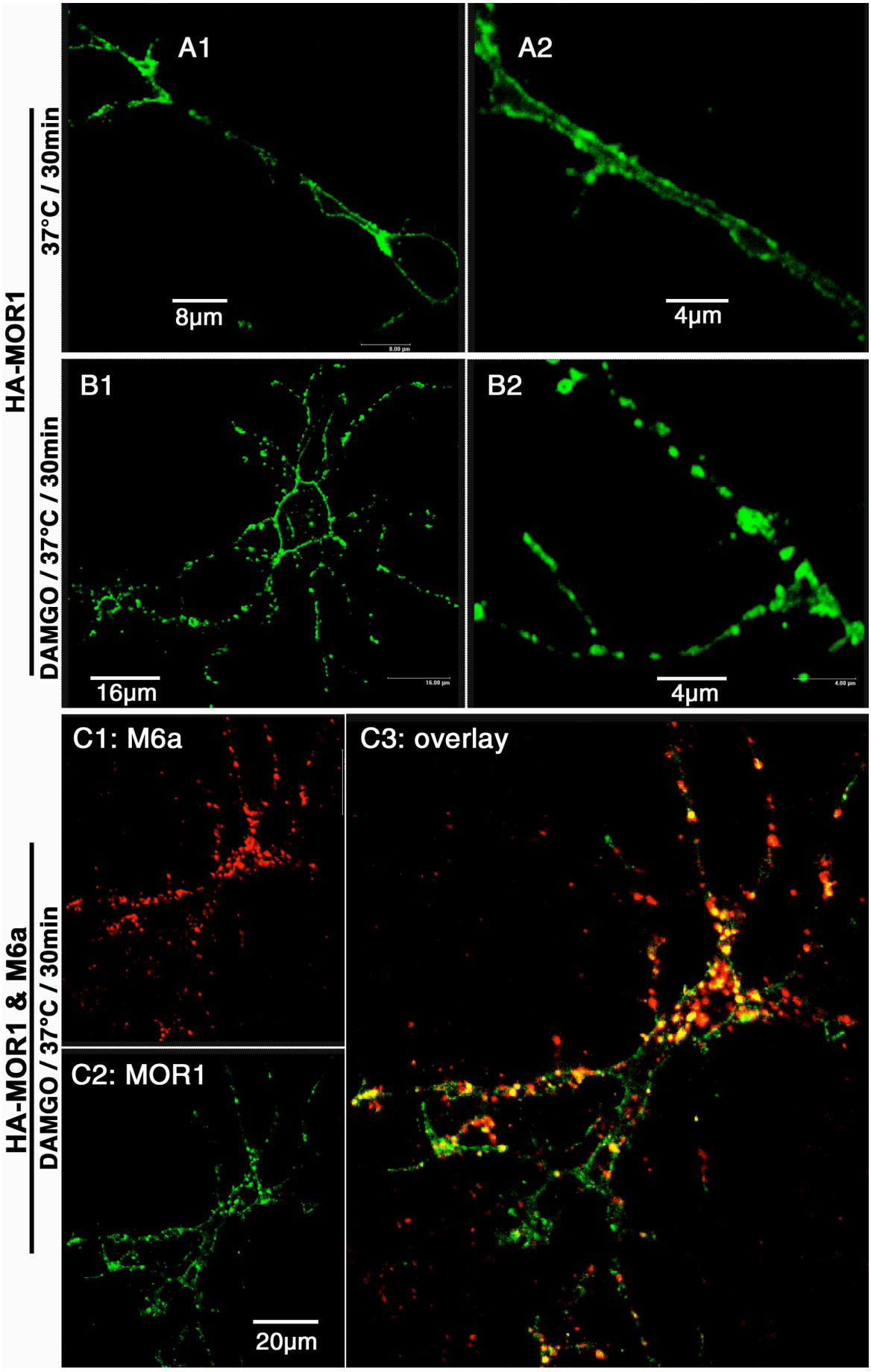
HA-MOR1
37°C / 30min
DAMGO / 37°C / 30min
A1
8µm
A2
4µm
B1
16µm
B2
4µm
HA-MOR1 & M6a
DAMGO / 37°C / 30min
C1: M6a
C2: MOR1
20µm
C3: overlay

Figure 4.20. The effect of M6a on MOR1 internalization in co-transfected primary cultured neurons. Newly prepared cortical cells (E17) were grown on poly-D-lysine-coated glass coverslips for about 100 hours, and then subjected to transfection with HA-MOR1 and/or M6a expressing plasmids. 40 hours after transfection, the surface HA-MOR1 and/or M6a were labeled at 4 °C with anti-HA and/or anti M6a antibody for 1 hour. Subsequently, cells were incubated in the presence or absence of 10 μM DAMGO at 37°C for 30 min, and then fixed immediately. Distribution of HA-MOR1 and/or M6a was detected by confocal microscopy as described under "Methods". In cells transiently expressing HA-MOR1 alone (A-B), the constitutive and agonist-induced internalization of HA-MOR1 were shown in A1 and B1, respectively. Part of the processes in A1 and B1 was shown in a higher magnification image (A2 and B2, respectively). In cells transiently co-expressing HA-MOR1 and M6a, the agonist-induced co-internalization of HA-MOR1 and M6a was shown in C. The overlay image of C1-C2 was shown in large magnification (4 folds versus C1 or C2). Note that: 1) HA-MOR1 and M6a are co-localized and co-internalized in transfected neurons. 2) M6a enhances agonist-induced internalization of HA-MOR1 in the cell body (C as compared to B). Shown are representative results from one of two independent experiments.

Since the endogenous μ-opioid receptor and the membrane glycoprotein M6a were under detectable level using available anti-MOR1 and anti-M6a antibodies in primary cultured cortical neurons (E17), we introduced exogenous MOR1 and M6a by transient transfection. As depicted in Figure 4.19, a remarkable co-localization between MOR1 and M6a was observed, both in the cell body and processes of primary cultured neuron transiently co-expressing HA-MOR1 and Myc-M6a.

To examine the internalization of MOR1 and/or M6a directly, we performed surface-labelling using anti-HA and/or anti-M6a antibodies to observe the internalization of surface MOR1 and/or M6a proteins. In cells transiently expressing HA-MOR1 alone, a constitutive internalization of receptors was hardly visible (Figure 4.20, A). However, 30 minutes after the incubation of 10 μM DAMGO, a clear agonist-mediated internalization of receptors could be detected (Figure 4.20, B). There was a pronounced internalization of the receptors in the processes of the neurons (Figure 4.20, B2) whereas only a few of receptors in the cell body were endocytosed (Figure 4.20, B1). In contrast, in cells co-expressing MOR1 and M6a, 10 μM DAMGO stimulated a remarkable co-internalization of the receptor and M6a in both of the cell body and processes (Figure 4.20, C1-C3). This observation provided the direct evidence that MOR1 and M6a co-internalized in transfected neurons, and M6a might enhance the receptor internalization. This is in line with the observed co-localization and co-internalization of MOR1 and M6a in HEK293 cells (Figure 4.11).

4.17 M6a attenuates MOR1 desensitization in primary cultured neurons

Next, we examined whether the M6a effect on receptor desensitization in the HEK293 cell model is physiologically relevant to native neurons.

As shown in Figure 4.21, DAMGO had no significant effect on forskolin-mediated cAMP accumulation in primary cultured cortical neurons. This suggested that the number of endogenous μ-opioid receptors in the cultured cortical neurons is too small to cause a significant decrease in cAMP levels. Thus, cortical neurons were transfected with MOR1 and M6a. In both of MOR1 and MOR1-M6a transfected cortical neurons, 10 μM DAMGO generated about 25% inhibition of forskolin-induced cAMP accumulation (Figure 4.21). This indicated that M6a has no effect on the ability of MOR1 to inhibit adenylate cyclase.

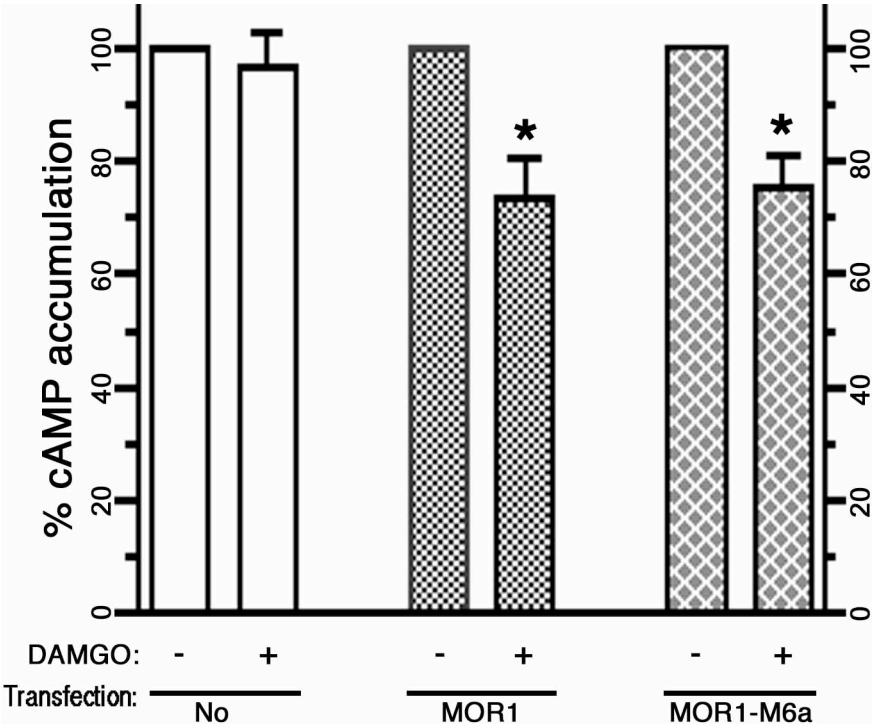

Figure 4.21. M6a does not influence inhibition of adenylate cyclase by MOR1 agonist in co-transfected primary cultured neurons. Newly prepared cortical neurons (E17) were transfected or not transfected with HA-MOR1 and/or Myc-M6a plasmid using a "Rat Neuron Nucleofector Solution", and then seeded in poly-D-lysine-coated plate. 4-5 days after transfection, cells were treated with 5 μM forskolin in the presence or absence of 10 μM DAMGO for 10 min. Forskolin-mediated cAMP accumulation was determined as described under "Methods". The cAMP accumulation in the absence of agonist was defined as 100%. Values represent mean ± SEM of 3-4 independent measurements performed in triplicate. Asterisk indicates a very significant difference ($p<0.01$) (One-way ANOVA followed by Bonferroni test).

As shown in Figure 4.22, after 1h of 10 μM DAMGO pretreatment, there was no significant difference in DAMGO-induced receptor desensitization betwen MOR1 and MOR1-M6a transfected cells. In marked contrast, 4 hours after agonist pretreatment, DAMGO-induced receptor desensitization was significantly reduced in MOR1-M6a co-

transfected cells as compared with MOR1 transfected cells. This was in agrement with the finding that over-expression of M6a decreased DAMGO-induced MOR1 desensitization in HEK293 cells (Figure 4.17). Thus, the mechanisms of agonist-induced receptor desensitization seen to be similar in HEK293 cells and primary cultured cortical neurons. This indicates that M6a regulates the signaling of the μ-opioid receptor in native neurons.

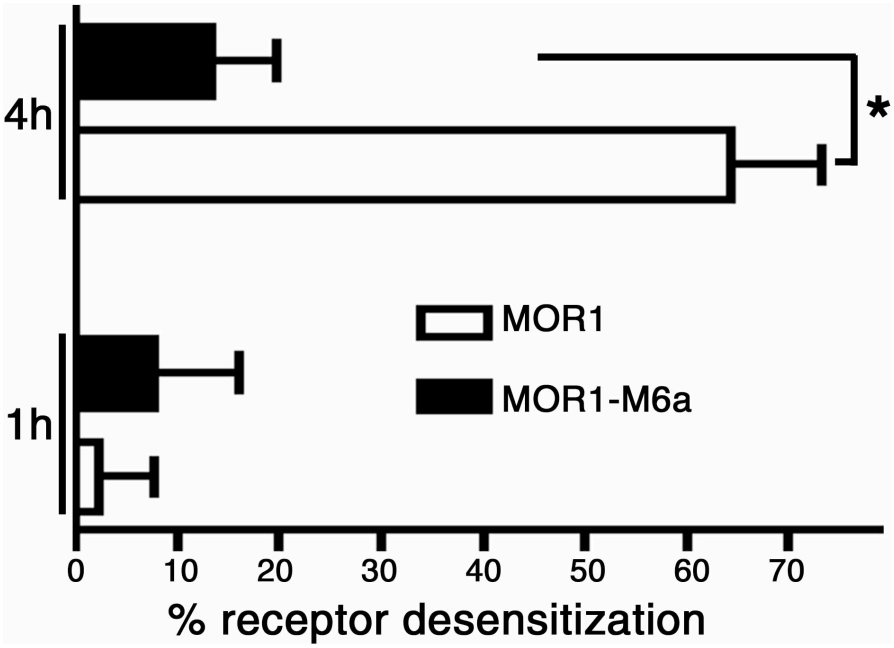

Figure 4.22. DAMGO-induced μ-opioid receptor desensitization in transfected primary cultured neurons. Newly prepared cortical neurons (E17) were transfected with HA-MOR1 and/or Myc-M6a plasmids using a "Rat Neuron Nucleofector Solution", and then seeded in poly-D-lysine-coated plate. 4-5 days after transfection, cells were preincubated with 10 μM DAMGO for 1 and 4 h. The agonist-induced receptor desensitization was determined as described under "Methods". Maximum agonist-induced inhibition of cAMP accumulation without agonist preincubation was defined as 100%. Values represent mean ± SEM of 5-6 independent measurements performed in triplicate. Asterisk indicates a very significant difference ($p<0.01$) (One-way ANOVA followed by Bonferroni test).

5 Discussion

5.1 Interaction of the *μ*-opioid receptor with the membrane glycoprotein M6a

In the present study, several lines of evidences suggest a direct interaction between MOR1 and M6a. First, the interaction between MOR1 and M6a was verified in yeast mating and ß-galactosidase assay (previous data from our group). Second, M6a was specifically pulled down by MOR1 in co-immunoprecipitation experiments. Third, M6a showed a strong positive signal with MOR1 in BRET assay. Moreover, the strict co-localization and co-internalization of MOR1 and M6a in both transfected HEK293 cells and primary cultured neurons provided additional support for the direct interaction of MOR1 and M6a. An interaction with MOR1 was found for M6a and M6b, but not for DM20, another close member from the same glycoprotein family. In rat brain, the interaction appears to be specific for M6a since double in situ hybridization revealed a co-localization of MOR1 with M6a, but not with M6b or PLP/DM20.

To investigate the binding domain of MOR1 with M6a, we constructed a number of truncation mutants of MOR1. Although the carboxyl terminus of MOR1 is not the direct binding region for M6a, the interaction of MOR1B (a splice variant of MOR1) with M6a was stronger than that with MOR1. This indicates that the carboxyl tail might influence the interacting-conformation of the μ-opioid receptor. MOR1 and MOR1B share 100% amino acid sequence identity up to amino acid 386 but differ by the last 12 amino acids at the carboxyl terminus (Figure 1.2) (Zimprich et al., 1995). The carboxyl terminal tail of the μ-opioid receptor has been shown to be an important domain for regulating receptor trafficking (Koch et al., 1998; Wolf et al., 1999; El Kouhen et al., 2001). In fact, MOR1B undergoes faster internalization and recycling both in the presence or absence of μ-agonist compared with MOR1 (Koch et al., 1998). Therefore, we speculate that MOR1B may form a highly favorable conformation to interact with M6a.

A truncated MOR1 containing the 4^{th} and 5^{th} transmembrane domains (amino acids 186-303) interacted with full length M6a (Figure 4.4B). Thus, it appears likely that the 4^{th} and 5^{th} transmembrane domains of MOR1 are important for the interaction with M6a. Unexpectedly, the BRET analysis revealed that M6a had two binding domains for MOR1 (Figure 4.4C). This was further supported by the finding of two dominant negative mutants of M6a on the DAMGO-induced MOR1-internalization (Figure 4.14). Both M6a negative mutants (amino acids 1-108 and 129-255) contain two transmembrane domains, suggesting that two transmembrane domains of M6a are necessary to form a binding conformation in MOR1-M6a interaction. We do not know whether under physiological condition only one binding domain of M6a is sufficient to form a functional complex between MOR1 and M6a. It is possible that both of them are necessary to form a functional complex. An alternative speculation is that these two binding domains might play a role in the formation of homo- or hetero-dimerization of GPCRs. This hypothesis is further supported by the

findings that M6a interacts with other GPCRs, and that MOR1 forms homo-dimers in the present studies.

5.2 Co-expression of MOR1 with members of the PLP/DM20 family in rat brain

Using specific riboprobes, different expression patterns of M6a, M6b and DM20 mRNAs were found in rat brain. Since we used a riboprobe directed against a sequence of both DM20 and PLP, both DM20 and PLP mRNAs were measured in our experiments. PLP/DM20 is strongly expressed in white matter (myelinated-oligodendrocyte containing) regions, including the corpus callosum and the fimbria/fornix. There is no co-expression of MOR1 and PLP/DM20 mRNAs. This is in agreement with previous reports showing that MOR1 is expressed in neurons whereas PLP/DM20 is expressed in oligodendrocytes (Arvidsson et al., 1995; Mansour et al., 1994, 1995a, 1995b; Yan et al., 1993, 1996). M6b mRNA is expressed in both of white and gray matter areas in rat brain. In all regions, co-expression between MOR1 and M6b is undetectable. However, we cannot exclude the possibility that there may be a co-expression between MOR1 and M6b in other regions not investigated.

The co-expression between MOR1 and M6a mRNAs occurs in many regions of rat brain, including thalamus and cerebral cortex (Figure 4.8). Since the distribution of MOR1 and M6a mRNAs is correlated well with their antigens in the central nervous system (Delfs et al., 1994; Mansour et al., 1995a, 1995b; Yan et al., 1996; Roussel et al., 1998; Stumm et al., 2004), it is reasonable to assume that MOR1 and M6a proteins are colocalized in native neurons, indicating an interaction between MOR1 and M6a under physiological conditions.

Interaction of receptors with scaffold, anchoring or adaptor proteins, such as M6a, is important for internalization and post-endocytotic sorting (see reviews in Brady and Limbird, 2002; Hall and Lefkowitz, 2002; Bockaert et al., 2004). Based on the frequent co-expression and strong interaction between MOR1 and M6a, a potential role of M6a in the regulation of μ-opioid receptors is reasonable.

5.3 The role of M6a in the trafficking of opioid receptors

Previous researchers have shown that the cytoplasmic tail of opioid receptors plays a key role in receptor trafficking and signaling. Recently, a number of proteins that bind to the cytoplasmic tail of opioid receptors have been identified by yeast two-hybrid screen, and functionally characterized. For example, a protein interacting with DOR1, the G protein-coupled receptor-associated sorting protein (GASP) was found to modulate the lysosomal sorting and functional down-regulation of DOR1 (Whistler et al., 2002). Phospholipase D2 interacts with MOR1 and accelerates agonist-induced μ-opioid receptor internalization (Koch et al., 2003). Filamin A, a cytoskeletal protein binds to MOR1 and to several other membrane proteins, appears to be necessary for normal MOR1 trafficking (Onoprishvili et al., 2003). Periplakin, a cytolinker protein, interacts with MOR1 and reduces the coupling of G proteins (Feng et al., 2003). Another protein which interacts with MOR1 is protein kinase C-interacting protein (PKCI) which functions as a negative

regulator in MOR1 desensitization, phosphorylation, and in mediating morphine analgesia (Guang et al., 2004). It seems that the carboxyl tail domain of opioid receptors is the predominant region involved in receptor regulation. If this is true, a chimeric DOR1 with the tail of MOR1 (DOR1/MT) should have an identical phenotype as wild type MOR1. However, this is not the case since the DOR1/MT is targeted to lysosome while MOR1 is not (Afify et al., 1998; Wang et al., 2003). In addition, the rate and magnitude of agonist-induced internalization of this chimera are not identical to that of the corresponding wild type receptors (Wang et al., 2003). Moreover, C-terminally truncated MOR1 (Qiu et al., 2003) and DOR1 (Murray et al., 1998) undergo receptor internalization. The important C-tail motif of MOR-derived endocytic recycling sequence (MRS) in opioid receptor post-endocytic sorting (Tanowitz and von Zastrow, 2003) fails to explain that MOR1B without this MRS shows faster recycling compared with MOR1 (Koch et al., 1998). All these suggest that other motifs in addition to the carboxyl tail could participate in the intracellular trafficking of the opioid receptors. This view is further supported by recent studies that the DOR1 carboxyl tail alone could not direct targeting of receptors to lysosomal compartments. Instead, a di-leucine motif within the 3rd intracellular loop in conjunction with the carboxyl tail sequence regulates the lysosomal targeting of DOR1 (Wang et al., 2003). Interestingly, although the di-leucine motif by itself could affect DOR1 internalization kinetics, it has minimal effects on the intracellular trafficking of MOR1 (Wang et al., 2003). These observations indicate that multiple motifs within opioid receptors regulate the receptor trafficking.

When MOR1 and M6a are co-expressed in HEK293 cells, MOR1 shows strict co-localization with M6a not only at the plasma membrane, but also in endosome-like vesicles of the cytosol. This result is surprising because MOR1 is normally found mainly at the cell surface in HEK293 cells (Koch et al., 1998, 2001, 2003). Hypertonic sucrose, an inhibitor of receptor internalization (Heuser and Anderson, 1989), significantly inhibits M6a-mediated distribution of MOR1 in cytoplasm, whereas monensin, an inhibitor of receptor recycling (Stein et al., 1984; Kaiser et al., 1988), greatly augments this distribution. This suggests a possible role of M6a in the constitutive trafficking of MOR1. Furthermore, we directly confirmed by both confocal microscopy and quantitative ELISA that over-expression of M6a enhances the constitutive internalization of MOR1. Thus, it is reasonable to speculate that M6a-enhanced distribution of MOR1 in cytosolic vesicles is due to M6a-augmented receptor internalization. M6a and proteolipid protein (PLP) belong to the PLP/DM20 family and show high homology. However, in contrast to M6a, over-expression of PLP induces an abnormal accumulation of PLP and cholesterol in the late endosomal/lysosomal compartment (Simons et al., 2002).

M6a also augments agonist-stimulated internalization of MOR1. In addition, using a pulse-chase experiment (Tsao and von Zastrow, 2000; Tulipano et al., 2004), we have demonstrated that M6a and MOR1 share a similar trafficking pathway like transferrin

receptors, which are rapidly recycled by recycling endosomes. Therefore, with the co-expression of M6a, endocytosed MOR1 might be sorted preferably to recycling endosomes for recycling. This is in line with the present findings that M6a enhances the recycling of endocytosed MOR1, and decreases the down-regulation of MOR1.

It is well demonstrated that the internalization of GPCRs is mediated by many biological molecules, such as kinase, β-arrestin, AP-2, clathrin and dynamin (reviewed in Ferguson, 2001; Claing et al., 2002; Mousavi et al., 2004). In contrast, the mechanism of post-endocytic sorting and recycling of internalized receptors is far from clear. There are some evidences that a specific sequence present in the cytoplasmic tail of MOR1 is necessary for rapid recycling of internalized receptors (Tanowitz and von Zastrow, 2003). From our experiments, M6a appears to be an important protein involved in the regulation of opioid receptor recycling.

As mentioned earlier, Whistler et al. (2002) identified a protein termed GASP (G protein-coupled receptor-associated sorting protein) that binds preferentially to the cytoplasmic tail of DOR1. The authors demonstrated that the strong interaction of DOR1-GASP modulates the post-endocytic sorting between receptors destined for lysosomal degradation and those to be recycled to the cell surface. Our data revealed that the strong interaction of MOR1-M6a leads to the sorting of MOR1 into endosomes for recycling, and inhibits MOR1 sorted into lysosomes for proteolytic degradation. Thus, it is reasonable to assume that the different intracellular trafficking between MOR1 and DOR1 may be caused by the competition between M6a and GASP during endosomal sorting of the receptors. Consistent with this, GASP binds much less strongly to the cytoplasmic tail of MOR1 than to DOR1 in vitro and apparently not at all in vivo (Whistler et al., 2002), and we observed a lower interaction of M6a with DOR1 compared to MOR1 (Figure 4.5). Therefore, a strong interaction of MOR1 with M6a might induce the rapid MOR1 recycling, whereas a strong interaction of DOR1 with GASP might target DOR1 into lysosomes for degradation during post-endocytic sorting diagrammed in Figure 5.1. Consistent with this hypothesis, over-expression of M6a led to the sorting of internalized DOR1 to recycling pathway (Figure 4.15B, lower panel), and over-expression of a dominant negative mutant of GASP inhibited the sorting of DOR1 to lysosomes (Whistler et al., 2002).

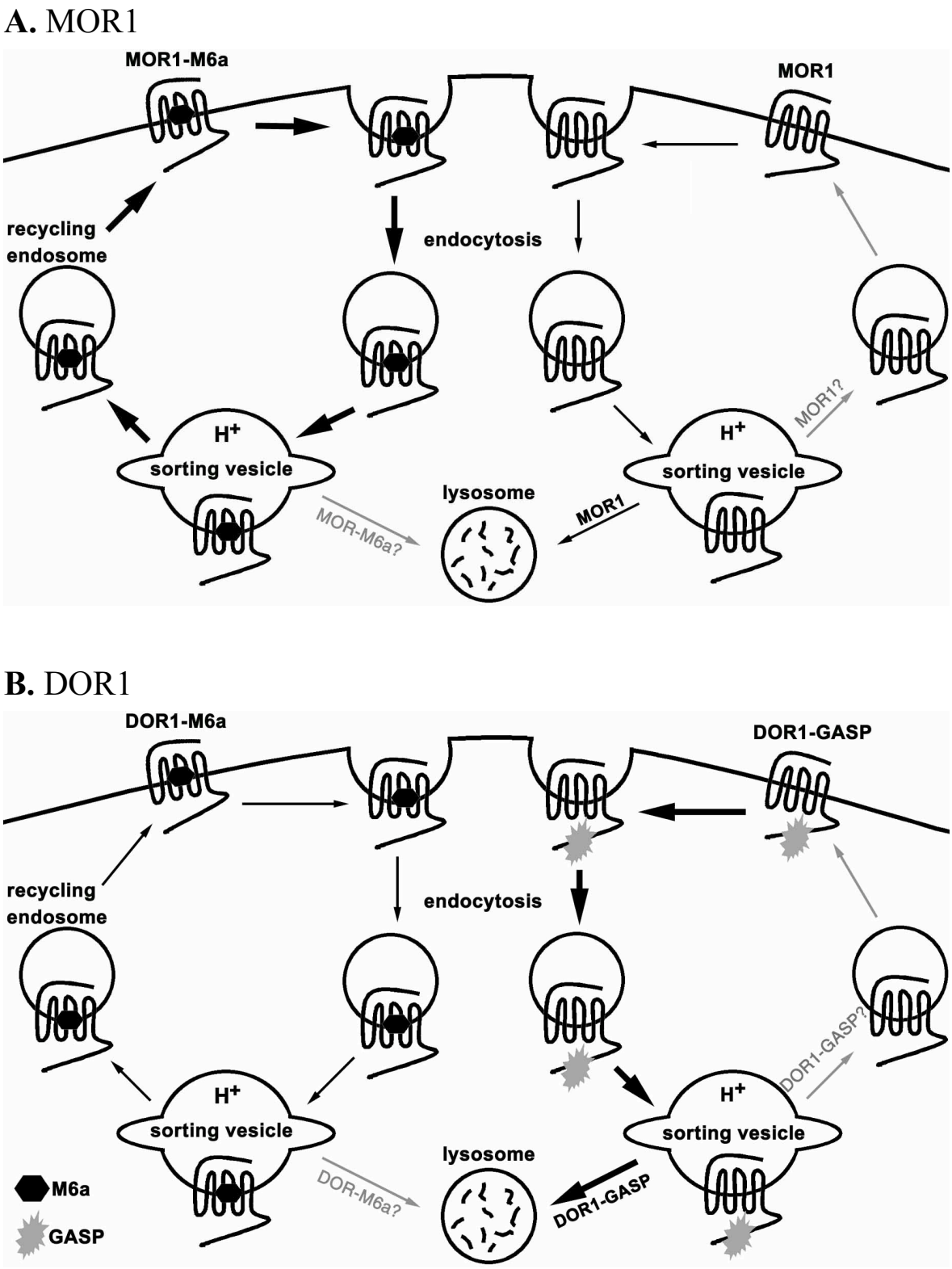

Figure 5.1. A model of the post-endocytic sorting of opioid receptors. A strong interaction between MOR1 and M6a lead to the sorting of MOR1 into endosomes for recycling whereas a strong interaction of DOR1 with GASP targets DOR1 into lysosomes for degradation during post-endocytic sorting. Thus, endocytosized MOR1 predominantly recycles to cell surface when internalized DOR1 is mainly sorted into lysosomes for proteolysis. Events unlikely to occur are indicated in gray line.

It is generally believed that glycoproteins of the PLP/DM20 family function as structural proteins for myelination. The present studies provide evidences supporting that the membrane glycoprotein M6a regulates μ-opioid receptor trafficking, thereby offering a new function of PLP/DM20 family other than its structural role in myelination. It appears that the interaction of MOR1 with M6a might be an important step in the initiation of clathrin-mediated receptor internalization and the following endosomal sorting of internalized receptors. Possibly, M6a is involved in actin cytoskeleton formation and thus induces receptor transport into cytoplasm. In support to this hypothesis, M6 protein (M6a/M6b) was observed to be concentrated selectively in the actin-rich, leading edge lamellipodia and philopodia of neuronal growth cones (Baumrind et al., 1992), and be transported there by actin-dependent mechanisms (Sheetz et al., 1990). This is also in line with the suggestion that a common feature of PLP/DM20 family is its association with the actin cytoskeleton (Kalwy et al., 1997). Another possibility is that, M6a might change the property of clathrin-coated vesicles and endosomes, e.g. charge and pH value, and thus influences vesicle transportation and endosome sorting. This hypothesis is supported by the observation that all tetraspan proteolipids, including members of PLP/DM20 family, contribute to the formation of pore structures in a wide spectrum of cellular system (Kitagawa et al., 1993). Moreover, Rhombex-29, a new member of PLP/DM20 family, was suggested to be responsible for transporting $^{+}$H (Shimokawa and Miura, 2000).

Taken together, we have demonstrated a function of M6a on opioid receptor trafficking in both transfected HEK293 cells and primary cultured neurons. M6a might also modulate the intracellular trafficking of other receptors. This view is supported by the observation that M6a interacts to another opioid receptor (DOR1) and with the somatostatin receptor 2A (sst2A). In addition, the interaction of M6a with sst2A is in line with the fact that the sst2A receptor shows a rapid internalization and recycling (Tulipano et al., 2004).

5.4 The effect of M6a on signal regulation of the *μ*-opioid receptor

While the functional property of M6a on MOR1 trafficking has been established most clearly using HEK293 cells, our studies in primary cultured neurons suggest that those also occur in native neurons. Moreover, in locus coeruleus neurons, an agonist's ability to produce rapid desensitization was found to correlate well with its effectiveness at promoting receptor internalization in HEK293 cells (Alvarez et al., 2002; Bailey et al., 2003). Thus, it is reasonable to believe that the HEK293 cell system is a good model for the analysis of the functional role of M6a in MOR1 signal regulation. M6a knockout mice (generously provided by Prof. Klaus-Armin Nave, Göttingen) are currently generated for future analysis. The effects of M6a on MOR1 signal regulation in vivo will be investigated in living animals.

5.4.1 Receptor down-regulation

In the present study we showed that over-expression of M6a attenuated the DAMGO-induced down-regulation of MOR1 in HEK293 cells. It is reasonable to speculate that M6a decreased receptor down-regulation because it augmented receptor recycling (Figure 4.12). The splice variants, MOR1D and MOR1E which show a more rapid internalization compared with MOR1 and MOR1C, induce a faster receptor down-regulation compared with MOR1 and MOR1C (Koch et al., 2001). One explanation for this observation is that the enhanced receptor internalization of MOR1D or MOR1E also increases receptor sorting to lysosomes for degradation whereas the strong interaction of MOR1 with M6a directs receptors to recycling pathway, and thus decreases receptor down-regulation. This model predicts a weaker interaction of M6a with MOR1D and MOR1E as compared with MOR1 and MOR1C. This hypothesis could be easily tested in co-expression studies.

5.4.2 Receptor desensitization

In the present study, we find that M6a augments both internalization and recycling of the μ-opioid receptor. This altered trafficking has clear consequences on the desensitization of MOR1. Thus, over-expression of M6a significantly decreased the rate of DAMGO-induced receptor desensitization in both HEK293 cells (Figure 4.17) and primary cultured neurons (Figure 4.22). Agonist-induced internalization of G protein-coupled receptors is a process that can contribute to desensitization of signal transduction by a loss of functional receptors at the plasma membrane (Law et al., 1984; Hoxie et al., 1993; Roettger et al., 1995; Pak et al., 1996). On the other hand, internalization also contributes to functional resensitization by promoting receptor recycling to cell surface (Ferguson et al., 1998; Lefkowitz et al., 1998; Koch et al., 1998, 2001; Law et al., 2000a). The slower rate of desensitization in M6a co-expressing cells is predominantly due to enhanced receptor recycling since the recycling blocker monensin markedly enhances the DAMGO-induced receptor desensitization in these cells (Figure 4.17). These findings confirm a series of recent reports showing that MOR1 desensitization is controlled by receptor internalization and recycling of internalized receptors to cell surface (Qiu et al., 2003; Beyer et al., 2004; Koch et al., 2004, 2005). Onoprishvili and colleagues (2003) recently reported that an enhanced internalization of MOR1 by co-expression of filamin A increases DAMGO-mediated receptor desensitization in melanoma cells. It might be that filamin A enhances receptor internalization without increasing receptor recycling. Consistent with this finding is the observation that over-expression of filamin A increases the μ-opioid receptor down-regulation (Onoprishvili et al., 2003), whereas M6a decreases receptor down-regulation in the present studies.

Peptide agonists, such as DAMGO, and many opioid alkaloids induce rapid endocytosis of the μ-opioid receptor in a number of cell types. By contrast, the alkaloid drug morphine is weak in promoting receptor internalization (Arden et al., 1995; Keith et

al., 1996, 1998; Whistler and von Zastrow, 1998; Bushell et al., 2002; Borgland et al., 2003; Celver et al., 2004). Since receptor trafficking is an important regulator of agonist-induced receptor desensitization, the significant differences of DAMGO- and morphine-mediated receptor trafficking should lead to differences in receptor desensitization. Whereas some studies have shown MOR1 desensitization by morphine (Avidor-Reiss et al., 1995; Koch et al., 2001, 2004, 2005; Borgland et al., 2003; Beyer et al., 2004; Dang and Williams, 2005), other reports claim that morphine is incapable of producing MOR1 desensitization (Blake et al., 1997; Whistler and von Zastrow, 1998; Zhang et al., 1998; Whistler et al., 1999; Finn and Whistler, 2001; Alvarez et al., 2002; Bailey et al., 2003). In our studies, we clearly found that chronic administration (4h) of morphine leads to a significant MOR1 desensitization, which occurs at a higher rate compared with that after DAMGO. This could be explained by the inability of morphine to induce MOR1 internalization and recycling which lead to receptor resensitization.

Phosphorylation of MOR1 by GRK2 is a necessary requirement of MOR1 internalization. Since morphine-activated MOR1 is known to be a poor substrate for GRK2-mediated phosphorylation (Whistler and von Zastrow, 1998; Zhang et al., 1998), morphine-mediated receptor phosphorylation might be insufficient for MOR1 receptor internalization. Recent findings in our group have shown that morphine results in a slow but persistent MOR1 phosphorylation at serine 375. This long-term phosphorylation causes prolonged desensitization, since the lack of internalization and recycling prevents receptor resensitization (Schulz et al., 2004).

An important factor influencing agonist-induced desensitization is the magnitude of expressed receptors. For instance, a high expression level of receptors has been shown to decrease the rate of agonist-induced receptor desensitization (Law et al., 2000a), and even masks receptor desensitization in short-term agonist exposure since a part of functional receptors is sufficient to produce maximal inhibition of adenylate cyclase.

In our experiments, we found a lower agonist-induced receptor desensitization than in previous experiments reported by Koch et al. (1998, 2001), since the expression level of MOR1 was 3-fold higher than in their experiments.

5.5 Molecular basis of opiate tolerance

Despite considerable progresses, the molecular and cellular mechanisms responsible for the development of opiate tolerance are incompletely understood (see reviews in Kieffer and Evans, 2002; Zuo, 2005). The classical hypothesis is that desensitization and internalization of the μ-opioid receptor contribute directly to tolerance by decreasing the number of functional surface receptors (see Kieffer and Evans, 2002 for a review). In contrast to this hypothesis, recent studies including that from our group have well demonstrated that agonist-induced μ-opioid receptor internalization plays an important role in reducing the development of opiate tolerance (Koch et al., 1998, 2001, 2004, 2005; Whistler et al., 1999; Finn and Whistler, 2001; Williams et al., 2001). Furthermore, it has

been reported that increased μ-opioid receptor endocytosis in response to morphine reduces the development of opiate tolerance in an animal model (He et al., 2002; He and Whistler, 2005).

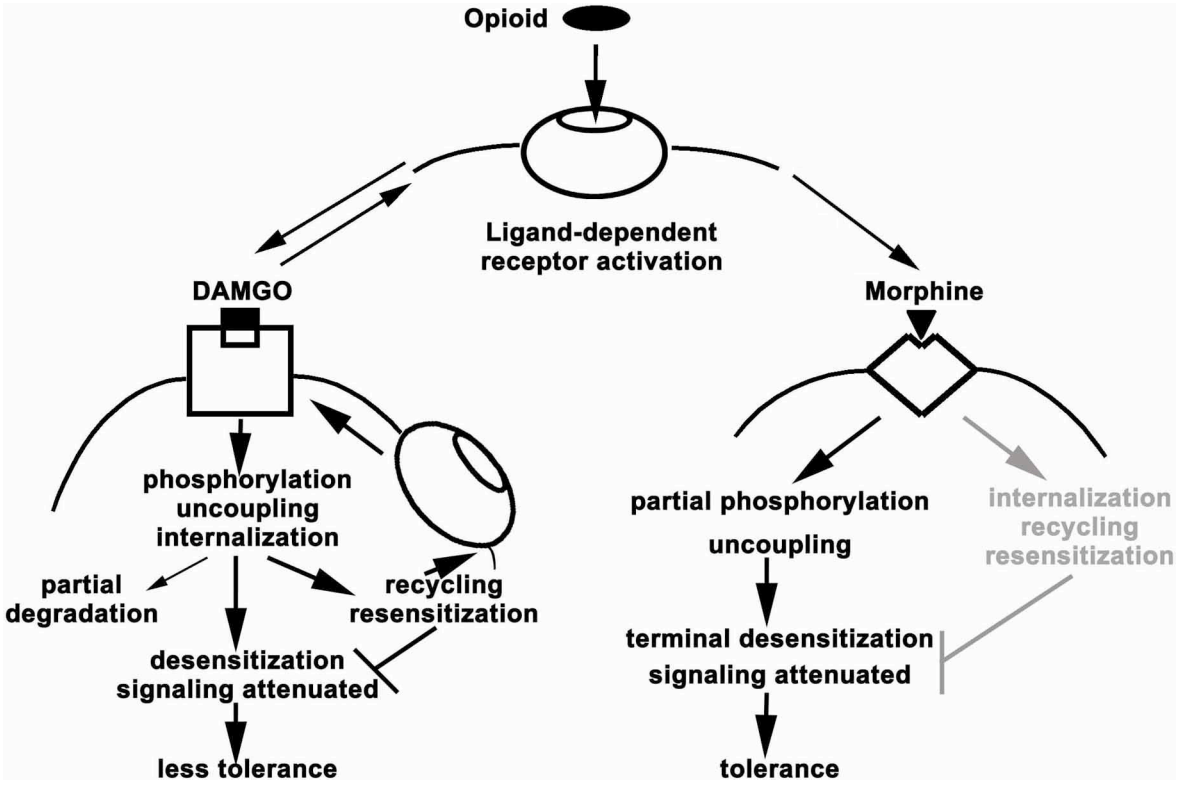

Figure 5.2. A hypothesis for opiate tolerance. In the presence of "internalizing" opioids, exemplified by DAMGO, signaling is continued rather than rapidly terminated because of receptor resensitization. Downstream adaptations, therefore, are limited by receptor recycling. In contrast, a "non-internalizing" opioid such as morphine is unable to efficiently trigger receptor resensitization, and thus leads to receptor desensitization finally. Tolerance develops from attenuated or terminated receptor signaling. The empty μ-opioid receptor is shown as a circle; while DAMGO- and morphine- bound receptors are schematized as a square and a diamond, respectively. Events unlikely to occur are indicated in gray.

Though it is clear that internalization of opioid receptors reduces the development of opiate tolerance, the mechanisms whereby this occurs are still controversially discussed. The RAVE (receptor activity versus endocytosis) model suggested that abnormally maintained signaling in the presence of non-internalizing agonists (e.g. morphine) leads to the development of opiate tolerance, whereas interrupted receptor signaling by receptor internalization attenuates opiate tolerance (Whistler et al., 1999; Kieffer and Evans, 2002). However, there are increasing evidences for an alternative model in which internalization followed by recycling continuously resensitizes the receptors and thus counteracts desensitization. For instance a recent publication demonstrated that the endocytotic efficacies of opioids are negatively correlated with the development of receptor desensitization (Koch et al., 2005). In line with this study, our experiments show that

agonist-induced MOR1 trafficking prolongs receptor signaling by augmenting receptor resensitization. As depicted in Figure 5.2, in our hypothesis, receptor uncoupling is mediated predominantly by phosphorylation, and internalization is the only way in which the μ-opioid receptor can be dephosphorylated and then resensitized. Agonists (e.g. morphine), which promote receptor phosphorylation but not receptor internalization, cause prolonged desensitization and signaling attenuation of opioid receptors. The attenuated signaling contributes to the development of opiate tolerance.

In summary, in cells co-expressing MOR1 and M6a, the attenuation of DAMGO-mediated receptor desensitization results from augmented receptor internalization and recycling by interaction with M6a. Morphine leads to a faster receptor desensitization after prolonged agonist exposure than DAMGO, since morphine is incapable to induce receptor trafficking. Furthermore, in the presence of the recycling inhibitor monensin, the internalizing agonist DAMGO induces rapid receptor desensitization whereas the non-internalizing agonist morphine does not. These results provide evidences that the trafficking of the μ-opioid receptor is negatively correlated with the development of agonist-induced receptor desensitization. Receptor desensitization is crucially important in opioid pharmacology, since it contributes to the development of opiate tolerance (Yu et al., 1997; Polakiewicz et al., 1998; Whistler et al., 1999; Bohn et al., 1999, 2000; Fin and Whistler, 2001; He et al., 2002; Koch et al., 1998, 2001, 2004, 2005). We therefore hypothesize that the interaction between MOR1 and M6a attenuates the development of opiate tolerance since M6a-enhanced receptor trafficking decreases receptor desensitization and prolongs receptor signaling.

6 Summary

Opiates such as morphine are still the best analgesic choice in the treatment of chronic and serious pain. The clinical utility of opiates is limited by adaptive changes in the nervous system occurring after prolonged or repeated drug administration. These adaptations are believed to contribute to physiological tolerance and dependence to opiates. All of these adaptive changes are initiated by the binding of opiate drugs to opioid receptors that are also activated by endogenous opioid neuropeptides. The μ-opioid receptor (MOR1) is of primary importance for mediating analgesic and addictive effects of clinically important opiate drugs. Understanding the mechanisms of MOR1 regulation is a key step to develop drugs and/or therapy, which result in effective analgesia without the detrimental adaptive responses.

There is increasing evidence that receptor-associated proteins modulate the signal transduction of MOR1. Several proteins which interact with MOR1 including the membrane glycoprotein M6a (M6a) were previously identified by our group using a yeast two-hybrid assay. To confirm the protein-protein interactions in mammalian cells, the proteins were tagged with bioluminescent/fluorescent epitopes and their interactions were assayed by a bioluminescence resonance energy transfer (BRET) technique. Of all proteins investigated, M6a showed the strongest interaction with MOR1. This interaction was also confirmed by co-immunoprecipitation experiments. Furthermore, the transmembrane domains of MOR1 and M6a that are important for the interaction were characterized. In addition, we demonstrated the interaction of M6a with a number of GPCRs, suggesting that M6a might play a general role in the regulation of GPCRs.

M6a is a member of the proteolipid protein (PLP)/DM20 family of unclear function. Double in situ hybridization showed a widespread co-expression between MOR1 and M6a in many regions of rat brain. In addition, in transfected HEK293 cells, MOR1 co-internalizes with M6a, and then co-recycles to cell surface by recycling endosomes. This is associated with an augmented internalization and recycling of the μ-opioid receptor. In HEK293 cells, a physiological role of endogenous M6a in MOR1 internalization was revealed since over-expression of M6a dominant negative mutants prevents agonist-mediated endocytosis of MOR1. In addition, by enhancing receptor recycling M6a decreases receptor degradation in lysosomes, consistent with the observed decrease in down-regulation of MOR1. M6a also binds to and co-internalizes with the δ-opioid receptor (DOR1). The interaction between DOR1 and M6a directs receptor post-endocytotic sorting into recycling pathway, which further provides support for a role of M6a in receptor recycling.

M6a-augmented MOR1 trafficking results in decreased receptor desensitization. Importantly, while the functional property of M6a on the trafficking and signal regulation of the μ-opioid receptor has been established in HEK293 cells, our studies in primary cultured neurons suggest a similar function also in native neurons.

Taken together, M6a might function as an adaptor protein in receptor trafficking, and be involved in reducing the development of opiate tolerance. Therefore, our work revealed a new function of the PLP/DM20 glycoprotein family other than its structural role in myelination.

7 References

Abbadie, C., Pan, Y., Drake, C. T., and Pasternak, G. W. (2000). Comparative immunohistochemical distributions of carboxy terminus epitopes from the mu-opioid receptor splice variants MOR-1D, MOR-1 and MOR-1C in the mouse and rat CNS. Neuroscience *100*, 141-153.

Afify, E. A., Law, P. Y., Riedl, M., Elde, R., and Loh, H. H. (1998). Role of carboxyl terminus of mu- and delta-opioid receptor in agonist-induced down-regulation. Brain Res Mol Brain Res *54*, 24-34.

Ahn, S., Nelson, C. D., Garrison, T. R., Miller, W. E., and Lefkowitz, R. J. (2003). Desensitization, internalization, and signaling functions of beta-arrestins demonstrated by RNA interference. Proc Natl Acad Sci U S A *100*, 1740-1744.

Alvarez, V. A., Arttamangkul, S., Dang, V., Salem, A., Whistler, J. L., Von Zastrow, M., Grandy, D. K., and Williams, J. T. (2002). mu-Opioid receptors: Ligand-dependent activation of potassium conductance, desensitization, and internalization. J Neurosci *22*, 5769-5776.

Arden, J. R., Segredo, V., Wang, Z., Lameh, J., and Sadee, W. (1995). Phosphorylation and agonist-specific intracellular trafficking of an epitope-tagged mu-opioid receptor expressed in HEK 293 cells. J Neurochem *65*, 1636-1645.

Arvidsson, U., Riedl, M., Chakrabarti, S., Lee, J. H., Nakano, A. H., Dado, R. J., Loh, H. H., Law, P. Y., Wessendorf, M. W., and Elde, R. (1995). Distribution and targeting of a mu-opioid receptor (MOR1) in brain and spinal cord. J Neurosci *15*, 3328-3341.

Avidor-Reiss, T., Bayewitch, M., Levy, R., Matus-Leibovitch, N., Nevo, I., and Vogel, Z. (1995). Adenylylcyclase supersensitization in mu-opioid receptor-transfected Chinese hamster ovary cells following chronic opioid treatment. J Biol Chem *270*, 29732-29738.

Avidor-Reiss, T., Nevo, I., Levy, R., Pfeuffer, T., and Vogel, Z. (1996). Chronic opioid treatment induces adenylyl cyclase V superactivation. Involvement of Gbetagamma. J Biol Chem *271*, 21309-21315.

Bailey, C. P., and Connor, M. (2005). Opioids: cellular mechanisms of tolerance and physical dependence. Curr Opin Pharmacol *5*, 60-68.

Bailey, C. P., Couch, D., Johnson, E., Griffiths, K., Kelly, E., and Henderson, G. (2003). Mu-opioid receptor desensitization in mature rat neurons: lack of interaction between DAMGO and morphine. J Neurosci *23*, 10515-10520.

Bare, L. A., Mansson, E., and Yang, D. (1994). Expression of two variants of the human mu opioid receptor mRNA in SK-N-SH cells and human brain. FEBS Lett *354*, 213-216.

Baumrind, N. L., Parkinson, D., Wayne, D. B., Heuser, J. E., and Pearlman, A. L. (1992). EMA: a developmentally regulated cell-surface glycoprotein of CNS neurons that is concentrated at the leading edge of growth cones. Dev Dyn *194*, 311-325.

Beyer, A., Koch, T., Schröder, H., Schulz, S., and Höllt, V. (2004). Effect of the A118G polymorphism on binding affinity, potency and agonist-mediated endocytosis, desensitization, and resensitization of the human mu-opioid receptor. J Neurochem *89*, 553-560.

Blake, A. D., Bot, G., Freeman, J. C., and Reisine, T. (1997). Differential opioid agonist regulation of the mouse mu opioid receptor. J Biol Chem *272*, 782-790.

Bockaert, J., Fagni, L., Dumuis, A., and Marin, P. (2004). GPCR interacting proteins (GIP). Pharmacol Ther *103*, 203-221.

Böhm, S. K., Grady, E. F., and Bunnett, N. W. (1997). Regulatory mechanisms that modulate signalling by G-protein-coupled receptors. Biochem J *322 (Pt 1)*, 1-18.

Bohn, L. M., Dykstra, L. A., Lefkowitz, R. J., Caron, M. G., and Barak, L. S. (2004). Relative opioid efficacy is determined by the complements of the G protein-coupled receptor desensitization machinery. Mol Pharmacol *66*, 106-112.

Bohn, L. M., Gainetdinov, R. R., Lin, F. T., Lefkowitz, R. J., and Caron, M. G. (2000). Mu-opioid receptor desensitization by beta-arrestin-2 determines morphine tolerance but not dependence. Nature *408*, 720-723.

Bohn, L. M., Lefkowitz, R. J., Gainetdinov, R. R., Peppel, K., Caron, M. G., and Lin, F. T. (1999). Enhanced morphine analgesia in mice lacking beta-arrestin 2. Science *286*, 2495-2498.

Bolan, E. A., Pan, Y. X., and Pasternak, G. W. (2004). Functional analysis of MOR-1 splice variants of the mouse mu opioid receptor gene Oprm. Synapse *51*, 11-18.

Borgland, S. L., Connor, M., Osborne, P. B., Furness, J. B., and Christie, M. J. (2003). Opioid agonists have different efficacy profiles for G protein activation, rapid desensitization, and endocytosis of mu-opioid receptors. J Biol Chem *278*, 18776-18784.

Boute, N., Jockers, R., and Issad, T. (2002). The use of resonance energy transfer in high-throughput screening: BRET versus FRET. Trends Pharmacol Sci *23*, 351-354.

Brady, A. E., and Limbird, L. E. (2002). G protein-coupled receptor interacting proteins: emerging roles in localization and signal transduction. Cell Signal *14*, 297-309.

Brüggemann, I., Schulz, S., Wiborny, D., and Höllt, V. (2000). Colocalization of the mu-opioid receptor and calcium/calmodulin-dependent kinase II in distinct pain-processing brain regions. Brain Res Mol Brain Res *85*, 239-250.

Bushell, T., Endoh, T., Simen, A. A., Ren, D., Bindokas, V. P., and Miller, R. J. (2002). Molecular components of tolerance to opiates in single hippocampal neurons. Mol Pharmacol *61*, 55-64.

Campagnoni, A. T. (1988). Molecular biology of myelin proteins from the central nervous system. J Neurochem *51*, 1-14.

Campagnoni, A. T., and Skoff, R. P. (2001). The pathobiology of myelin mutants reveal novel biological functions of the MBP and PLP genes. Brain Pathol *11*, 74-91.

Capeyrou, R., Riond, J., Corbani, M., Lepage, J. F., Bertin, B., and Emorine, L. J. (1997). Agonist-induced signaling and trafficking of the mu-opioid receptor: role of serine and threonine residues in the third cytoplasmic loop and C-terminal domain. FEBS Lett *415*, 200-205.

Celver, J., Xu, M., Jin, W., Lowe, J., and Chavkin, C. (2004). Distinct domains of the mu-opioid receptor control uncoupling and internalization. Mol Pharmacol *65*, 528-537.

Chen, Y., Mestek, A., Liu, J., Hurley, J. A., and Yu, L. (1993a). Molecular cloning and functional expression of a mu-opioid receptor from rat brain. Mol Pharmacol *44*, 8-12.

Chen, Y., Mestek, A., Liu, J., and Yu, L. (1993b). Molecular cloning of a rat kappa opioid receptor reveals sequence similarities to the mu and delta opioid receptors. Biochem J *295 (Pt 3)*, 625-628.

Cheng, Z. J., Yu, Q. M., Wu, Y. L., Ma, L., and Pei, G. (1998). Selective interference of beta-arrestin 1 with kappa and delta but not mu opioid receptor/G protein coupling. J Biol Chem *273*, 24328-24333.

Childers, S. R. (1991). Opioid receptor-coupled second messenger systems. Life Sci *48*, 1991-2003.

Claing, A., Laporte, S. A., Caron, M. G., and Lefkowitz, R. J. (2002). Endocytosis of G protein-coupled receptors: roles of G protein-coupled receptor kinases and beta-arrestin proteins. Prog Neurobiol *66*, 61-79.

Craig, A. D., Bushnell, M. C., Zhang, E. T., and Blomqvist, A. (1994). A thalamic nucleus specific for pain and temperature sensation. Nature *372*, 770-773.

Cvejic, S., and Devi, L. A. (1997). Dimerization of the delta opioid receptor: implication for a role in receptor internalization. J Biol Chem *272*, 26959-26964.

Dang, V. C., and Williams, J. T. (2005). Morphine-induced {micro}-opioid receptor desensitization. Mol Pharmacol.

Davis, K. D., Kwan, C. L., Crawley, A. P., and Mikulis, D. J. (1998). Functional MRI study of thalamic and cortical activations evoked by cutaneous heat, cold, and tactile stimuli. J Neurophysiol *80*, 1533-1546.

Delfs, J. M., Kong, H., Mestek, A., Chen, Y., Yu, L., Reisine, T., and Chesselet, M. F. (1994). Expression of mu opioid receptor mRNA in rat brain: an in situ hybridization study at the single cell level. J Comp Neurol *345*, 46-68.

Deng, H. B., Yu, Y., Pak, Y., O'Dowd, B. F., George, S. R., Surratt, C. K., Uhl, G. R., and Wang, J. B. (2000). Role for the C-terminus in agonist-induced mu opioid receptor phosphorylation and desensitization. Biochemistry *39*, 5492-5499.

Deng, H. B., Yu, Y., Wang, H., Guang, W., and Wang, J. B. (2001). Agonist-induced mu opioid receptor phosphorylation and functional desensitization in rat thalamus. Brain Res *898*, 204-214.

Diaz, R. S., Monreal, J., and Lucas, M. (1990). Calcium movements mediated by proteolipid protein and nucleotides in liposomes prepared with the endogenous lipids from brain white matter. J Neurochem *55*, 1304-1309.

Diehl, H. J., Schaich, M., Budzinski, R. M., and Stoffel, W. (1986). Individual exons encode the integral membrane domains of human myelin proteolipid protein. Proc Natl Acad Sci U S A *83*, 9807-9811.

Drake, C. T., and Milner, T. A. (1999). Mu opioid receptors are in somatodendritic and axonal compartments of GABAergic neurons in rat hippocampal formation. Brain Res *849*, 203-215.

Dunn, K. W., McGraw, T. E., and Maxfield, F. R. (1989). Iterative fractionation of recycling receptors from lysosomally destined ligands in an early sorting endosome. J Cell Biol *109*, 3303-3314.

El Kouhen, R., Burd, A. L., Erickson-Herbrandson, L. J., Chang, C. Y., Law, P. Y., and Loh, H. H. (2001). Phosphorylation of Ser363, Thr370, and Ser375 residues within the carboxyl tail differentially regulates mu-opioid receptor internalization. J Biol Chem *276*, 12774-12780.

Evans, C. J., Keith, D. E., Jr., Morrison, H., Magendzo, K., and Edwards, R. H. (1992). Cloning of a delta opioid receptor by functional expression. Science *258*, 1952-1955.

Feng, G. J., Kellett, E., Scorer, C. A., Wilde, J., White, J. H., and Milligan, G. (2003). Selective interactions between helix VIII of the human mu-opioid receptors and the C terminus of periplakin disrupt G protein activation. J Biol Chem *278*, 33400-33407.

Ferguson, S. S. (2001). Evolving concepts in G protein-coupled receptor endocytosis: the role in receptor desensitization and signaling. Pharmacol Rev *53*, 1-24.

Ferguson, S. S., Zhang, J., Barak, L. S., and Caron, M. G. (1998). Molecular mechanisms of G protein-coupled receptor desensitization and resensitization. Life Sci *62*, 1561-1565.

Finn, A. K., and Whistler, J. L. (2001). Endocytosis of the mu opioid receptor reduces tolerance and a cellular hallmark of opiate withdrawal. Neuron *32*, 829-839.

Freedman, N. J., and Lefkowitz, R. J. (1996). Desensitization of G protein-coupled receptors. Recent Prog Horm Res *51*, 319-351; discussion 352-313.

Fukuda, K., Kato, S., Mori, K., Nishi, M., and Takeshima, H. (1993). Primary structures and expression from cDNAs of rat opioid receptor delta- and mu-subtypes. FEBS Lett *327*, 311-314.

Gagescu, R., Demaurex, N., Parton, R. G., Hunziker, W., Huber, L. A., and Gruenberg, J. (2000). The recycling endosome of Madin-Darby canine kidney cells is a mildly acidic compartment rich in raft components. Mol Biol Cell *11*, 2775-2791.

Garbern, J., Cambi, F., Shy, M., and Kamholz, J. (1999). The molecular pathogenesis of Pelizaeus-Merzbacher disease. Arch Neurol *56*, 1210-1214.

George, S. R., O'Dowd, B. F., and Lee, S. P. (2002). G-protein-coupled receptor oligomerization and its potential for drug discovery. Nat Rev Drug Discov *1*, 808-820.

Golub, T., Wacha, S., and Caroni, P. (2004). Spatial and temporal control of signaling through lipid rafts. Curr Opin Neurobiol *14*, 542-550.

Gomes, I., Gupta, A., Filipovska, J., Szeto, H. H., Pintar, J. E., and Devi, L. A. (2004). A role for heterodimerization of mu and delta opiate receptors in enhancing morphine analgesia. Proc Natl Acad Sci U S A *101*, 5135-5139.

Gomes, I., Jordan, B. A., Gupta, A., Trapaidze, N., Nagy, V., and Devi, L. A. (2000). Heterodimerization of mu and delta opioid receptors: A role in opiate synergy. J Neurosci *20*, RC110.

Goodman, O. B., Jr., Krupnick, J. G., Gurevich, V. V., Benovic, J. L., and Keen, J. H. (1997). Arrestin/clathrin interaction. Localization of the arrestin binding locus to the clathrin terminal domain. J Biol Chem *272*, 15017-15022.

Goodman, O. B., Jr., Krupnick, J. G., Santini, F., Gurevich, V. V., Penn, R. B., Gagnon, A. W., Keen, J. H., and Benovic, J. L. (1996). Beta-arrestin acts as a clathrin adaptor in endocytosis of the beta2-adrenergic receptor. Nature *383*, 447-450.

Gourlay, G. K. (2005). Advances in opioid pharmacology. Support Care Cancer *13*, 153-159.

Greer, J. M., and Lees, M. B. (2002). Myelin proteolipid protein--the first 50 years. Int J Biochem Cell Biol *34*, 211-215.

Guang, W., Wang, H., Su, T., Weinstein, I. B., and Wang, J. B. (2004). Role of mPKCI, a novel mu-opioid receptor interactive protein, in receptor desensitization, phosphorylation, and morphine-induced analgesia. Mol Pharmacol *66*, 1285-1292.

Gurevich, V. V., and Benovic, J. L. (1997). Mechanism of phosphorylation-recognition by visual arrestin and the transition of arrestin into a high affinity binding state. Mol Pharmacol *51*, 161-169.

Hall, R. A., and Lefkowitz, R. J. (2002). Regulation of G protein-coupled receptor signaling by scaffold proteins. Circ Res *91*, 672-680.

Harrison, L. M., Kastin, A. J., and Zadina, J. E. (1998). Opiate tolerance and dependence: receptors, G-proteins, and antiopiates. Peptides *19*, 1603-1630.

Hasbi, A., Allouche, S., Sichel, F., Stanasila, L., Massotte, D., Landemore, G., Polastron, J., and Jauzac, P. (2000). Internalization and recycling of delta-opioid receptor are dependent on a phosphorylation-dephosphorylation mechanism. J Pharmacol Exp Ther *293*, 237-247.

He, L., Fong, J., von Zastrow, M., and Whistler, J. L. (2002). Regulation of opioid receptor trafficking and morphine tolerance by receptor oligomerization. Cell *108*, 271-282.

He, L., and Whistler, J. L. (2005). An opiate cocktail that reduces morphine tolerance and dependence. Curr Biol *15*, 1028-1033.

Helynck, G., Luu, B., Nussbaum, J. L., Picken, D., Skalidis, G., Trifilieff, E., Van Dorsselaer, A., Seta, P., Sandeaux, R., Gavach, C.*, et al.* (1983). Brain proteolipids. Isolation, purification and effect on ionic permeability of membranes. Eur J Biochem *133*, 689-695.

Heuser, J. E., and Anderson, R. G. (1989). Hypertonic media inhibit receptor-mediated endocytosis by blocking clathrin-coated pit formation. J Cell Biol *108*, 389-400.

Heydorn, A., Sondergaard, B. P., Ersboll, B., Holst, B., Nielsen, F. C., Haft, C. R., Whistler, J., and Schwartz, T. W. (2004). A library of 7TM receptor C-terminal tails. Interactions with the proposed post-endocytic sorting proteins ERM-binding phosphoprotein 50 (EBP50), N-ethylmaleimide-sensitive factor (NSF), sorting nexin 1 (SNX1), and G protein-coupled receptor-associated sorting protein (GASP). J Biol Chem *279*, 54291-54303.

Hodes, M. E., and Dlouhy, S. R. (1996). The proteolipid protein gene: double, double, ... and trouble. Am J Hum Genet *59*, 12-15.

Hopkins, C. R., and Trowbridge, I. S. (1983). Internalization and processing of transferrin and the transferrin receptor in human carcinoma A431 cells. J Cell Biol *97*, 508-521.

Hoxie, J. A., Ahuja, M., Belmonte, E., Pizarro, S., Parton, R., and Brass, L. F. (1993). Internalization and recycling of activated thrombin receptors. J Biol Chem *268*, 13756-13763.

Inoue, K. (2005). PLP1-related inherited dysmyelinating disorders: Pelizaeus-Merzbacher disease and spastic paraplegia type 2. Neurogenetics *6*, 1-16.

Inouye, H., and Kirschner, D. A. (1991). Folding and function of the myelin proteins from primary sequence data. J Neurosci Res *28*, 1-17.

Johnston, C. A., and Watts, V. J. (2003). Sensitization of adenylate cyclase: a general mechanism of neuroadaptation to persistent activation of Galpha(i/o)-coupled receptors? Life Sci *73*, 2913-2925.

Jordan, B. A., and Devi, L. A. (1999). G-protein-coupled receptor heterodimerization modulates receptor function. Nature *399*, 697-700.

Kaiser, J., Stockert, R. J., and Wolkoff, A. W. (1988). Effect of monensin on receptor recycling during continuous endocytosis of asialoorosomucoid. Exp Cell Res *174*, 472-480.

Kalwy, S. A., Smith, R., and Kidd, G. J. (1997). Myelin proteolipid protein expressed in COS-1 cells is targeted to actin-associated surfaces. J Neurosci Res *48*, 201-211.

Kaplan, T. J., Skyers, P. R., Tabori, N. E., Drake, C. T., and Milner, T. A. (2004). Ultrastructural evidence for mu-opioid modulation of cholinergic pathways in rat dentate gyrus. Brain Res *1019*, 28-38.

Keith, D. E., Anton, B., Murray, S. R., Zaki, P. A., Chu, P. C., Lissin, D. V., Monteillet-Agius, G., Stewart, P. L., Evans, C. J., and von Zastrow, M. (1998). mu-Opioid receptor internalization: opiate drugs have differential effects on a conserved endocytic mechanism in vitro and in the mammalian brain. Mol Pharmacol *53*, 377-384.

Keith, D. E., Murray, S. R., Zaki, P. A., Chu, P. C., Lissin, D. V., Kang, L., Evans, C. J., and von Zastrow, M. (1996). Morphine activates opioid receptors without causing their rapid internalization. J Biol Chem *271*, 19021-19024.

Kieffer, B. L. (1999). Opioids: first lessons from knockout mice. Trends Pharmacol Sci *20*, 19-26.

Kieffer, B. L., Befort, K., Gaveriaux-Ruff, C., and Hirth, C. G. (1992). The delta-opioid receptor: isolation of a cDNA by expression cloning and pharmacological characterization. Proc Natl Acad Sci U S A *89*, 12048-12052.

Kieffer, B. L., and Evans, C. J. (2002). Opioid tolerance-in search of the holy grail. Cell *108*, 587-590.

Kieffer, B. L., and Gaveriaux-Ruff, C. (2002). Exploring the opioid system by gene knockout. Prog Neurobiol *66*, 285-306.

Kim, D. S., Chin, H., and Klee, W. A. (1995). Agonist regulation of the expression of the delta opioid receptor in NG108-15 cells. FEBS Lett *376*, 11-14.

Kitagawa, K., Sinoway, M. P., Yang, C., Gould, R. M., and Colman, D. R. (1993). A proteolipid protein gene family: expression in sharks and rays and possible evolution from an ancestral gene encoding a pore-forming polypeptide. Neuron *11*, 433-448.

Ko, J. L., Arvidsson, U., Williams, F. G., Law, P. Y., Elde, R., and Loh, H. H. (1999). Visualization of time-dependent redistribution of delta-opioid receptors in neuronal cells during prolonged agonist exposure. Brain Res Mol Brain Res *69*, 171-185.

Ko, M. C., Lee, H., Harrison, C., Clark, M. J., Song, H. F., Naughton, N. N., Woods, J. H., and Traynor, J. R. (2003). Studies of micro-, kappa-, and delta-opioid receptor density and G protein activation in the cortex and thalamus of monkeys. J Pharmacol Exp Ther *306*, 179-186.

Kobayashi, T., Yamaji-Hasegawa, A., and Kiyokawa, E. (2001). Lipid domains in the endocytic pathway. Semin Cell Dev Biol *12*, 173-182.

Koch, T., Brandenburg, L. O., Liang, Y., Schulz, S., Beyer, A., Schröder, H., and Höllt, V. (2004). Phospholipase D2 modulates agonist-induced mu-opioid receptor desensitization and resensitization. J Neurochem *88*, 680-688.

Koch, T., Brandenburg, L. O., Schulz, S., Liang, Y., Klein, J., and Höllt, V. (2003). ADP-ribosylation factor-dependent phospholipase D2 activation is required for agonist-induced mu-opioid receptor endocytosis. J Biol Chem *278*, 9979-9985.

Koch, T., Kroslak, T., Averbeck, M., Mayer, P., Schröder, H., Raulf, E., and Höllt, V. (2000). Allelic variation S268P of the human mu-opioid receptor affects both desensitization and G protein coupling. Mol Pharmacol *58*, 328-334.

Koch, T., Kroslak, T., Mayer, P., Raulf, E., and Höllt, V. (1997). Site mutation in the rat mu-opioid receptor demonstrates the involvement of calcium/calmodulin-dependent protein kinase II in agonist-mediated desensitization. J Neurochem *69*, 1767-1770.

Koch, T., Schulz, S., Pfeiffer, M., Klutzny, M., Schröder, H., Kahl, E., and Höllt, V. (2001). C-terminal splice variants of the mouse mu-opioid receptor differ in morphine-induced internalization and receptor resensitization. J Biol Chem *276*, 31408-31414.

Koch, T., Schulz, S., Schröder, H., Wolf, R., Raulf, E., and Höllt, V. (1998). Carboxyl-terminal splicing of the rat mu opioid receptor modulates agonist-mediated internalization and receptor resensitization. J Biol Chem *273*, 13652-13657.

Koch, T., Widera, A., Bartzsch, K., Schulz, S., Brandenburg, L. O., Wundrack, N., Beyer, A., Grecksch, G., and Höllt, V. (2005). Receptor endocytosis counteracts the development of opioid tolerance. Mol Pharmacol *67*, 280-287.

Kohout, T. A., Lin, F. S., Perry, S. J., Conner, D. A., and Lefkowitz, R. J. (2001). beta-Arrestin 1 and 2 differentially regulate heptahelical receptor signaling and trafficking. Proc Natl Acad Sci U S A *98*, 1601-1606.

Kouhen, O. M., Wang, G., Solberg, J., Erickson, L. J., Law, P. Y., and Loh, H. H. (2000). Hierarchical phosphorylation of delta-opioid receptor regulates agonist-induced receptor desensitization and internalization. J Biol Chem *275*, 36659-36664.

Kovoor, A., Nappey, V., Kieffer, B. L., and Chavkin, C. (1997). Mu and delta opioid receptors are differentially desensitized by the coexpression of beta-adrenergic receptor kinase 2 and beta-arrestin 2 in xenopus oocytes. J Biol Chem *272*, 27605-27611.

Kraus, J., Horn, G., Zimprich, A., Simon, T., Mayer, P., and Höllt, V. (1995). Molecular cloning and functional analysis of the rat mu opioid receptor gene promoter. Biochem Biophys Res Commun *215*, 591-597.

Krupnick, J. G., and Benovic, J. L. (1998). The role of receptor kinases and arrestins in G protein-coupled receptor regulation. Annu Rev Pharmacol Toxicol *38*, 289-319.

LaForge, K. S., Yuferov, V., and Kreek, M. J. (2000). Opioid receptor and peptide gene polymorphisms: potential implications for addictions. Eur J Pharmacol *410*, 249-268.

Lagenaur, C., Kunemund, V., Fischer, G., Fushiki, S., and Schachner, M. (1992). Monoclonal M6 antibody interferes with neurite extension of cultured neurons. J Neurobiol *23*, 71-88.

Laporte, S. A., Oakley, R. H., Holt, J. A., Barak, L. S., and Caron, M. G. (2000). The interaction of beta-arrestin with the AP-2 adaptor is required for the clustering of beta 2-adrenergic receptor into clathrin-coated pits. J Biol Chem *275*, 23120-23126.

Laporte, S. A., Oakley, R. H., Zhang, J., Holt, J. A., Ferguson, S. S., Caron, M. G., and Barak, L. S. (1999). The beta2-adrenergic receptor/betaarrestin complex recruits the clathrin adaptor AP-2 during endocytosis. Proc Natl Acad Sci U S A *96*, 3712-3717.

Law, P. Y., Erickson, L. J., El-Kouhen, R., Dicker, L., Solberg, J., Wang, W., Miller, E., Burd, A. L., and Loh, H. H. (2000a). Receptor density and recycling affect the rate of agonist-induced desensitization of mu-opioid receptor. Mol Pharmacol *58*, 388-398.

Law, P. Y., Hom, D. S., and Loh, H. H. (1983). Opiate receptor down-regulation and desensitization in neuroblastoma X glioma NG108-15 hybrid cells are two separate cellular adaptation processes. Mol Pharmacol *24*, 413-424.

Law, P. Y., Hom, D. S., and Loh, H. H. (1984). Down-regulation of opiate receptor in neuroblastoma x glioma NG108-15 hybrid cells. Chloroquine promotes accumulation of tritiated enkephalin in the lysosomes. J Biol Chem *259*, 4096-4104.

Law, P. Y., and Loh, H. H. (1999). Regulation of opioid receptor activities. J Pharmacol Exp Ther *289*, 607-624.

Law, P. Y., Wong, Y. H., and Loh, H. H. (2000b). Molecular mechanisms and regulation of opioid receptor signaling. Annu Rev Pharmacol Toxicol *40*, 389-430.

Lefkowitz, R. J. (1998). G protein-coupled receptors. III. New roles for receptor kinases and beta-arrestins in receptor signaling and desensitization. J Biol Chem *273*, 18677-18680.

Lefkowitz, R. J., Pitcher, J., Krueger, K., and Daaka, Y. (1998). Mechanisms of beta-adrenergic receptor desensitization and resensitization. Adv Pharmacol *42*, 416-420.

Li, S., Zhu, J., Chen, C., Chen, Y. W., Deriel, J. K., Ashby, B., and Liu-Chen, L. Y. (1993). Molecular cloning and expression of a rat kappa opioid receptor. Biochem J *295 (Pt 3)*, 629-633.

Lin, L. F., and Lees, M. B. (1982). Interactions of dicyclohexylcarbodiimide with myelin proteolipid. Proc Natl Acad Sci U S A *79*, 941-945.

Liu, J. G., and Anand, K. J. (2001). Protein kinases modulate the cellular adaptations associated with opioid tolerance and dependence. Brain Res Brain Res Rev *38*, 1-19.

Lohse, M. J. (1993). Molecular mechanisms of membrane receptor desensitization. Biochim Biophys Acta *1179*, 171-188.

Lusa, S., Blom, T. S., Eskelinen, E. L., Kuismanen, E., Mansson, J. E., Simons, K., and Ikonen, E. (2001). Depletion of rafts in late endocytic membranes is controlled by NPC1-dependent recycling of cholesterol to the plasma membrane. J Cell Sci *114*, 1893-1900.

Macklin, W. B., Campagnoni, C. W., Deininger, P. L., and Gardinier, M. V. (1987). Structure and expression of the mouse myelin proteolipid protein gene. J Neurosci Res *18*, 383-394.

Maher, C. E., Martin, T. J., and Childers, S. R. (2005). Mechanisms of mu opioid receptor/G-protein desensitization in brain by chronic heroin administration. Life Sci *77*, 1140-1154.

Mansour, A., Fox, C. A., Akil, H., and Watson, S. J. (1995a). Opioid-receptor mRNA expression in the rat CNS: anatomical and functional implications. Trends Neurosci *18*, 22-29.

Mansour, A., Fox, C. A., Burke, S., Akil, H., and Watson, S. J. (1995b). Immunohistochemical localization of the cloned mu opioid receptor in the rat CNS. J Chem Neuroanat *8*, 283-305.

Mansour, A., Fox, C. A., Thompson, R. C., Akil, H., and Watson, S. J. (1994). mu-Opioid receptor mRNA expression in the rat CNS: comparison to mu-receptor binding. Brain Res *643*, 245-265.

Marchese, A., and Benovic, J. L. (2001). Agonist-promoted ubiquitination of the G protein-coupled receptor CXCR4 mediates lysosomal sorting. J Biol Chem *276*, 45509-45512.

Marie, N., Lecoq, I., Jauzac, P., and Allouche, S. (2003). Differential sorting of human delta-opioid receptors after internalization by peptide and alkaloid agonists. J Biol Chem *278*, 22795-22804.

Matthes, H. W., Maldonado, R., Simonin, F., Valverde, O., Slowe, S., Kitchen, I., Befort, K., Dierich, A., Le Meur, M., Dolle, P.*, et al.* (1996). Loss of morphine-induced analgesia, reward effect and withdrawal symptoms in mice lacking the mu-opioid-receptor gene. Nature *383*, 819-823.

Meng, F., Xie, G. X., Thompson, R. C., Mansour, A., Goldstein, A., Watson, S. J., and Akil, H. (1993). Cloning and pharmacological characterization of a rat kappa opioid receptor. Proc Natl Acad Sci U S A *90*, 9954-9958.

Mestek, A., Hurley, J. H., Bye, L. S., Campbell, A. D., Chen, Y., Tian, M., Liu, J., Schulman, H., and Yu, L. (1995). The human mu opioid receptor: modulation of functional desensitization by calcium/calmodulin-dependent protein kinase and protein kinase C. J Neurosci *15*, 2396-2406.

Milner, R. J., Lai, C., Nave, K. A., Lenoir, D., Ogata, J., and Sutcliffe, J. G. (1985). Nucleotide sequences of two mRNAs for rat brain myelin proteolipid protein. Cell *42*, 931-939.

Minami, M., Toya, T., Katao, Y., Maekawa, K., Nakamura, S., Onogi, T., Kaneko, S., and Satoh, M. (1993). Cloning and expression of a cDNA for the rat kappa-opioid receptor. FEBS Lett *329*, 291-295.

Mousavi, S. A., Malerod, L., Berg, T., and Kjeken, R. (2004). Clathrin-dependent endocytosis. Biochem J *377*, 1-16.

Mukherjee, S., Zha, X., Tabas, I., and Maxfield, F. R. (1998). Cholesterol distribution in living cells: fluorescence imaging using dehydroergosterol as a fluorescent cholesterol analog. Biophys J *75*, 1915-1925.

Mukobata, S., Hibino, T., Sugiyama, A., Urano, Y., Inatomi, A., Kanai, Y., Endo, H., and Tashiro, F. (2002). M6a acts as a nerve growth factor-gated Ca(2+) channel in neuronal differentiation. Biochem Biophys Res Commun *297*, 722-728.

Murray, S. R., Evans, C. J., and von Zastrow, M. (1998). Phosphorylation is not required for dynamin-dependent endocytosis of a truncated mutant opioid receptor. J Biol Chem *273*, 24987-24991.

Nadon, N. L., Miller, S., Draeger, K., and Salvaggio, M. (1997). Myelin proteolipid DM20: evidence for function independent of myelination. Int J Dev Neurosci *15*, 285-293.

Nave, K. A., Lai, C., Bloom, F. E., and Milner, R. J. (1987). Splice site selection in the proteolipid protein (PLP) gene transcript and primary structure of the DM-20 protein of central nervous system myelin. Proc Natl Acad Sci U S A *84*, 5665-5669.

Nestler, E. J., and Aghajanian, G. K. (1997). Molecular and cellular basis of addiction. Science *278*, 58-63.

Nomura, K., Reuveny, E., and Narahashi, T. (1994). Opioid inhibition and desensitization of calcium channel currents in rat dorsal root ganglion neurons. J Pharmacol Exp Ther *270*, 466-474.

Olinsky, S., Loop, B. T., DeKosky, A., Ripepi, B., Weng, W., Cummins, J., Wenger, S. L., Yan, Y., Lagenaur, C., and Narayanan, V. (1996). Chromosomal mapping of the human M6 genes. Genomics *33*, 532-536.

Onoprishvili, I., Andria, M. L., Kramer, H. K., Ancevska-Taneva, N., Hiller, J. M., and Simon, E. J. (2003). Interaction between the mu opioid receptor and filamin A is involved in receptor regulation and trafficking. Mol Pharmacol *64*, 1092-1100.

Pak, Y., Kouvelas, A., Scheideler, M. A., Rasmussen, J., O'Dowd, B. F., and George, S. R. (1996). Agonist-induced functional desensitization of the mu-opioid receptor is mediated by loss of membrane receptors rather than uncoupling from G protein. Mol Pharmacol *50*, 1214-1222.

Pak, Y., O'Dowd, B. F., and George, S. R. (1997). Agonist-induced desensitization of the mu opioid receptor is determined by threonine 394 preceded by acidic amino acids in the COOH-terminal tail. J Biol Chem *272*, 24961-24965.

Pan, L., Xu, J., Yu, R., Xu, M. M., Pan, Y. X., and Pasternak, G. W. (2005). Identification and characterization of six new alternatively spliced variants of the human mu opioid receptor gene, Oprm. Neuroscience *133*, 209-220.

Pan, Y. X., Xu, J., Bolan, E., Abbadie, C., Chang, A., Zuckerman, A., Rossi, G., and Pasternak, G. W. (1999). Identification and characterization of three new alternatively spliced mu-opioid receptor isoforms. Mol Pharmacol *56*, 396-403.

Pan, Y. X., Xu, J., Bolan, E., Chang, A., Mahurter, L., Rossi, G., and Pasternak, G. W. (2000). Isolation and expression of a novel alternatively spliced mu opioid receptor isoform, MOR-1F. FEBS Lett *466*, 337-340.

Pasternak, D. A., Pan, L., Xu, J., Yu, R., Xu, M. M., Pasternak, G. W., and Pan, Y. X. (2004). Identification of three new alternatively spliced variants of the rat mu opioid receptor gene: dissociation of affinity and efficacy. J Neurochem *91*, 881-890.

Pasternak, G. W. (1993). Pharmacological mechanisms of opioid analgesics. Clin Neuropharmacol *16*, 1-18.

Pasternak, G. W., and Standifer, K. M. (1995). Mapping of opioid receptors using antisense oligodeoxynucleotides: correlating their molecular biology and pharmacology. Trends Pharmacol Sci *16*, 344-350.

Pert, C. B., and Snyder, S. H. (1973). Opiate receptor: demonstration in nervous tissue. Science *179*, 1011-1014.

Peyron, R., Laurent, B., and Garcia-Larrea, L. (2000). Functional imaging of brain responses to pain. A review and meta-analysis (2000). Neurophysiol Clin *30*, 263-288.

Pfleger, K. D., and Eidne, K. A. (2003). New technologies: bioluminescence resonance energy transfer (BRET) for the detection of real time interactions involving G-protein coupled receptors. Pituitary *6*, 141-151.

Pierce, K. L., Premont, R. T., and Lefkowitz, R. J. (2002). Seven-transmembrane receptors. Nat Rev Mol Cell Biol *3*, 639-650.

Polakiewicz, R. D., Schieferl, S. M., Dorner, L. F., Kansra, V., and Comb, M. J. (1998). A mitogen-activated protein kinase pathway is required for mu-opioid receptor desensitization. J Biol Chem *273*, 12402-12406.

Puttfarcken, P. S., and Cox, B. M. (1989). Morphine-induced desensitization and down-regulation at mu-receptors in 7315C pituitary tumor cells. Life Sci *45*, 1937-1942.

Qiu, Y., Law, P. Y., and Loh, H. H. (2003). Mu-opioid receptor desensitization: role of receptor phosphorylation, internalization, and representation. J Biol Chem *278*, 36733-36739.

Rausell, E., Bickford, L., Manger, P. R., Woods, T. M., and Jones, E. G. (1998). Extensive divergence and convergence in the thalamocortical projection to monkey somatosensory cortex. J Neurosci *18*, 4216-4232.

Readhead, C., Schneider, A., Griffiths, I., and Nave, K. A. (1994). Premature arrest of myelin formation in transgenic mice with increased proteolipid protein gene dosage. Neuron *12*, 583-595.

Roettger, B. F., Rentsch, R. U., Pinon, D., Holicky, E., Hadac, E., Larkin, J. M., and Miller, L. J. (1995). Dual pathways of internalization of the cholecystokinin receptor. J Cell Biol *128*, 1029-1041.

Roussel, G., Trifilieff, E., Lagenaur, C., and Nussbaum, J. L. (1998). Immunoelectron microscopic localization of the M6a antigen in rat brain. J Neurocytol *27*, 695-703.

Salahpour, A., Angers, S., and Bouvier, M. (2000). Functional significance of oligomerization of G-protein-coupled receptors. Trends Endocrinol Metab *11*, 163-168.

Schindler, P., Luu, B., Sorokine, O., Trifilieff, E., and Van Dorsselaer, A. (1990). Developmental study of proteolipids in bovine brain: a novel proteolipid and DM-20 appear before proteolipid protein (PLP) during myelination. J Neurochem *55*, 2079-2085.

Schmidt, H., Schulz, S., Klutzny, M., Koch, T., Handel, M., and Höllt, V. (2000). Involvement of mitogen-activated protein kinase in agonist-induced phosphorylation of the mu-opioid receptor in HEK 293 cells. J Neurochem *74*, 414-422.

Schulz, S., and Höllt, V. (1998). Opioid withdrawal activates MAP kinase in locus coeruleus neurons in morphine-dependent rats in vivo. Eur J Neurosci *10*, 1196-1201.

Schulz, S., Mayer, D., Pfeiffer, M., Stumm, R., Koch, T., and Höllt, V. (2004). Morphine induces terminal micro-opioid receptor desensitization by sustained phosphorylation of serine-375. Embo J *23*, 3282-3289.

Schulz, S., Schreff, M., Koch, T., Zimprich, A., Gramsch, C., Elde, R., and Höllt, V. (1998). Immunolocalization of two mu-opioid receptor isoforms (MOR1 and MOR1B) in the rat central nervous system. Neuroscience *82*, 613-622.

Self, D. W., and Nestler, E. J. (1995). Molecular mechanisms of drug reinforcement and addiction. Annu Rev Neurosci *18*, 463-495.

Sharma, S. K., Klee, W. A., and Nirenberg, M. (1975). Dual regulation of adenylate cyclase accounts for narcotic dependence and tolerance. Proc Natl Acad Sci U S A *72*, 3092-3096.

Sheetz, M. P., Baumrind, N. L., Wayne, D. B., and Pearlman, A. L. (1990). Concentration of membrane antigens by forward transport and trapping in neuronal growth cones. Cell *61*, 231-241.

Shih, S. C., Katzmann, D. J., Schnell, J. D., Sutanto, M., Emr, S. D., and Hicke, L. (2002). Epsins and Vps27p/Hrs contain ubiquitin-binding domains that function in receptor endocytosis. Nat Cell Biol *4*, 389-393.

Shimokawa, N., and Miura, M. (2000). Rhombex-29, a novel gene of the PLP/DM20-M6 family cloned from rat medulla oblongata by differential display. J Neurosci Res *62*, 1-8.

Sim-Selley, L. J., Selley, D. E., Vogt, L. J., Childers, S. R., and Martin, T. J. (2000). Chronic heroin self-administration desensitizes mu opioid receptor-activated G-proteins in specific regions of rat brain. J Neurosci *20*, 4555-4562.

Simon, E. J., Hiller, J. M., and Edelman, I. (1973). Stereospecific binding of the potent narcotic analgesic (3H) Etorphine to rat-brain homogenate. Proc Natl Acad Sci U S A *70*, 1947-1949.

Simons, M., Kramer, E. M., Macchi, P., Rathke-Hartlieb, S., Trotter, J., Nave, K. A., and Schulz, J. B. (2002). Overexpression of the myelin proteolipid protein leads to accumulation of cholesterol and proteolipid protein in endosomes/lysosomes: implications for Pelizaeus-Merzbacher disease. J Cell Biol *157*, 327-336.

Simons, M., Kramer, E. M., Thiele, C., Stoffel, W., and Trotter, J. (2000). Assembly of myelin by association of proteolipid protein with cholesterol- and galactosylceramide-rich membrane domains. J Cell Biol *151*, 143-154.

Simons, R., Alon, N., and Riordan, J. R. (1987). Human myelin DM-20 proteolipid protein deletion defined by cDNA sequence. Biochem Biophys Res Commun *146*, 666-671.

Sinoway, M. P., Kitagawa, K., Timsit, S., Hashim, G. A., and Colman, D. R. (1994). Proteolipid protein interactions in transfectants: implications for myelin assembly. J Neurosci Res *37*, 551-562.

Stafford, K., Gomes, A. B., Shen, J., and Yoburn, B. C. (2001). mu-Opioid receptor downregulation contributes to opioid tolerance in vivo. Pharmacol Biochem Behav *69*, 233-237.

Stein, B. S., Bensch, K. G., and Sussman, H. H. (1984). Complete inhibition of transferrin recycling by monensin in K562 cells. J Biol Chem *259*, 14762-14772.

Stumm, R. K., Rummel, J., Junker, V., Culmsee, C., Pfeiffer, M., Krieglstein, J., Höllt, V., and Schulz, S. (2002). A dual role for the SDF-1/CXCR4 chemokine receptor system in adult brain: isoform-selective regulation of SDF-1 expression modulates CXCR4-dependent neuronal plasticity and cerebral leukocyte recruitment after focal ischemia. J Neurosci *22*, 5865-5878.

Stumm, R. K., Zhou, C., Schulz, S., and Höllt, V. (2004). Neuronal types expressing mu- and delta-opioid receptor mRNA in the rat hippocampal formation. J Comp Neurol *469*, 107-118.

Tanowitz, M., and Von Zastrow, M. (2002). Ubiquitination-independent trafficking of G protein-coupled receptors to lysosomes. J Biol Chem *277*, 50219-50222.

Tanowitz, M., and von Zastrow, M. (2003). A novel endocytic recycling signal that distinguishes the membrane trafficking of naturally occurring opioid receptors. J Biol Chem *278*, 45978-45986.

Terenius, L. (1973). Characteristics of the "receptor" for narcotic analgesics in synaptic plasma membrane fraction from rat brain. Acta Pharmacol Toxicol (Copenh) *33*, 377-384.

Tsao, P. I., and von Zastrow, M. (2000). Type-specific sorting of G protein-coupled receptors after endocytosis. J Biol Chem *275*, 11130-11140.

Tsao, P. I., and von Zastrow, M. (2001). Diversity and specificity in the regulated endocytic membrane trafficking of G-protein-coupled receptors. Pharmacol Ther *89*, 139-147.

Tulipano, G., Stumm, R., Pfeiffer, M., Kreienkamp, H. J., Höllt, V., and Schulz, S. (2004). Differential beta-arrestin trafficking and endosomal sorting of somatostatin receptor subtypes. J Biol Chem *279*, 21374-21382.

von Zastrow, M. (2003). Mechanisms regulating membrane trafficking of G protein-coupled receptors in the endocytic pathway. Life Sci *74*, 217-224.

von Zastrow, M. (2004). A cell biologist's perspective on physiological adaptation to opiate drugs. Neuropharmacology *47 Suppl 1*, 286-292.

von Zastrow, M., Svingos, A., Haberstock-Debic, H., and Evans, C. (2003). Regulated endocytosis of opioid receptors: cellular mechanisms and proposed roles in physiological adaptation to opiate drugs. Curr Opin Neurobiol *13*, 348-353.

Waldhoer, M., Bartlett, S. E., and Whistler, J. L. (2004). Opioid receptors. Annu Rev Biochem *73*, 953-990.

Wang, D., Sun, X., Bohn, L. M., and Sadee, W. (2005). Opioid receptor homo- and heterodimerization in living cells by quantitative bioluminescence resonance energy transfer. Mol Pharmacol *67*, 2173-2184.

Wang, H. L. (2000). A cluster of Ser/Thr residues at the C-terminus of mu-opioid receptor is required for G protein-coupled receptor kinase 2-mediated desensitization. Neuropharmacology *39*, 353-363.

Wang, H. L., Chang, W. T., Hsu, C. Y., Huang, P. C., Chow, Y. W., and Li, A. H. (2002). Identification of two C-terminal amino acids, Ser(355) and Thr(357), required for short-term homologous desensitization of mu-opioid receptors. Biochem Pharmacol *64*, 257-266.

Wang, J. B., Imai, Y., Eppler, C. M., Gregor, P., Spivak, C. E., and Uhl, G. R. (1993). mu opiate receptor: cDNA cloning and expression. Proc Natl Acad Sci U S A *90*, 10230-10234.

Wang, W., Loh, H. H., and Law, P. Y. (2003). The intracellular trafficking of opioid receptors directed by carboxyl tail and a di-leucine motif in Neuro2A cells. J Biol Chem *278*, 36848-36858.

Whistler, J. L., Chuang, H. H., Chu, P., Jan, L. Y., and von Zastrow, M. (1999). Functional dissociation of mu opioid receptor signaling and endocytosis: implications for the biology of opiate tolerance and addiction. Neuron *23*, 737-746.

Whistler, J. L., Enquist, J., Marley, A., Fong, J., Gladher, F., Tsuruda, P., Murray, S. R., and Von Zastrow, M. (2002). Modulation of postendocytic sorting of G protein-coupled receptors. Science *297*, 615-620.

Whistler, J. L., and von Zastrow, M. (1998). Morphine-activated opioid receptors elude desensitization by beta-arrestin. Proc Natl Acad Sci U S A *95*, 9914-9919.

Williams, J. T., Christie, M. J., and Manzoni, O. (2001). Cellular and synaptic adaptations mediating opioid dependence. Physiol Rev *81*, 299-343.

Wolf, R., Koch, T., Schulz, S., Klutzny, M., Schröder, H., Raulf, E., Buhling, F., and Höllt, V. (1999). Replacement of threonine 394 by alanine facilitates internalization and resensitization of the rat mu opioid receptor. Mol Pharmacol *55*, 263-268.

Wolozin, B. L., and Pasternak, G. W. (1981). Classification of multiple morphine and enkephalin binding sites in the central nervous system. Proc Natl Acad Sci U S A *78*, 6181-6185.

Yabaluri, N., and Medzihradsky, F. (1997). Down-regulation of mu-opioid receptor by full but not partial agonists is independent of G protein coupling. Mol Pharmacol *52*, 896-902.

Yan, Y., Lagenaur, C., and Narayanan, V. (1993). Molecular cloning of M6: identification of a PLP/DM20 gene family. Neuron *11*, 423-431.

Yan, Y., Narayanan, V., and Lagenaur, C. (1996). Expression of members of the proteolipid protein gene family in the developing murine central nervous system. J Comp Neurol *370*, 465-478.

Yasuda, K., Raynor, K., Kong, H., Breder, C. D., Takeda, J., Reisine, T., and Bell, G. I. (1993). Cloning and functional comparison of kappa and delta opioid receptors from mouse brain. Proc Natl Acad Sci U S A *90*, 6736-6740.

Yu, Y., Zhang, L., Yin, X., Sun, H., Uhl, G. R., and Wang, J. B. (1997). Mu opioid receptor phosphorylation, desensitization, and ligand efficacy. J Biol Chem *272*, 28869-28874.

Zadina, J. E., Chang, S. L., Ge, L. J., and Kastin, A. J. (1993). Mu opiate receptor down-regulation by morphine and up-regulation by naloxone in SH-SY5Y human neuroblastoma cells. J Pharmacol Exp Ther *265*, 254-262.

Zadina, J. E., Harrison, L. M., Ge, L. J., Kastin, A. J., and Chang, S. L. (1994). Differential regulation of mu and delta opiate receptors by morphine, selective agonists and antagonists and differentiating agents in SH-SY5Y human neuroblastoma cells. J Pharmacol Exp Ther *270*, 1086-1096.

Zhang, J., Ferguson, S. S., Barak, L. S., Bodduluri, S. R., Laporte, S. A., Law, P. Y., and Caron, M. G. (1998). Role for G protein-coupled receptor kinase in agonist-specific regulation of mu-opioid receptor responsiveness. Proc Natl Acad Sci U S A *95*, 7157-7162.

Zimprich, A., Simon, T., and Höllt, V. (1995). Cloning and expression of an isoform of the rat mu opioid receptor (rMOR1B) which differs in agonist induced desensitization from rMOR1. FEBS Lett *359*, 142-146.

Zubieta, J. K., Smith, Y. R., Bueller, J. A., Xu, Y., Kilbourn, M. R., Jewett, D. M., Meyer, C. R., Koeppe, R. A., and Stohler, C. S. (2001). Regional mu opioid receptor regulation of sensory and affective dimensions of pain. Science *293*, 311-315.

Zuo, Z. (2005). The role of opioid receptor internalization and beta-arrestins in the development of opioid tolerance. Anesth Analg *101*, 728-734, table of contents.

8 List of figures and table

9 Abbreviations

ABTS	2,2'-azino-di-[3-ethylbenzthiazoline sulfonate (6)]
AC	Adenylate cyclase
ANOVA	Analysis of variance
ATCC	American Type Culture Collection (Rockville, MD)
B_{max}	the number of maximal [^{3}H] DAMGO binding site
BRET	Bioluminescence resonance energy transfer
cAMP	Adenosine 3',5'-cylic-monophosphate
cDNA	Complemetary deoxyribonucleic acid
CHO	Chinese hamster ovary
CNS	Central nervous system
CRE	cAMP response element
CREB	CRE binding protein
DAMGO	[D-Ala^2, *N*-Me-Phe^4, Gly^5-ol]-enkephalin, Tyr-D-Ala-Gly-N-methyl-Phe-Gly-ol
DMEM	Dulbecco's Modified Eagle Medium
DNA	Deoxyribonucleic acid
DOR1	The δ-opioid receptor isoform 1
DOR1/MT	A chimeric DOR1 which the entire cytoplasmic tail of DOR1 has been replaced by the entire cytoplasmic tail of MOR1.
DPDPE	[D-Pen^2, D-Pen^5] enkephalin, Tyr-D-Pen-Gly-Phe-D-PenOH
DPX	Distrene, dibutyl Phthalate, Xylene
DSP	Dithiobis-(succinimi-dylpropionate)
DTT	Dithiothreitol
E. coli	Escherichia coli
EDTA	Ethylenediaminetetraacetic acid
ELISA	Enzyme-linked immunoabsorbent assay
FCS	Fetal calf serum
E17	Embryonic day 17
G-protein	Heterotrimeric guanine nucletide binding protein
G418 sulfate	Geneticin, a 2-deoxystreptamine antibiotic produced by *Microspora rhodorangea*
GASP	G protein-coupled receptor-associated sorting protein
GDP	Guanosine 5'-diphosphate
GFP	Green fluorescent protein
GPCR	G protein-coupled receptor
GRK	G protein-coupled receptor kinase
GTP	Guanosine 5'-triphosphate
HA	Human influenza virus hemagglutinin (YPYDVPDYA)

HA-MOR1	Amino-terminally HA-tagged MOR1
HEK	Human embryonic kidney
HEPES	N-2-hydroxyethylpiperazine-N□2-ethanesulfonic acid
i.p.	Intraperitoneally
K_D	Dissociation constant
MAP	Mitogen activated protein
MOR1	The μ-opioid receptor isoform 1
MOR1B	A splice variant of MOR1
MRS	MOR-derived endocytic recycling sequence
Myc	Epitope tag (sequence: MASMQKLISEEDL)
Myc-M6a	Amino-terminally Myc-tagged M6a
PBS	Phosphate-buffered saline
PCR	Polymerase chain reaction
PKA	Protein kinase A
Rluc	Renilla luciferase
RPMI	Roswell Park Memorial Institute
rpm	round per minte
RT	Room temperature
RT-PCR	Reverse transcription-PCR
SDS	Sodium dodecyl sulphate
SDS-PAGE	Sodium dodecyl sulphate - polyacrylamide gel electrophoresis
SEM	Stand error of the mean
SSC	Sodium chloride/sodium citrate
TPBS	Tris/phosphate-buffered saline

10 Appendix

10.1 Curriculum vitae

Name:	Daifei Wu
Gender:	Male
Date of birth:	Apr. 3, 1969
Place of birth:	Fujian, China
Marital status:	Single
Nationality:	Chinese

Education & Experience:

Mar. 2002--now:	Ph.D. student Department of Pharmacology and Toxicology, Medical Faculty, Otto-von-Guericke-University, Magdeburg, Germany.
Jul. 1997--Feb. 2002:	Assistant researcher National Key Lab of Biotechnology Haikou, China
Sep. 1994--Jun.1997:	Master student (top Student) Chinese Academy of Tropical Agricultural Sciences, Hainan, China
Sep. 1990--Jun. 1994:	Bachelor student (top Student) South China University of Tropical Agriculture, Hainan, China

Magdeburg, July 6, 2006

……

Daifei Wu

10.2 Publications and presentations

10.2.1 Publications

Wu DF, et al. Membrane glycoprotein M6a is a modulator of μ-opioid receptor trafficking and desensitization. Neuron 2006, in submission.

Wu DF, et al. Interaction of the μ-Opioid Receptor with Synaptophysin Influences Receptor Trafficking and Signaling. Mol Pharmacol. 2006, in revision.

Koch T, **Wu DF**, Yang LQ, Brandenburg LO, Höllt V. Role of phospholipase D2 in the agonist-induced and constitutive endocytosis of G-protein couple receptors. J Neurochem. 2006, 97:365-72.

Börner C, **Wu DF**, Höllt V, Kraus J. Expression of functional μ-opioid receptors induced by cytokines in Jurkat T cells. J Neuroimmunol. 2006, submitted.

Wu DF, et al. The phospholipase D2 is involved in the endocytosis and signaling of cannabinoid receptor CB1. Naunyn-Schmiedeberg's Archives of Pharmacology. 2006, 372 (supplement 1).

Koch T, **Wu DF**, Kahl E, Köpplin R, Höllt V. Buprenorphine and the active metabolite norbuprenorphine differ in the MOPr internalization and desensitization. Naunyn-Schmiedeberg's Archives of Pharmacology. 2006, 372 (supplement 1).

Yang LQ, Koch T, **Wu DF**, Goschke A, Höllt V. Role of phospholipase D2 in agonist-induced DOPr endocytosis. Naunyn-Schmiedeberg's Archives of Pharmacology. 2006, 372 (supplement 1).

Koch T, Brandenburg LO, **Wu D**, Liang Y, Schulz S, Höllt V. Identification of mu opioid receptor-interacting proteins involved in receptor regulation and trafficking. Naunyn-Schmiedeberg's Archives of Pharmacology. 2004, 369 (supplement 1).

Pfeiffer M, Kirscht S, Stumm R, Koch T, **Wu DF**, Laugsch M, Schröder H, Höllt V, Schulz S. Heterodimerization of substance P and mu-opioid receptors regulates receptor trafficking and resensitization. J Biol Chem. 2003, 278(51): 51630-7.

10.2.2 Conference presentation and poster

Wu DF, Koch T, Höllt V. Interaction of the mu-opioid receptor with synaptophysin influences receptor endocytosis and signaling. Poster on the 37th International Narcotic Research Conference (INRC). St. Paul, Minnesota, USA. 2006

Koch T, **Wu DF**, Kahl E, Strohm F and Höllt V. Mu-opioid receptor-stimulated synthesis of reactive oxygen species (ROS) is mediated via phospholipase D2. Poster on the 37th INRC. St. Paul, USA. 2006

Wu DF, Koch T, Höllt V. Activation of phospholipase D2 by cannabinoid receptors (CB1) plays a role in CB1 trafficking. Oral presentation on the 47th Spring Meeting, the German society of experimental and clinical pharmacology and toxicocogy. Mainz, Germany. 2006

Koch T, **Wu D**, Yang L, Brandenburg L.O., Höllt V. Regulation of G-protein coupled receptor endocytosis by phospholipase D2. Poster on the 36th INRC. Annapolis Maryland, USA. 2005

Höllt V, Grecksch G, Koch T, Pfeiffer M, Schulz S, Stumm R, **Wu D**. Mu opioid receptor internalization and desensitization. Symposium lecture on the 36th INRC. Annapolis, USA. 2005

Wu D, Koch T, Liang Y, Höllt V. Membrane glycoprotein M6a influences mu opioid receptor trafficking, desensitization and superactivation. Oral presentation on the 35th INRC. Kyoto, Japan. 2004

Koch T, Brandenburg LO, **Wu D**, Liang Y, Schulz S, Höllt V. Identification of mu opioid receptor-interacting proteins involved in receptor regulation and trafficking. Oral presentation on the 45th spring meeting, the German society of experimental and clinical pharmacology and toxicology. Mainz, Germany. 2004

Wu D, Liang Y, Koch T, Höllt V. Glycoprotein M6a interacts with the rMOR1: An analysis by Bioluminescence Resonance Energy Transfer (BRET^2). Poster on the 34th INRC, Perpignan, 2003

Liang Y, **Wu D**, Koch T, Höllt V. Heat shock cognate protein 70 (Hsc70) and synaptophysin interact with the mu opioid receptor. Poster on the 34th INRC. Perpignan, France. 2003

Schröder H, Koch T, Schulz S, **Wu D**, Höllt V. Modulation of mu opioid receptor by coexpressed metabotropic GluR5 receptor in HEK 293 cells. Poster on the 34th INRC. Perpignan, France. 2003

10.3 Acknowledgement

All experiments in this dissertation were carried out in Department of Pharmacology and Toxicology, Medical Faculty, Otto-Von-Guericke-University Magdeburg, Germany. Here I would like to express my sincere thanks to those people who made my Ph.D. studies both educational and pleasurable.

Prof. Dr. Volker Höllt, who is my adviser, guided my way to Germany and provided me continuous supports in my Ph.D. research works. There are so many times that I am always deeply moved by his patience and kindness. His constant advice, encouragement as well as his great help will always be cherished. From him I learned not only scientific knowledge, but also his decent personality.

I am greatly indebted to my practical adviser Dr. Thomas Koch for his guidance throughout my time in his group. He gave me much constructive advice all through my graduate study. His enthusiasm, spirit of hard work and tireless effort in guiding graduate students give me tremendous courage and confidence.

I would like to thank Dr. Stefan Schulz for his helpful advice and assistance in confocal microscopy. I am indebted to him for kindly providing me the scientific resources in his group.

I would like to thank Dr. Ralf Stumm for his help in in situ hybridization and preparation of primary neurons, Dr. Helmut Schröder for his help in radioligand binding assay, Dr. Manuela Pfeiffer for her help in BRET assay, Dr. Giovanni Tulipano for his help in ELISA assay.

I would like to express my special thanks to the lab member Jenny (Yingjian Liang) for her willingness to share her scientific experience, and for her great help in cell culture, immunoprecipitation and confocal microscopy. After she left Magdeburg, her constructive advice and helpful discussion continued throughout my research works.

I would like to express my gratitude to my lab members, Andrea Goschke, Sandra Großeheilmann, Evelyn Kahl and Sabrina Sattelkau, for their friendly help both in my work and daily life. I thank Anke Reichenauer, Karina Schäfer, Michaela Böx and Dana Mayer for their excellent technical assistance in my experiments.

I would like to express my special thanks to my previous mentor, Prof. Dr. Chunfa Zhang (NICHD, NIH, USA), for supporting my decision to pursue a Ph.D. degree in Germany. I benefit from his continues encouragement and suggestions in Germany all the time.

At last, I am extremely indebted to my parents for their invaluable support throughout my life.

11 Zusammenfassung

Opiate wie Morphin sind nach wie vor das Mittel der Wahl bei der Behandlung von starken und chronischen Schmerzen. Der klinische Einsatz der Opiate wird jedoch durch adaptative Veränderungen des Nervensystems eingeschränkt, die nach langer oder wiederholter Opiatgabe auftreten können und zur physiologischen Toleranz und Abhängigkeit gegenüber Opiaten beitragen. Diese adaptiven Veränderungen werden durch die Bindung von endogenen wie auch exogenen Opiaten an den Opiatrezeptor ausgelöst. Der µ-Opioidrezeptor (MOR1) ist von besonderer Bedeutung für die Vermittlung der analgetischen und adaptiven Effekte von klinisch relevanten Opiaten. Die Aufklärung der Mechanismen, welche an der Regulation der µ-Opioidrezeptoraktivität beteiligt sind, ist möglicherweise der Schlüsselschritt zur Entwicklung neuer Drogen oder veränderter analgetischer Therapien.

In der letzten Zeit mehren sich die Hinweise, dass die Signaltransduktion des µ-Opioidrezeptors durch verschiedene rezeptor-assoziierte Proteine moduliert werden kann. In Vorarbeiten wurden mit Hilfe der Yeast-Two-Hybrid Technik bereits verschiedene µ-opioidrezeptor-interagierende Proteine von unserer Arbeitsgruppe identifiziert, zu denen auch das membranständige Glykoprotein M6a (M6a) gehört. Um die Interaktion dieser Proteine mit dem MOR1 in Säugerzellen zu bestätigen, wurden die zu untersuchenden Proteine mit Biolumineszens/Fluoreszens-Epitopen markiert und mittels Bioluminszens-Resonanz-Energie-Transfer Technik (BRET) untersucht. Von allen untersuchten Proteinen zeigte das M6a die stärkste Interaktion mit dem µ-Opioidrezeptor. Diese Interaktion konnte auch mit Hilfe der Koimmunopräzipitations-Technik immuncytochemisch nachgewiesen werden. Weitere Untersuchungen zeigten, dass die Transmembrandomänen des MOR1 und des M6a für die Protein-Protein-Interaktion wichtig sind. Zusätzlich konnte gezeigt werden, dass das M6a mit einer Reihe weiterer G-Protein-gekoppelter Rezeptoren (GPCRs) interagieren kann, was auf eine möglicherweise wichtige Funktion des M6a bei der Regulation dieser Rezeptoren hindeutet.

Das M6a-Protein, dessen Funktion bei Beginn dieser Studie noch unklar war, gehört zur Familie der Proteolipid-Protein (PLP)/DM20 Familie. Doppel-*in situ* Hybridisierungen zeigten eine Koexpression von MOR1 und M6a in vielen Hirnregionen, was eine Interaktion dieser Proteine auch unter *in vivo* Bedingungen möglich macht. Im Weiteren konnte gezeigt werden, dass MOR1 und M6a in transfizierten HEK293 Zellen kointernalisieren und mittels Recycling-Endosomen gemeinsam zur Zellmembran zurücktransportiert werden. Zusätzlich führt die Interaktion mit dem M6a Protein zu einer Verstärkung der Internalisierung und Rezyklisierung des µ-Opioidrezeptors. In HEK293 Zellen konnte ebenfalls gezeigt werden, dass das endogen exprimierte M6a Protein eine wichtige physiologische Funktion bei der MOR1 Internalsierung besitzt, da die Überexpression einer dominant-negativen M6a Mutante die agonisten-vermittelte Internalisierung des MOR1 verhinderte. Zusätzlich konnte gezeigt werden, dass das M6a die Herunterregulation des MOR1 vermindert, was auf die M6a-induzierte verstärkte Rezeptorrezyklisierung zurückgeführt werden kann. M6a bindet und kointernalisiert auch mit dem □-Opioidrezeptor (DOR1). Die Interaktion des DOR1 mit M6a führt, ähnlich wie beim MOR1, zu einer Verstärkung der Rezeptorrezyklisierung, was ebenfalls für eine Rolle des M6a bei der Rezeptorrezyklisiserung spricht.

Der verstärkte intrazelluläre Transport des MOR1 führt nachweislich zu einer verzögerten Rezeptordesensitisierung. Die genannten funktionellen Eigenschaften des M6a Proteins auf den intrazellulären Transport und die Signaltransduktion des µ-Opioidrezeptors wurden in überexprimierenden HEK293 Zellen, aber auch in primären kultivierten Neuronen nachgewiesen.

Zusammengefasst konnten wir zeigen, dass das M6a eine wichtige Funktion als Adapterprotein bei dem intrazellulären µ-Opioidrezeptortransport übernimmt und an der Verminderung der Entwicklung einer Opiattoleranz beteiligt ist. Somit zeigt unsere Arbeit, dass die Familie der PLP/DM20 Glycoproteine neben ihrer strukturellen Rolle bei der Myelinisierung auch eine neue Funktion bei der Regulation der Aktivität von GPCRs übernehmen kann.